AUTOBAHN: A GENE THAT HAS A ROLE IN AUXIN INFLUX IN *ARABIDOPSIS* LEAVES?

JASMINE JAY TAMARA GARRETT
B.Sc., University of Lethbridge, 2003

A Thesis
Submitted to the School of Graduate Studies
Of the University of Lethbridge
In Partial Fulfillment of the
Requirements for the Degree

MASTERS OF SCIENCE

Biological Sciences
University of Lethbridge
LETHBRIDGE, ALBERTA, CANADA

Abstract

The development of leaf vascular patterns is a highly regulated process. The plant hormone auxin is critical for vascular patterning: auxin canalization is proposed to cause files of cells to accumulate higher auxin levels and develop into veins. Thus, the response of cells to auxin and transport of auxin are critical to establish proper cell fate. We have characterized a mutation in the *Arabidopsis thaliana* gene named AUTOBAHN (ABN). *abn* leaves produce leaves that proliferate disorganized, overlapping veins parallel to the midvein with no differentiation of higher order veins. *abn* leaves show no normal aspects of the secondary auxin response though double mutant analysis suggest that ABN functions independently of previously characterized auxin response pathways. Wild type plants grown on an influx inhibitor phenocopy *abn* suggesting that *abn* is defective in carrier-mediated auxin influx.

Table of Contents

List of Tables

List of Figures

List of Abbreviations

Genes and Proteins

ABC	ATP-BINDING CASSETTE
ABN	AUTOBAHN
ABP	AUXIN BINDING PROTEIN
ARE	AUXINE-RESPONSE ELEMENT
ARF	AUXIN-RESPONSE FACTOR
ATHB8	ARABIDOPSIS THALIANA HOMEOBOX8
AUX	AUXIN
AXR1	AUXIN RESISTANT1
AXR2	AUXIN RESISTANT2
AXR4	AUXIN RESISTANT4
AXR6	AUXIN RESISTANT6
BDL	BODENLOS
CUL1	CULLIN1
CVP	COTYLEDON VASCULR PATTERN
FKD	FORKED
GEF	GTP EXCHANGE FACTOR
GL1-1	GLABROUS1-1
LAX	LIKE AUX1
MDR	MULTIPLE DRUG RESISTANCE
MRP	MULTIDRUG- RELATED PROTEIN

MP	MONOPTEROS
PID	PINOID
PIN1	PIN FORMED1
RTY	ROOTY
SCF	SKP1/CULLIN/F-BOX
SFC	SCARFACE
VAN	VASCULAR NETWORK
VEP1	VEIN PATTERNING1

Chemicals

2,4-D	2,4-dichlorophenoxyacetic acid
EMS	ethyl methane sulfonate
DMSO	dimethyl sulfoxide
IAA	indole-3-acetic acid
NAA	1-naphthaleneacetic acid
NOA	1-napthoxyacetic acid
NPA	naphthylphthalamic acid
X-gluc	5-bromo-4-chloro-3-indoyl glucuronide

Terms

AT	*Arabidopsis thaliana*
BP	branch point
Col	Columbia ecotype

CCD	charge-coupled device
DAG	days after germination
FEV	freely ending vein
Ler	Landsberg ecotype
PCR	polymerase chain reaction
RAM	root apical meristem
RF	recombination frequency
SAM	shoot apical meristem
SSLP	simple sequence length polymorphism
VI	vascular island

Introduction

Vascular systems are essential for the viability of plants and are comprised of two major types of conducting tissues: xylem and phloem. Xylem primarily transports water and dissolved minerals that are absorbed from the soil and phloem primarily transports photosynthates and hormones throughout the plant. Xylem and phloem are arranged into vascular bundles called veins. The spatial arrangement of leaf veins forms a multitude of patterns throughout different taxa in the plant kingdom. It is important to understand the development of venation patterns as they confer transport efficiency and mechanical stability to the entire plant.

In leaves of dicots, there are three major types of veins that contribute to the mature vascular pattern: 1) the midvein, which connects with the stem vascular system; 2) secondary veins, which branch from the midvein and develop into the lamina and; 3) tertiary and higher order veins, which branch from secondary veins or each other and do not meet with the midvein (Sieburth, 1999). Classical studies suggest that the midvein differentiates towards the leaf tip (acropetal differentiation) whereas secondary and higher order veins differentiate primarily towards the leaf base (basipetal differentiation) (Nelson and Dengler, 1997). However considerable debate over the direction of vein differentiation exists: recent analysis, based on proposed routes of auxin transport, suggests that the development of the midvein may be basipetal (Benkova et al., 2003) while ATHB8::GUS expression suggests that the development of secondary veins may be simultaneously acropetal and basipetal (Mattsson et al., 1999, Scarpella et al., 2004). The plant hormone auxin is known to be critical for plant vascular tissue formation and

patterning. Auxin has been shown to play a critical role in many aspects of plant growth and development (reviewed in Aloni, 1995) including tropisms (Rosen et al., 1999; Friml et al., 2002), patterning of early embryos (Jürgens, 2001; Friml 2003), root patterning and elongation (Blilou et al., 2005), lateral root initiation (Casimiro et al., 2001), the positioning and expansion of leaves and flowers (Berleth and Sachs, 2001; Benkova et al., 2003; Reindhardt et al, 2003), and vascular differentiation (Berleth et al, 2000; Aloni, 2003). Although the importance of auxin has been well established, we are only beginning to understand the molecular details of auxin signaling and transport.

Auxin is a unique signaling molecule as it is actively transported in a polar fashion from its source in young plant tissues and apical meristems to sites of action. Auxin transport in shoots is basipetal and is facilitated by the actions of specific influx and efflux carrier proteins located in the plasma membrane. The chemiosmotic hypothesis helps to explain polarized auxin transport. This model suggests that polar auxin flow is due to the asymmetrical distribution of influx and efflux carrier proteins (Estelle, 1998). The chemiosmotic model suggests that, in the shoot, influx carriers are located on the apical sides and that the efflux carriers are positioned to the basal sides of the cell; therefore, auxin can only be transported unidirectionally. In this model protonated IAA is cotransported into cells with a proton and loses its proton to become negatively charged. The anionic form of IAA can only be transported out of the cell through an efflux carrier. The *PIN1* gene encodes the transmembrane component of an auxin efflux carrier in shoot vascular tissue (Bennett et al., 1998; Galweiler et al., 1998, Blilou et al., 2005). Plants mutant for *PIN1* are defective in polar auxin transport resulting in a variety of defects including a lack of floral buds and an increase in marginal

venation in the leaves (Gälweiler et al., 1998, Mattsson et al., 1999). In shoots, PIN proteins are basally located in the cell corresponding with the direction of auxin flow (Friml, 2003), thus supporting the chemiosmotic hypothesis. To maintain their basal positioning, PIN proteins are proposed to continuously cycle between the plasma membrane and endosomes and may quickly respond to external cues (Geldner et al, 2003, Muday et al., 2003). Recycling of the PIN efflux carriers requires GNOM, an ADP ribosylation factor-GTP exchange factor (ARF-GEF) that regulates vesicle budding (Steinmann et al., 1999). Additionally PID, a protein kinase, is involved in ensuring the proper polarity of PIN (Friml et al., 2004). The exact involvement of PID is not known but it has been shown that high concentrations of PID lead to apical PIN localization and low levels of PID lead to basal localization of PIN (Friml et al., 2004).

Another class of proteins that are linked to auxin eflux belongs to the ATP-binding cassette (ABC) protein family (Luschnig, 2002). This large gene family is composed of several smaller clusters, of which cluster II are proposed to contain proteins that may be involved in auxin transport (Noh et al., 2001). Cluster II ABC proteins have several membrane-spanning domains and a cytosolic ATP-binding site. The multidrug resistance (MDR) and multidrug-related (MRPs) proteins belong to this group and have been shown to directly or indirectly remove substrates, such as organic anions, from the cytosol by hydrolyzing ATP (Noh et al., 2001). Plants mutant for AtMRP5 and AtMDR1 have defects similar to other auxin transport mutants such as decreased primary root elongation, early lateral root initiation and decreased apical dominance (Luschnig, 2002). It is suggested that these proteins may act independently or along with other transport proteins to transport auxin across the plasma membrane (Luschnig, 2002).

The importance of influx in polar transport has not been as well established as efflux but auxin influx carriers are proposed to catalyze the uptake of auxin from the extracellular space. The *AUX1* gene encodes a component of an influx carrier (Bennett at al., 1996, Marchant et al., 1998). *aux1* mutants have roots that are agravitropic, show decreased sensitivity to auxin and have defects in embryo patterning (Parry et al., 2001). Moreover, the agravitropic phenotype is rescued by exogenous application of 1-NAA, a highly permeable auxin that bypasses the influx carrier (Yamamoto and Yamamoto, 1998; Marchant et al., 1999). AUX1 is expressed in the shoot apical meristem; however, no shoot defects are apparent in *aux1* plants suggesting that different proteins may be involved in influx in the roots and shoots (Pickett et al., 1990; Marchant et al., 1999; Marchant et al., 2002). Influx is proposed to be important for directing the initial flux of auxin into leaf primordia as inhibiting influx with the chemical NOA, which sufficiently phenocopies *aux1* in roots, causes defects in the positioning of primordia but does not abolish organogenesis (Imhoff et al., 2000; Swarup et al., 2001). Plants mutant for AXR4, a proposed regulator of the influx carrier (Yamamoto and Yamamoto, 1999), are resistant to auxin, have agravitropic roots and the aerial portion of the plants is largely wild type (Hobbie and Estelle, 1995).

Other possible groups of genes controlling auxin influx in shoots are the LAX (Like AUX1) and ANT1 proteins. LAX proteins were identified based on their significant homology to AUX1 (Parry et al., 2001). ANT1 belongs to a small family of amino acid transporters that has been shown to transport IAA and 2,4-D (Chen et al., 2001). The role of these proteins in auxin influx has yet to be defined. More components

of auxin influx need to be identified to further characterize the role influx plays in developmental and regulatory processes.

Regulated auxin transport, both efflux and influx, is necessary to ensure that the proper cells receive auxin in order to respond and develop appropriately. Once inside the cell, auxin signals a cascade of events that eventually leads to the regulation of Aux/IAA gene expression. The signal cascade in response to auxin is proposed to initiate at the plasma membrane where IAA binds to ABP1 (auxin-binding protein 1), a specific receptor at the plasma membrane (Jones et al., 1998, reviewed in Napier, 1995). ABP1 primarily resides in the ER, but continuously cycles between the plasma membrane and the ER (Warwicker, 2001). It has been shown that binding of auxin to ABP1 can cause numerous changes at the cell membrane including modifications to ion channels or transporters (Napier et al., 2002).

Auxin is thought to modify the expression of auxin-inducible genes through a complex degradation pathway involving the SCF protein complex. SCF catalyzes the ubiquitination of specific proteins that targets them for degradation (Patton et al., 1998). The F-box subunit of SCF directly interacts with the targeted proteins allowing the Cullin and RBX1 subunits to catalyze the addition of ubiquitin, targeting the proteins for proteolysis by 26S proteosomes (Leyser, 2002). Support for the auxin-induced ubiquitination of target proteins is mounting as specific proteins involved in this system are identified (Leyser et al., 1993; Ruegger et al., 1998; del Prozo et al., 1998). Auxin's involvement in this pathway is not fully understood, though it is thought that auxin directly or indirectly increases the affinity of the F-box for the target proteins (Leyser,

2002). One model suggests that auxin initiates a phosphorylation cascade, the end product then mediating ubiquitination (Skowyra et al., 1997).

Aux/IAA proteins are some of the proteins targeted for degradation by SCF resulting in an endogenously short half-life (Leyser, 2002). Aux/IAA proteins also have a nuclear localization sequence allowing them to enter into the nucleus and modify gene expression by binding to auxin response factors (ARFs) (Leyser, 2002). In the absence of AUX/IAAs, ARF homodimers bind to auxin response elements (AREs) in auxin-regulated genes to up regulate gene expression (Ulmasov et al., 1997). A repeated sequence (TGTCTC-containing motif) has been shown to be sufficient to bind ARFs. An auxin-inducible reporter gene construct, DR5:GUS, was created by fusing tandem repeats of a modified ARE motif to the GUS reporter gene (Ulmasov et al., 1997). This construct enables the response to high levels of auxin to be easily assessed in plant tissues by providing the 5-bromo-4-chloro-3-indoyl glucuronide (x-gluc) substrate.

One well-characterized auxin response pathway in early embryonic development involves ARF5/MONOPTEROS (MP) (Hardtke and Berleth, 1998; Ulmasov et al, 1999), AUXIAA12/BODENLOS (BDL) (Hamann et al, 2002) and CUL1/AXR6 (Hellmann et al., 2003). *bdl*, *mp,* and *axr6* mutants are defective in apical-basal patterning in the embryo resulting in seedlings that lack basal structures (Berleth and Jurgens, 1993, Hardtke and Berleth, 1998; Hamman et al., 1999; Hobbie et al., 2000). Double mutant analyses have shown that all three are involved in the same pathway (Hellmann et al., 2003). The *mp* mutation is a loss of function allele consistent with the idea that MP cannot activate downstream genes in response to auxin. On the other hand, *bdl* is a gain of function mutation such that BDL, which normally binds to and represses ARFs, is not

degraded. Thus ARFs are continuously repressed causing the same negative effect on gene expression as the *mp* mutant (Hellmann et al., 2003). AXR6 is a component of the SCF complex and thus normally functions to degrade AUX/IAA proteins, such as BDL (Hellmann et al., 2003). *axr6* mutants are proposed to have an increased concentration of BDL causing the formation of BDL MP dimers and subsequent decreased gene expression in response to auxin (Hellmann et al., 2003). There are at least 24 AUX/IAA (Zrogg et al., 2001) and at least 10 ARF proteins (Ulmasov et al., 1999) that may interact in overlapping and distinct pathways to finely tune the cellular response to auxin.

The formation of files of vascular cells depends on both auxin transport and auxin response. The 'signal-flow canalization' hypothesis of auxin transport helps to explain vascular tissue development with respect to auxin transport and cellular response to auxin (Sachs, 1981, 1989, 1991). In this model, a small increase in the concentration of auxin in a cell ultimately causes more auxin to accumulate in that cell while draining neighboring cells of the hormone (Nelson and Dengler, 1997). The increased amount of auxin is proposed to cause the cell to become more efficient at transporting auxin as it elongates and situates auxin efflux carriers to the basal end of the cell. Furthermore, increased levels of auxin trigger the cells to differentiate into mature vascular tissue. Because of basipetal auxin transport, downstream cells accumulate auxin and the net effect is the formation of a canal of mature vascular tissue called a vein.

Mutants with defects in auxin transport or response may also have altered vasculature, consistent with the auxin canalization model. As well as being defective in polar auxin transport, *pin1* mutants have increased vasculature along the margin of leaves (Mattsson et al., 1999; Steinmann et al., 1999). *mp, bdl* and *axr6* are defective in auxin

response and show a reduction in cotyledon vasculature (Hardtke and Berleth, 1998; Hamman et al., 1999; Hobbie et al., 2000; Steynen and Schultz, 2003). AXR1 is involved in auxin response through an ubiquitin-degredation pathway (del Pozo and Estelle, 1999) and AXR2 is an auxin-inducible AUX/IAA protein (Nagpal et al., 2000). *axr1* and *axr2* mutants show a variety of auxin-related defects including a simplified vascular pattern (Steynen and Schultz, 2003). Furthermore, VASCULAR NETWORK (VAN) proteins are putative regulators of internal cell patterning and *van7* mutants, which are allelic to *gnom,* show disruptions in minor veins in leaves (Koizumi et al., 2000). *forked-1 (fkd-1)* mutants also show disrupted vascular patterning in leaves and the FKD-1 protein is proposed to respond to threshold levels of auxin required for distal vein meeting in leaves (Steynen and Schultz, 2003).

While the canalization model explains the differentiation of xylem and phloem from existing parenchyma cells it does not account for the existence of prepatterning of specific cells to become vasculature (Sachs 1990; Sachs 1991). Several vascular patterning mutants have been identified with unclear links to auxin canalization. The *cvp* (*cotyledon vascular pattern*) mutants show cotyledons with decreased vein meeting, however auxin synthesis, transport and perception appear normal (Carland et al, 1999). The altered venation pattern is due to a defect in the underlying prepatterning of cells to become vasculature that does not appear to depend on auxin canalization (Carland et al. 1999). CVP1 is a sterol methyltransferase and is important for signaling involved in cell differentiation and elongation along the cell axis (Carland et al., 2002). Sterol signaling has also been implicated for patterning processes beyond vasculature (Otsuga et al., 2001; McConnell et al., 2001). CVP2 is an inositol triphosphate signal that may regulate several

second messengers, including Ca^{2+}, important in a signal transduction pathway that leads to the specification of cells for a vascular cell fate (Carland and Nelson, 2004). The *scarface (scf)* mutant shows disrupted vascular patterning in leaves but shows normal differentiation resulting in a mutant phenotype that lacks vascular meeting (Deyholos et al., 2000). VEIN PATTERNING1 (VEP1) is a protein involved in apoptosis and *vep1* mutants show a reduction in vein meeting and a decrease in the total number of minor veins in leaves (Yang et al., 1997). The identification of such mutants suggests that the development of vascular patterns is a complex process involving several distinct and overlapping mechanisms in addition to auxin canalization.

A model is emerging to explain the role of auxin in the development of leaf venation patterns. Polar auxin transport creates sites of auxin maxima in the leaf where strong cellular auxin responses are evident (Aloni, 2003; Mattsson et al., 2003). Initially, an external source of auxin is transported into emerging leaf primordia from the stem vascular system toward the distal tip creating a strong distal auxin response that drives formation of the midvein (Aloni, 2003; Benkova et al., 2003; Reinhardt et al., 2003; Steynen and Schultz, 2003). Efflux carriers are localized and leaves with polar auxin transport inhibited by NPA or the *pin1* mutation show no distal auxin response or midvein differentiation (Mattsson et al., 1999; Sieburth, 1999). This result suggests that auxin efflux is required for midvein differentiation. Next, a secondary, internal source of auxin is positioned along the leaf margin, and internal transport accounts for the differentiation of secondary veins (Mattsson et al., 1999; Sieburth, 1999). In support of this idea, leaves treated with NPA show a ring of DR5::GUS expression along the leaf margin and differentiation of a thick band of vascular tissue follows (Mattsson et al.,

2003; Sieburth, 2003). Furthermore, there may be additional sources of auxin in the lamina of the leaf that have a role in the development of higher order veins (Aloni, 2003; Steynen and Schultz, 2003). Thus both polar auxin transport and auxin response are essential for vascular patterning formation in leaves.

To identify genes controlling the process of vascular development, mutants defective in vascular pattern formation have been isolated in the model plant, *Arabidopsis thaliana*. We have characterized a mutation in a gene named AUTOBAHN (ABN). The *abn* allele shows partial dominance with the heterozygotes showing an intermediate phenotype between that of wild type and *abn* homozygotes. *abn* plants produce leaves that proliferate disorganized, overlapping veins that are parallel to the midvein. Additionally the leaves show no differentiation of higher order veins. Our results suggest that *abn* is defective in carrier-mediated auxin uptake, a process required to establish the secondary source of auxin that allows for the differentiation of higher order veins.

Materials and Methods

Plant Materials

Glabrous (*gl1-1*) seed of Columbia ecotype (Col) used for EMS mutagenesis was obtained courtesy of George Haughn (Department of Botany, University of British Columbia, Vancouver, BC). *pin1-1*, mp^{G92}, mp^{BS1354} *and* mp^{G12} were generously provided by Thomas Berleth (University of Toronto, Toronto, ON) and *bdl* by Gerd Jurgens (University of Tubingen, Tubingen, Germany). DR5::GUS expressing seed was donated by Jane Murfett (University of Missouri, Columbia, MO). *fkd-1* was previously isolated from this laboratory (Steynen and Schultz, 2003). All other seed material was purchased from the Arabidopsis Biological Resource Center (Columbus, Ohio).

Chemicals

i) Hormones and Inhibitors

2,4-dichlorophenoxyacetic acid (2,4-D) and 1-naphthaleneacetic acid (NAA) were purchased from Sigma (St. Louis, MO); naphthylphthalamic acid (NPA) was purchased from Chem Service (West Chester, PA); 1-napthoxyacetic acid (NOA) was purchased from Lancaster Synthesis (Pelham, NH).

ii) AT medium (Estelle and Somerville, 1987)

$Ca(NO_3)_2$, $MgSO_4$, $MnCl_2$, NaCl and KNO_3 were obtained through BDH Inc. (Toronto, ON); KH_2PO_4, H_3BO_3, $CuSO_4$, $ZnSO_4$, Na_2MoO_4 and $CoCl_2$ were obtained from Sigma-Aldrich and FeEDTA was purchased from JT Baker (Phillipsburg, NJ). Agar was purchased from EM Science (Gibbstown, NJ).

iii) PCR and Gel Electrophoresis

KCl was from Fisher Scientific (Fair Lawn, NJ); ethidium bromide was purchased from Sigma; DNTP's and primers were synthesized by Invitrogen (Burlington, ON); Taq DNA Polymerase was purchased from Fischer Scientific (Ottawa, ON); agarose was purchased from EM Science; all other chemicals were purchased from BDH Inc..

iv) GUS Staining and Leaf Clearing (Kang and Dengler, 2002)

5-bromo-4-chloro-3-indoyl glucuronide (X-gluc) was purchased from Rose Scientific; $K_3Fe_3(CN)_6$ and dimethyl formamide were purchased from Sigma. $NaPO_4$ and EDTA were obtained from BDH Inc.; nonidet P40 was obtained from EM Science.

v) Solvents and Others

Dimethyl sulfoxide (DMSO) and ethyl methane sulfonate (EMS) were purchased from Sigma-Aldrich. Cytoseal was obtained though Stephen's Scientific (Kalamazoo, MI). All other chemicals and solvents were obtained from VWR.

Growth Conditions

Seed were either planted on Metromix 200 soil (W.R. Grace Co., Marysville, OK) in 100 cm^2 pots or on Petri plates containing Arabidopsis thaliana (AT) growth medium (Ruegger et. al., 1997). Pots were covered with plastic and both pots and plates were incubated at 4°C in the dark for 3 days, after which they were transferred to growth chambers (Percival Scientific, Perry, IA) with 24 hours of light at an intensity of 130 $\mu mol \bullet sec^{-1} \bullet m^{-2}$ from Sylvania Cool White, Grow Lux, and incandescent bulbs (Osram Sylvania Inc, Danvers, MA). Chambers were set at 20°C and 60% relative humidity. The

day of transfer to the growth chambers was considered to be the day of germination or 0 days after germination (DAG). Plastic wrap from the pots was removed 7 DAG.

Mutagenesis and Mutant Isolation

Approximately 2000 Columbia ecotype *gl1-1* seeds were treated with 0.25% v/v EMS for 16 hours then rinsed with distilled water and air dried on filter paper. The resultant M1 seeds were sown on soil at a density of 50 seeds per pot, grown to maturity and single plant M2 seeds were harvested for mutant screening. M2 seeds were sown on soil at a density of 25 seeds per pot. Cotyledons and first leaves were screened for aberrations in venation patterning at 14 DAG. Tissues were mounted in cytoseal, which provides partial clearing, and analyzed using a dissecting microscope. Putative vasculature mutants were grown to maturity and M3 seed was harvested and subsequently re-screened. The *abn* mutant was one of several identified from this initial screen. *abn* was back-crossed to Col three times before any analysis was performed.

Microscopy and Imaging

A Stemi 2000 dissecting light microscope was used for analysis of mature cotyledons, leaves and flowers (Carl Zeiss Inc., Thornwood, NY). Tissues were viewed using a CCD camera (RS-170, Cohu Inc., Electronics Division, San Diego, CA) that connected the microscope to a computer with NIH Image (http://rsb.info.nih.gov/nih-image/).

For cotyledon and leaf developmental analysis and the assessment of the effect of auxins and inhibitors on such development, an Eclipse E600 compound light microscope

was used (Nikon, Mississauga, ON). All photographs were taken with a Coolpix 990 digital camera (Nikon, Mississauga, ON) and images were adjusted using Adobe Photoshop 5.0 (Adobe Systems Inc., San Jose, CA).

Mapping

abn was crossed into the Landsberg (Ler) background and F2 seed was obtained for the mapping population. DNA was extracted from the leaves of plants showing the homozygous mutant phenotype according to Dellaporta et al. (1983). PCR-based mapping was performed using simple sequence length polymorphisms (SSLPs) between Col and Ler as described in Bell and Ecker (1994).

Phenotypic Analysis of Foliar Organs

To analyze and compare the cotyledons and leaves of all genotypes, seed were sown on soil at a density of 9 seed per pot. Cotyledons and first leaves were removed and mounted in cytoseal at 14 DAG and 21 DAG respectively. The shape and vascular pattern of tissues were scored using NIH Image. The shape was scored at the blade midpoint as a ratio of length to width. The vascular pattern was scored for the number of freely ending veins (FEV), branch points (BP), areoles, and vascular islands (VI). Additionally, the distance from the margin of the blade to the external-most vein was scored from both sides of the blade at the midpoint.

To assess floral morphology, whole flowers from *abn* homozygotes and Col flowers were removed and dissected when their petals had fully emerged. Dissections were performed under a dissecting light microscope and were scored for the number and

position of sepals, stigma, petals and stamens. In addition, the sepals and petals were cleared in 70% ethanol and the vascular pattern was scored using a compound light microscope.

Phenotypic Analysis of Whole Plant

To analyze whole plant morphology, F2 seed were sown on soil at a density of 9 seed per pot. Plants were scored for phyllotaxy, time of emergence of rosette leaves, time to flowering. Additionally the total number of rosette leaves, height of primary inflorescence, and number of main and secondary inflorescences were determined at 28 DAG. We also determined the rate of leaf intiation in wild type and an F2 population segregating for *abn*. The total number of rosette leaves was measured every 48 hours between 12 DAG and 21DAG and the rate was calculated as the number of leaves/day.

To assess root phenotype, *abn* F2, Col and *axr1-12* seed were planted on both AT plates and plates containing 1μM 2,4-D. Six seed were planted per plate and were grown vertically. Roots were scored for the length of the primary root at 7 DAG; the number of lateral roots (LRs), the distance from the root apical meristem (RAM) to the distal-most LR, and the length of the LRs were measured at 14 DAG. Additionally, root gravitropism was determined by rotating the plates 90° and measuring the ability to respond to gravity after 24 hours.

To assess stem vasculature, *abn* homozygote, heterozygote and Col wild type stems were sectioned by hand and stained with toluidine blue. Vascular pattern was viewed under a compound light microscope.

Generation of Double Mutants

Double mutants were generated between *abn* and the following mutants: *mp, axr6-2, bdl, pin1-1, axr2, axr1-12, axr4-2, fkd-1* and *aux1-7.* Double mutants were found in the F2 generations with the expected frequency (Table 1). Additionally, *mp* and *axr1-12* segregation data supports the molecular mapping of ABN to chromosome 1 (Table 1). For *bdl, axr2, axr1-12, axr4-2, fkd-1* and *aux1-7* double mutants, seed from the F2 plants that were heterozygous for *abn* but homozygous for the double mutant was harvested. Mature analysis on the cotyledons and leaves was done on the resultant F3 plants, with the exception of *axr1-12*and *axr2-1*, which were analyzed in an F2. For *mp, axr6* and *pin1-1*, the F2 seed was used for mature analysis as both mutants are infertile and a homozygous population was not obtainable.

Leaf Developmental Analysis on AT, NPA, NOA, 2,4-D and NAA

abn plants expressing the DR5:GUS fusion were created by crossing *abn* mutants with DR5:GUS plants (Ulmasov et al., 1997). F2 plants were screened for those showing root tip GUS expression and segregating for the *abn* mutation. These lines were pooled and used for all analysis. *abn* DR5:GUS and wild type DR5:GUS seeds were planted at a density of 50 seed per plate on unsuplemented AT plates and AT plates containing 30μM NPA, 30μM NOA, 1μM 2,4-D or 0.4 μM NAA. 100 *abn* DR5:GUS F2 seedlings and 25 DR5:GUS seedlings were GUS-stained and cleared as described by Steynen and Schultz (2003) for each day of analysis. Seedlings were dissected by hand under a dissecting microscope and were mounted on slides with 50% glycerol. Analysis was done using a compound light microscope.

Results

Mutant Isolation and Mapping

A population of Columbia ecotype (Col-0) Arabidopsis seed was mutagenized with EMS and the resultant M1 generation was single plant harvested. M2 families were screened for putative leaf vascular patterning mutants. We identified from this initial screen a mutant that proliferates disorganized, overlapping veins that develop parallel to the midvein in both the cotyledons and leaves. The resulting vascular pattern looks like a multi-lane highway of veins, therefore, we named the mutant *autobahn (abn). abn* plants produce narrow, irregularly shaped leaves and are male sterile. The remaining plant morphology appears normal.

After back-crossing *abn* to wild-type, the F1 has a vascular pattern phenotype intermediate between the *abn* homozygote and wild type in both the cotyledons and leaves. The F2 population segregates in accordance with Mendelian ratios for a single, nuclear, semi-dominant mutation (1:2:1, $x^2 = 0.613$, df = 2, n=1043).

In order to map the ABN gene, *abn* was crossed to Landsberg erecta (Ler) and the segregating F2 population was used for molecular mapping (Bell and Ecker, 1994). The ABN gene mapped to Chromosome I to a position of 24 cM using the simple sequence length polymorphism markers nga248 (1-40) (R.F.=15.8%, n=48 chromosomes) and nga63 (1-11) (R.F.=13.6%, n=82 chromosomes).

First Leaf Phenotype and Vascular Development

In order to characterize the *abn* leaf phenotype, the mature vascular pattern of *abn* homozygotes, *abn* heterozygotes and wild type leaves was quantified and compared (Table 2). We scored the complexity and openness of the vascular pattern by determining the number of freely ending veins (FEV), branch points (BP), areoles (an area completely enclosed by veins) and vascular islands (VIs) (Table 2). The placement of the vascular pattern was assessed by determining the margin size, providing a measure of whether the veins are centralized or expand towards to the margin. The margin size was scored by measuring, at the midpoint of the blade, the distance from the margin to the outer-most vein on each half of the leaf and then averaging the distances and dividing by the total leaf width. Thus, a larger margin represents a more centralized venation pattern. Finally, the shape of the leaves was determined as the ratio of the length to the width at the blade midpoint.

Wild type leaves have a single midvein, several secondary loops that most often meet proximally, and higher order veins that either end freely in the leaf lamina or connect with veins other than the midvein to form small, closed areoles (Figure 1a). The *abn* heterozygous venation pattern is similar to wild type in that it consists of a single midvein, several secondary branches that form areoles, and higher order veins that branch into the lamina. A distinction from wild type is seen at the distal tip of the midvein, where the initial secondary veins often branch slightly proximal to the distal tip of the midvein and several small veins form at this site (Figure 1b). Whereas in wild type the distal junction between the first secondaries is relatively smooth, the additional veins in *abn* heterozygote leaves results in a much more complex, disorganized junction.

Additionally, the secondary branches are not as regularly spaced as in wild type and the vasculature is significantly more centralized than in wild type (Table 2). Furthermore the leaf shape of *abn* heterozygotes is more elongate than wild type (Table 2). The venation pattern of *abn* homozygotes (Figure 1c) is much more centralized and has reduced complexity compared to both wild type and *abn* heterozygotes (Table 2). Branches from the midvein are more randomly spaced and develop at irregular angles compared to wild type (Figure 1c). Furthermore, the size and shape of aeroles are irregular in *abn* homozygotes and *abn* leaf shape is significantly more elongate compared to wild type and heterozygous leaves (Figure 1c, Table 2).

To study the development of the vascular pattern, we assessed developing first leaves for the appearance of xylem cell wall thickening, which we considered equivalent to the differentiation of veins. In wild type, the differentiation of the midvein, which connects to the stem vasculature and extends to the distal tip of the leaf, is complete at 6 DAG. Two distal secondary veins branch from the distal tip of the midvein and differentiate in opposite directions along the margin. They loop back into the lamina in a basipetal direction and reconnect to the midvein at a more proximal location by 7 DAG. Additional secondary veins branch from existing secondaries and are regularly spaced. They develop in the same direction as previous secondaries and connect to the midvein proximally. Tertiary veins branch from the secondaries and quaternary branch from tertiaries. The later secondary veins develop simultaneously with higher order veins to create the mature reticulate vascular pattern. The development of the *abn* heterozygous leaf vascular pattern is a very similar to wild type with the midvein differentiating at 6 DAG and secondary branches extending from it and differentiating basipetally. The

midvein of *abn* homozygous leaves also differentiates first and is complete at 6 DAG, although it terminates farther from the distal tip than in wild type. There are no clear secondary branches that form at the distal tip of the midvein; rather, subsequent veins initiate at proximal points along the midvein and differentiate apically. These veins have a similar appearance and form very close to the midvein producing a mature phenotype that appears to be the result of a proliferation of midveins without the development of regularly patterned secondary veins.

Characteristics of the *abn* first leaf vein and midrib thickness support our hypothesis that *abn* leaves proliferate midveins at the expense of higher order veins. The midvein is the thickest vein in leaves with higher order vein thickness decreasing hierarchically (Nelson and Dengler, 1997; Dengler and Kang, 2001). The mid rib develops along with the midvein: leaves with midveins occupying more cells develop mid ribs that are correspondingly more pronounced (Nelson and Dengler, 1997). In *abn* leaves, all veins are of similar thickness to the wild type midvein. As well, the mid rib in *abn* leaves is more pronounced than in wild type.

Cotyledon Phenotype

Cotyledons have a much simpler venation pattern than leaves and thus cotyledons are useful for assessing basic patterning defects. We quantified the mature venation pattern of *abn* homozygotes, *abn* heterozygotes and wild type cotyledons by the same criteria as leaves (Table 3). Wild type cotyledons have a single midvein and most often 4 secondary veins that loop to form 4 areoles (Figure 2a). However there are occasionally

fewer areoles (average = 3.4) due to a smaller number of secondary veins or secondary veins that do not meet the midvein proximally.

Like wild type, *abn* heterozygote cotyledons always have a single midvein and most often four secondary veins that form closed areoles (Figure 2b). In contrast to wild type cotyledons, but like *abn* heterozygous leaves, the heterozygous cotyledons have additional veins that often extend from the distal tip of the midvein and either end freely or close to form small areoles. Thus *abn* heterozygotes have a more complex vascular pattern than wild type (Table 3). The placement of veins and the cotyledon shape are not significantly different to wild type (Table 3).

Like *abn* homozygous leaves, *abn* homozygote cotyledons have a disorganized vein pattern that consists of a midvein from which additional veins extend distally from the midvein at irregular positions (Figure 2c). The venation of *abn* homozygotes is significantly more complex and is more centralized than either heterozygote and wild type cotyledons (Table 3). Additionally, *abn* homozygote cotyledons are significantly more elongate than either wild type or heterozygote cotyledons (Table 3). Like the leaf phenotype, we believe the mature cotyledon phenotype is the result of midvein proliferation; however, we were unable to assess the development of the venation pattern in *abn* cotyledons; the sterility of *abn* homozygotes requires that a segregating population be used for all analyses. Within this population, the genotype of individual plants is certain only after the mature vascular pattern has been established in the cotyledons.

Auxin Response in *abn* Leaves

DR5:GUS Expression Pattern

Auxin plays a critical role in the development of leaf vascular patterns. Current models suggest that there are predominantly two distinct sources of auxin involved in leaf vascular development. The external, primary auxin source is transported into the leaf and is required for midvein development (Benkova et al., 2003; Reinhardt et al., 2003). The internal, secondary auxin source along the margin is transported into the interior of the leaf and may account for the development of secondary veins (Mattsson et al., 1999; Sieburth, 1999). The mature vascular pattern of *abn* leaves appears to result from a proliferation of midveins with no higher order vein differentiation, which may result from a defective secondary auxin source. Two models are consistent with such a defect: 1) *abn* leaves have aberrant cellular responses to auxin required for higher order vein differentiation or 2) *abn* leaves are defective in auxin transport required for higher order veins.

To test if *abn* leaves show altered auxin response, *abn* was introduced into the DR5:GUS background to assess auxin response in the leaves. This line, segregating for *abn* and homozygous for the DR5:GUS construct, was grown on AT plates and seedlings were scored at 24-hour intervals. We compared the intensity and pattern of DR5:GUS expression in *abn* leaves to that in wild type (Table 4). We found no change in the intensity of DR5:GUS expression in *abn* but the pattern of expression was altered.

In wild type first leaves, DR5:GUS expression is first evident in a single cell at the distal tip at 4 DAG before any vascular lignification has occurred (90.2%, n=122,

Table 4) (Figure 3a). At 5 DAG, expression remains at the distal tip but is also evident along the marginal zone predicting the position of secondary veins (14.8%, n=121) (Table 4, Figure 3b). As well, DR5:GUS expression is first observed in the lamina at 5 DAG in areas that seem to predict higher order vein formation (14%, n=121, Table 4). This lamina expression is most strongly observed at 6 DAG (39.5%, n=43) (Table 4, Figure 3c). Hydathode DR5:GUS expression is also first observed at 5 DAG, most often in 2 hydathodes (90.3%, n=31, Table 4). Hydathode expression continues through remaining leaf development (Figure 3c,d, Table 4).

Like wild type, *abn* heterozygous first leaves initially express DR5:GUS at the distal tip at 4 DAG (43.6%, n=110, Table 4), but expression is most prominent at 5 DAG (74.4%, n = 86) (Table 4, Figure 3e). The secondary marginal expression is never observed and tertiary expression is much less common than in wild type at 6 DAG (2.4%, n=82) (Table 4, Figure 3f). Furthermore, as in wild type expression in the hydathodes is evident at 5 DAG but is most often seen in only one hydathode (75%, n=4) (Table 4, Figure 3f,g).

Many *abn* homozygous leaf primordia did not expand or show any DR5:GUS expression at 10 DAG (44.3%, n=20, Table 4), which is significantly more than seen in *abn* heterozygotes (28%, n=93, Table 4) or wild type (13.3%, n=60, Table 4). A smaller proportion of *abn* homozygous first leaves express DR5:GUS in the distal tip compared to wild type (22.2%, n=27 at 4 DAG and 30.5% at 6 DAG) (Table 4, Figure 3i). *abn* homozygotes, like heterozygotes, do not express DR5:GUS along the secondary margin; however a thick band of cells just internal to the margin shows expression at 5 DAG (80%, n=30) (Table 4, Figure 3j,k). While this pattern is similar in timing and superficial

appearance to the secondary marginal expression in wild type leaves, we feel it is distinct since the expression is more central and the number of expressing cells staining is increased. As well, expression in this thick band never occurs simultaneously with expression at the distal tip (Table 4). Finally, *abn* homozygous leaves completely lack tertiary and hydathode staining (Table 4, Figure 3l).

In *abn* leaves, the initial auxin response at the distal tip occurs in fewer leaves, but when it does occur, expression is as in wild type. In contrast, subsequent auxin response in *abn* is altered. This suggests that the initial, distal auxin maximum required for the midvein development can form normally, but the internal, marginal auxin is altered. The altered response to the internal, marginal auxin may be due to a change in the source of auxin itself, altered auxin transport from that source, or a change in the cellular response to auxin.

Sepal and Petal Venation Pattern

All floral organs are thought to be derived from leaves. Therefore, we predicted that the venation pattern of other foliar organs in *abn* plants may show defects similar to those observed in leaves. The venation pattern of the sepals and petals in *abn* homozygous and wild type plants was examined and compared. The pattern of wild type sepals usually consists of 3 main veins (avg=3.4, n=43) that most often interconnect to form two closed loops (avg=2.05, n=43). While *abn* sepals have more major veins (avg=8.7, n=99) than wild type, they nevertheless form fewer closed loops (avg=1.72, n=99). The venation pattern of wild type petals always consist of a single main vein with several secondary branches (avg=4.3, n=40). *abn* petals have many more veins than wild

type petals (avg=7.4, n = 31). Thus, like *abn* leaves and cotyledons, *abn* perianth organs seem to proliferate major veins.

Plant Morphology

If an altered auxin response pattern exists in other parts of *abn* plants, we may see phenotypic changes. Additionally, vascular systems have a critical role for ensuring nutrients and water are appropriately transported throughout the plant; thus, the altered venation pattern in *abn* plants may have pleiotropic effects elsewhere in the plant. To assess if the *abn* mutation affects other areas of the plant, we examined *abn* flower, shoot, stem and root morphologies and compared them to wild type.

In addition to the vascular pattern of floral organs, we compared the structure of *abn* and wild type flowers to assess if *abn* shows aberrations in the positioning or number of pistils, stamen, sepals or petals. Wild type flowers consist of 4 concentric organ whorls in which organs are symmetrically arranged around a central pistil. We always observed 6 stamen, 4 petals and 4 sepals in wild type flowers (n=10). In contrast, *abn* homozygous flowers lack symmetrical organ arrangement and show altered numbers of organs as well as organ fusion. *abn* flowers (n=30) consist of a pistil surrounded by fewer stamen (avg=4.6) and petals (avg=2.2) but the same average number of sepals (avg=4.0) as observed in wild type. The morphology of *abn* floral organs is often aberrant; stamens may fuse in pairs (10%) or triplets (6.7%); petals are sometimes tubular (15.6%), folded at their distal tip (26.6%) or fused in pairs (1.6%); sepals also fuse in pairs (20%).

The aerial morphology of *abn* homozygote, *abn* heterozygote and wild type plants was compared by scoring the number of rosette leaves, number of secondary

inflorescences and the height of the plants at 28 DAG (Table 5). Additionally the time of bolting (2 cm inflorescence), flowering, and maturity (1 cm internode between first silique-bearing nodes) was compared between the genotypes (Table 5). Phylotaxy was also measured and no observable difference was discernable between the genotypes.

abn heterozygous plants bolt, produce flowers and mature several days earlier than wild type plants (Table 5). Additionally, *abn* heterozygotes produce fewer rosette leaves, secondary inflorescences and are significantly shorter than wild type plants at maturity (Table 5). Correspondingly, *abn* homozygotes produce bolts, flowers and reach maturation significantly earlier than both *abn* heterozygote and wild type plants (Table 5). Furthermore, *abn* homozygote plants produce significantly fewer rosette leaves, secondary inflorescences and are shorter than both heterozygous and wild type plants at maturity (Table 5). The rate of leaf initiation was determined in an F2 population segregating for *abn*. Within the entire population, the rate of initiation was significantly slower compared to a wild type population (data not shown), suggesting that the *abn* plants have a slower rate of leaf initiation than wild type.

abn homozygous, heterozygous and wild type stems were cross- sectioned and the vascular patterns were compared. There were no visible differences among the genotypes.

Auxin has well quantified effects on roots including response to gravity stimulus, lateral root initiation and elongation of the primary root. To assess auxin-related defects in root phenotype, *abn* homozygote, *abn* heterozygote, wild type and *axr1-12* plants were grown vertically on both unsuplemented AT plates and AT plates containing 1 μM 2,4-D. *axr1-12* plants served as a control group for the effects of 2,4-D.

Roots were scored for the number of lateral roots (LRs), the distance from the root apical meristem (RAM) to the distal-most LR, the length of the LRs, and the density of LRs (length of primary root / number of LRs) (Table 6). Additionally, gravitropism was assessed. For all properties scored, there was no significant difference between *abn* homozygote, heterozygote and wild type roots (Student's t-test, Table 6), while *axr1-12* roots were significantly different from all other genotypes (Student's t-test, data not shown).

Effects of Auxin Response Mutants on the *abn* Phenotype

axr1-12, axr2-1, fkd-1

Plants mutant for *AXR1* and *AXR2* have a decreased sensitivity to auxin (Lincoln et al., 1990; Timpte et al., 1994) and share similar phenotypes including decreased gravitropism, slowed growth of inflorescences, curled rosette leaves due to aberrant marginal leaf cell expansion, and simplified vascular patterns (Hobbie and Estelle, 1995; Steynen and Schultz, 2003). Plants mutant for *FKD1* show leaf specific defects including decreased distal vein meeting and *fkd-1* leaves show a more open vein pattern (Steynen and Schultz, 2003). We assessed *axr1-12, axr2-1* and *fkd-1* in combination with *abn* to provide some insight into the auxin defects in *abn* plants. If *abn* is defective in auxin response, we predict genetic intereactions to occur in the double mutants.

Both *axr1-12* and *axr2-1* have a more open venation pattern (Steynen and Schultz, 2003) and *axr1-12* leaf pattern is also simpler (Tables 2 and 3) (Figures 1d,g and 2d,g). *fkd1* cotyledons (Figure 2j) and leaves (Figure 2d) have significantly more FEV

and consequentially a reduction in the number of areoles and branch points (BPs) (Tables 2 and 3). *fkd1* leaves additionally show a marked increase in the number of vascular islands (VIs) (Table 2). As well, *axr1-12* and *axr2-1* cotyledons and leaves are rounder than wild type (Tables 2 and 3).

axr1-12, *axr2-1* and *fkd-1* in combination with both heterozygous and homozygous *abn* show essentially additive phenotypes. The *axr* double mutant cotyledons (Figure 2e,f,h,i) and leaves (Figure 1e,f,h,i) show a shape intermediate between the single mutants and centralized veins like *abn* single mutants (Tables 2 and 3). Like the *axr* single mutants, the double mutant cotyledons have a more open pattern (Table 3). The *fkd-1* double mutant cotyledons (Figure 2k,l) have an intermediate phenotype with a significant reduction in the number of areoles compared to *abn* single mutants (Table 3). The double mutant leaves (Figure 1k,l) show an intermediate venation pattern with an increase in FEVs like *fkd-1* and a similar number of areoles compared to *abn* (Table 2). The veins of the cotyledons are centralized like *abn* single mutants but are positioned intermediately in the leaves (Tables 2 and 3). These additive phenotypes suggest that ABN functions independently of these genes

mp, bdl and *axr6* Double Mutants

One explanation for the altered auxin response pattern observed in *abn* leaves is that *abn* is defective in a molecular auxin response pathway. MP, AXR6 and BDL act in auxin-response pathways and double mutants between *mp, axr6-2*and *bdl* with *abn* were generated to determine if ABN functions in the same pathway. *mp* and *axr6* mutants lack hypocotyls and roots, have incomplete vasculature in the cotyledons and produce few

leaves (Berleth and Jurgens, 1993; Przemeck et al., 1996; Hobbie et al., 2000), whereas *bdl* mutants have a weaker phenotype with normal shoots with fertile flowers (Hamman et al., 1999).

We observed that *mp* and *axr6-2* seedlings most often produce two cotyledons (70.2%, n=121; 80%, n=45) with severely reduced vasculature (Figure 2ab,y). Most *mp* cotyledons only developed a midvein (43.7%, n=206) and less frequently a midvein and one (25.2%, n=206) or two (14.1%, n=206) incomplete secondary veins that do not reconnect to the midvein to produce closed loops. Occasionally a small loop of vasculature was formed above the distal tip of the midvein (17.0%, n=206) that often had multiple small secondaries extending from it (10.2%, n=206). Most *axr6-2* cotyledons have a midvein and one (15.1%, n=53) or two secondaries (83%, n=53) that do not meet with the midvein proximally. Often there were vascular islands along the region where the secondary loops would usually form (45.3%, n=53) and very rarely the pattern consisted of only a midvein (1.9%, n=53). *bdl* seedlings produce normal shoots with fully developed cotyledons (Figure 2m) and leaves (Figure 1m). In our analysis, *bdl* cotyledons were more round than wild type with otherwise normal vascular pattern (Table 3) and leaves were more round and show a more complex vascular pattern than wild type (Table 2).

mp abn , *axr6-2 abn*, and *bdl abn* double mutants show additive phenotypes suggesting that ABN functions independently from this auxin response pathway. *axr6-2 abn* double mutants (Figure 2aa) make up 21.3 % of the population that is homozygous for *axr6-2* (n=94); like *axr6-2* single mutants they lack roots and a hypocotyl but the cotyledon venation pattern is like *abn* single mutants. While we expect half of the

remaining *axr6-2* seedlings to be heterozygous for *abn* (based on a 1:2:1 *abn* ratio), only 28.4% (n=74) have cotyledons with characteristics similar to *abn* heterozygotes (Figure 2z) indicating that a single copy of the mutant *ABN* gene is often not distinguishable in an *axr6* background. In the *axr6-2 abn* heterozygous cotyledons that had a visible phenotype, the venation pattern consists of a midvein with many small vascular strands at the distal tip and a reduction in the remaining vasculature. There is most often only one (14.3%) or two (33.3%) secondary veins formed that are freely ending proximally and vascular islands are infrequently observed (4.8%). Occasionally the secondary veins do meet distally to the midvein to form a closed loop (33.3%), which is never observed in *axr6* single mutant cotyledons.

The *mp abn* double mutant phenotype appears to be additive as it has characteristics of both single mutants (Figure 2ac): like *mp* single mutants, the seedling lacked a hypocotyl and roots and the venation pattern was like *abn* single mutants. Due to the small number of *mp abn* double mutants, no statistical analysis of the phenotype was possible. As in *axr6-2* seedlings, within the *mp* homozygous seedlings, plants with a single copy of the *abn* mutation were not distinguishable.

The *bdl abn* double mutant phenotype appears to be additive. The cotyledons (Figure 2n,o) have an intermediate venation pattern complexity that is centralized like *abn* single mutants (Table 3), and the leaves, on the other hand, show a venation pattern like *abn* single mutant that is intermediately centralized (Table 2). The cotyledons and leaves have an intermediate shape between the single mutants (Tables 2 and 3).

The additive phenotypes of these double mutants indicate that the aberrant auxin response pattern in *abn* leaves is not due to a defect in the molecular response to auxin.

Another explanation for the altered auxin response pattern in *abn* leaves is that auxin transport is altered. To examine auxin transport, we grew *abn* plants on different sources of exogenous auxin, transport inhibitors and generated double mutants with mutants defective in different aspects of auxin transport.

Effects of Polar Auxin Transport on *abn* Leaf Vascular Patterning

Efflux: NPA and *pin1-1*

pin1-1 mutants are defective in polar auxin transport and sometimes produce leaves with increased marginal venation (Galweiler et al., 1998; Mattson et al., 1999). *pin1-1* cotyledons (Figure 2p) and leaves (Figure 1p) are wider than wild type though the vein pattern does not differ greatly from wild type (Tables 2 and 3). The phenotype of *abn* leaves seems to be enhanced in the *pin1-1* background (Table 2). The *pin1-1 abn* double mutant cotyledons (Figure 2q,r) show an intermediate shape and the venation pattern does not differ significantly from *abn* single mutants (Table 3). The leaves of the double mutants, however, are highly elongated (Figure 1q,r) and the venation pattern is significantly more complex than either single mutant (Table 2). One explanation for the enhancement of the *abn* phenotype in the presence of the *pin1-1* mutation is that some aspect of transport is defective in *abn* and decreasing auxin efflux exacerbates the defect.

The effects of the *pin1-1* mutant can be phenocopied by growing seedlings on the auxin efflux inhibitor NPA which binds to and disrupts the ability of PIN1 to export auxin from cells (Lomax et al., 1995). High concentrations of NPA results in a proliferation of vascular tissue along the leaf margin without the development of a

midvein. Afterward, vascular strands emerge from the marginal zone and develop basipetally to create parallel veins that exit the leaf at the petiole. This observation has led to the hypothesis that the leaf margin is a source of auxin and for normal vascular differentiation in discrete cell files requires auxin efflux to transport auxin away from this source (Mattsson et al., 1999; Sieburth, 1999).

Wild type and *abn* plants expressing DR5:GUS were grown on 30μM NPA to assess the molecular auxin response and vascular development in leaves under the inhibitory effects of NPA. Like untreated leaves, NPA treated wild type leaves initially show an auxin response at the distal tip; however, it is not confined to a single cell but rather is diffuse across several cells (Figure 4a). This response spreads along the margin (Figure 4b). No acropetal midvein differentiation occurs. Later DR5:GUS expression is observed along two loops, one at the margin and one slightly interior to the margin (Figure 4c). Vascular tissue later differentiates basipetally from the interior loop toward the center of the leaf and parallel veins exit the leaf at the petiole. Late DR5:GUS expression is evident throughout the interior of the leaf blade concurrently with the marginal loops (Figure 4d). Unlike untreated wild type leaves, this internal expression pattern in NPA treated leaves does not appear to predict future vascular differentiation. Furthermore, no hydathode expression is evident.

abn heterozygotes show an initial response at the distal tip like wild type leaves (Figure 4e). The auxin response spreads along the margin but is discontinuous (Figure 4f). Like wild type, *abn* heterozygotes show a double loop of expression and vascular tissue forms along the interior loop but the loops are less uniform (Figure 4g). In contrast to wild type, a midvein differentiates acropetally along with the development of veins

from the marginal ring of vasculature. There is very little expression of DR5:GUS evident in the interior of the leaf and none in the hydathodes (Figure 4h).

abn homozygotes treated with NPA most often produce a large number of small leaf primordia (88.2% n =68, Table 4) that never develop into distinct leaves. In contrast, only 58.2% (n=153) of *abn* heterozygotes and a very small number of wild type seedlings (7.7% n=117) proliferate leaf primordia with no subsequent leaf development when treated with NPA (Table 4). Interestingly, this response is reminiscent of the effects of treating NPA induced pins with NOA, an influx inhibitor (Stieger et al., 2002). Later in development some of these primordia develop into leaves that are often tubular with an initial auxin response at the distal tip that is restricted to the distal-most ring of tissue (Figure 4j,k). This expression, in contrast to wild type and *abn* heterozygotes, does not predict vascular development. *abn* homozygote leaves maintain a similar, though more extreme, vascular pattern as untreated seedlings and show a proliferation of midveins. There is never any late DR5:GUS expression predicting higher order veins observed in the interior of the leaf nor in the hydathodes (Table 4, Figure 4l).

Influx: NOA, *aux1-7* and *axr4*

The increased severity of the *abn* phenotype in the presence of NPA or *pin1* suggests that *abn* may be defective in polar auxin transport. Moreover, like NPA-induced pins treated with NOA, *abn* seedlings treated with NPA proliferate undeveloped primordia. This suggests that like NOA, *abn* may inhibit active auxin influx. To test this, we treated *abn* homozygotes, *abn* heterozygotes and wild type seedlings with NOA and additionally generated double mutants of *abn* with *aux1-7* and *axr4-2*.

The molecular function of AXR4 is still unknown though it is proposed to be involved in the regulation of auxin influx (Hobbie and Estelle, 1995). *axr4* plants show global auxin-related defects including a decreased sensitivity to auxin and defects in root gravitropism. They have curled rosette leaves but do not show a vascular pattern defect in the cotyledons and leaves (Hobbie and Estelle, 1995). We found that *axr4-2* cotyledons (Figure 2s) are rounder than wild type though the vascular pattern is indistinguishable (Table 3). *axr4-2* mutants do not show any leaf abnormalities (Figure 1s) (Table 2). *abn* was observed to be epistatic to *axr4-2:* leaves that show the *abn* vascular phenotype do not curl downward like *axr4-2* mutant and are thus indistinguishable from the *abn* single mutants (Figures 1t,u and 2t,u). This suggests that the gene product of *ABN* acts upstream of AXR4 and may be involved with auxin influx in leaves.

To further examine the role of influx in *abn* plants, we generated double mutants with *aux1-7*. AUX1 encodes a protein that facilitates auxin uptake into cells (Marchant et al., 2002). AUX1 regulates the transport of auxin from its source in young leaf primordia toward its sink in root tissues (Marchant et al., 2002). *aux1-7* mutants are defective in AUX1-mediated auxin influx and show defects specific to roots including a reduced number of lateral roots and altered gravitropism (Parry et al., 2001). We found that *aux1* cotyledons (Figure 2v) do not differ significantly from wild type except that they are rounder (Table 3), while the leaves (Figure 1v) are the same shape but have a vascular pattern that is slightly more complex than wild type (Table 2). ABN and AUX1 appear to be functionally independent as the phenotype of the double mutants appears to be additive. The double mutant cotyledons (Figure 2w,x) have an intermediate shape and venation pattern complexity (Table 3). The double mutant leaves (Figure 1w,x) have the

same shape as *abn* single mutants with a venation pattern that shows an intermediate complexity between the two single mutants (Table 3). If ABN is involved directly with auxin influx, these results suggest that there may be a different mechanism for influx in the roots and shoots with AUX1 functioning in the roots and perhaps ABN in the shoots.

NOA, an auxin influx inhibitor, has been shown to phenocopy *aux1* mutants (Parry et al., 2001) and to affect leaf primordial initiation (Stieger et al., 2002). If *abn* is defective in auxin influx, treating wild type with NOA may phenocopy the *abn* leaf phenotype. *abn* and wild type plants expressing DR5:GUS were grown on 30 μM NOA to assess both the molecular auxin response and vascular development in leaves under the inhibitory effects of NOA. Like many *abn* homozygous leaves, NOA treated wild type leaves initially do not show a discrete auxin response at the distal tip but rather show a strong response in a crescent shape along a sizeable region of the distal tip and margin (Table 4, Figure 5a). Later expression is more confined to a lateral region along the distal margin (Figure 5b) with vascular differentiation initiating at the zone of expression and extending proximally (Figure 5b,c). Veins develop parallel to one another and meet distally though no distinct midvein is evident. The final vascular pattern appears similar to untreated *abn* heterozygotes (Figure 5d).

NOA treated *abn* heterozygotes have a similar initial auxin response as NOA treated wild type leaves (Table 4, Figure 5e). Also like wild type, later expression in *abn* heterozygotes is confined to the distal marginal zone and vascular differentiation initiates at the sites of DR5:GUS expression (Figure 5f-h). Unlike wild type leaves, *abn* heterozygous leaves acropetally develop a distinctive midvein (Figure 5g). The final

vascular pattern consists of an abundance of parallel veins with little distal meeting and closely resembles the vascular pattern of untreated *abn* homozygotes (Figure 5h).

abn homozygotes grown on NOA do not show a strong initial auxin response (Table 4, Figure 5i). Later DR5:GUS expression occurs along the periphery of the midvein, interior to the margin (Figure 5j,k). Vascular differentiation in *abn* does not appear to be affected by NOA treatment (Figure 5i-l). NOA treatment appears to phenocopy the *abn* mutation supporting the hypothesis that ABN is involved in auxin influx.

The effects of exogenous auxins on the *abn* phenotype: 2,4 D and NAA

The result that NOA partially phenocopies *abn* in wild type leaves but does not affect the *abn* homozygous phenotype supports the idea that *abn* is defective in auxin influx. If this is true, one would expect a synthetic auxin, such as 2,4-D, that relies on auxin influx to enter cells, to have no effect on the *abn* phenotype.

Wild type leaves treated with 1 μM 2,4-D often do not express DR5:GUS at the distal tip (Table 4). When they do, expression is evident in several cells simultaneously (Table 4, Figure 6a). Strong expression occurs next in a crescent shape that may cover more than half of the developing leaf primordium (Figure 6b). Late expression is constrained to the marginal tip as in untreated leaves (figure 6c,d). Tertiary and hydathode DR5:GUS expression are absent. Vascular differentiation is relatively unchanged however the distal vasculature recedes slightly from the distal tip causing a flattened apical ridge of vasculature (Figure 6d).

abn heterozygotes grown on 2,4-D show similar DR5:GUS expression as wild type at all stages though the strength of the auxin response is somewhat reduced (Table 4, Figure 6e-h). Like wild type leaves treated with 2,4-D, the vasculature in *abn* heterozygote leaves treated with 2,4-D appears unchanged except for a reduction in a prominent distal tip of vasculature to a more flattened apical ridge (Figure 6h). *abn* homozygotes grown on 2,4-D do not appear to have an altered auxin response compared to untreated *abn* leaves and the vascular development also appears unchanged (Figure 6i-l). That 2,4-D does not affect the *abn* phenotype supports the notion that the auxin response changes in *abn* leaves are due to defective carrier-mediated auxin influx.

To further assess if *abn* is defective in carrier-mediated influx or auxin uptake in general, we can expose *abn* plants to 1-NAA. This auxin is able to easily enter cells by diffusion, thus bypassing the influx carrier (Delbarre et al., 1996). If the *abn* defects are the result of a lack of auxin entering the cell, NAA should rescue the *abn* phenotype; however, if the *abn* defects are due to processes that require active auxin influx, NAA should not rescue the phenotype. 1-NAA has been shown to rescue the agravitropic roots of *aux1* plants (Yamamoto and Yamamoto, 1998; Marchant et al., 1999); however, 1-NAA is not able to rescue influx related defects in the shoot as primordial placement defects in plants inhibited with NOA were not rescued with NAA treatment (Stieger et al., 2002).

To assess if auxin response and vascular differentiation in the leaves is affected by 1-NAA, wild type and *abn* plants expressing DR5:GUS were grown on AT plates supplemented with 0.4 μM 1-NAA. For all genotypes, treatment with 1-NAA caused an increase in the number of seedlings whose primordia did not expand or express

DR5:GUS (Table 4). For those primordia that did expand, no change in auxin response or vascular development was noted for any genotype (Figure 7). The lack of phenotypic change in developing primordial supports that *abn* is defective in carrier-mediated auxin influx. Auxin enters *abn* leaves by diffusion thus the availability of a diffusible auxin, 1-NAA, does not change the phenotype. The increase in undeveloped primordia may be the result of increasing the amount of auxin entering the leaf via unregulated diffusion.

Discussion

We have identified a new vascular pattern mutant in *Arabidopsis thaliana* named *autobahn (abn)*. *abn* produces elongated leaves that proliferate disorganized, overlapping veins parallel to the midvein without higher order vein differentiation. *abn* flowers are male sterile and perianth organs have similar vein patterning defects as the leaves. Stems do not show vascular defects and roots have normal auxin responses, thus ABN seems to be specific to foliar organs. All aspects of the *abn* heterozygous phenotype are intermediate between wild type and *abn* homozygous phenotypes indicating that the phenotype is dosage dependent.

We have observed that *abn* leaves have an altered pattern of auxin response from analysis of an *abn* line that contains the DR5:GUS construct. In wild type leaves, three distinct classes of auxin response are evident: 1) primary, at the distal tip, 2) secondary, along the margin and, 3) higher order, in hydathodes as well as areas within the lamina that predict the differentiation of higher order veins (Aloni, 2003). The primary auxin response pattern is proposed to result from auxin entering leaves from the stem and forming a sink at the distal tip (Aloni, 2003; Benkova et al., 2003; Steynen and Schultz, 2003). Auxin from a secondary, internal source exists along the leaf margin and is proposed to be canalized into the leaf interior (Sieburth, 1999; Mattsson et al, 1999). Some *abn* leaves never establish the distal maxima and do not expand or form veins, while others show normal primary DR5:GUS expression and develop midveins. In contrast, the secondary and tertiary auxin responses never occur normally and no higher

order veins form. Thus, the primary transport of auxin into the *abn* leaves can be established normally while the secondary response cannot.

The aberrant secondary auxin response in *abn* may be explained by two different mechanisms: 1) *abn* is defective in the secondary molecular response to auxin or 2) *abn* is defective in auxin transport required for secondary auxin responses. Our results suggest that the altered auxin response pattern observed in *abn* leaves is due to a defect in carrier-mediated auxin influx. *abn* leaves are often not defective in establishing the distal tip maximum required for midvein formation but the defect in auxin influx causes multiple, rather than singular, midveins to differentiate at the expense of higher order veins. Additionally, the secondary source of auxin that is proposed to exist along the margin fails to be established in *abn* leaves and thus no higher order auxin response is observed and subsequent vasculature does not develop. Therefore, we suggest that auxin influx is important for regulated auxin transport into the leaf, activation of the marginal source of auxin and inhibition of the primary auxin source. ABN is a critical component for each of these processes.

abn is defective in carrier-mediated auxin influx

Wild type plants grown on NOA are agravitropic and insensitive to exogenously supplied auxin, thus phenocopying the *aux1* mutant, which is defective in auxin uptake in roots (Imhoff et al., 2000). Previous studies have not examined the effects of NOA on the venation pattern of leaves. When treated with NOA, wild type leaves show an auxin response pattern similar to *abn* followed by a proliferation of midveins that meet distally, closely resembling untreated *abn* heterozygotes. Furthermore, when grown on NOA, *abn*

heterozygote leaves show an altered auxin response pattern and a more extreme venation phenotype that closely resembles untreated *abn* homozygotes. The venation pattern phenotype and auxin response of *abn* homozygotes does not appear to be affected by NOA treatment. The result that NOA phenocopies the *abn* phenotype in wild type and *abn* heterozygous leaves but does not change *abn* homozygous phenotype suggests that *abn* is defective in carrier-mediated influx with a dosage effect seen in the heterozygote.

Double mutants constructed with mutants defective in auxin efflux, auxin response and auxin influx support this idea. Double mutant combinations with *abn* and several well-characterized auxin efflux and response mutants show additive phenotypes indicating that ABN is not involved in these pathways. *aux1-7* is defective in carrier-mediated influx; however, mutant plants show root-specific defects. Since *abn* shows shoot specific defects it is not surprising that *aux1-7 abn* double mutants show an additive phenotype. In contrast, *axr4-2* mutants show both root and shoot defects. The AXR4 protein is proposed to be a regulator of carrier-mediated influx (Hobbie and Estelle, 1995). *aux1-7* is epistatic to *axr4-2* with respect to the root phenotype (Hobbie and Estelle, 1995), and we have found that *abn* is epistatic to *axr4-2* with respect to the shoot phenotype.

Further support for our hypothesis comes from the lack of response of the *abn* phenotype to either 2,4-D or 1-NAA. 2,4-D enters cells via the influx carrier but exits independently of the efflux carrier (Delbarre et al., 1996). If *abn* is defective in carrier-mediated influx, *abn* seedlings should be resistant to 2,4-D. In support of our idea, *abn* seedlings grown on 2,4-D show no detectible change in auxin response or vascular development in the developing leaves whereas, 2,4-D treated wild type leaves show a

slight increase in auxin response at the distal tip and a widening of the vasculature. 1-NAA has been shown to diffuse readily into cells (Yamamoto and Yamamoto, 1998; Marchant et al., 1999) but cannot rescue leaf primordial positioning defects in NOA influx-inhibited plants (Stieger et al., 2002). This suggests that some aspects of leaf formation require auxin to enter via a carrier protein and that entry by diffusion cannot substitute. Developing *abn* leaves grown on 1-NAA show no detectible changes in auxin response or vascular differentiation compared to untreated leaves, supporting our proposal that *abn* is specifically defective in carrier-mediated auxin influx.

Shoots that have both influx and efflux inhibited by NOA and NPA respectively, are unable to undergo leaf organogenesis (Stieger et al., 2002). Consistent with the notion that *abn* is defective in carrier-mediated influx, *abn* plants treated with NPA show a similar phenotype to NOA treated plants exposed to NPA: they often do not form leaves and instead produce a large number of primordia from the SAM. Moreover, in the exceptional case of primordial expansion, leaves are often ring-shaped, similar to the leaves that form when NPA-induced shoot apical pins are exogenously exposed to 1-NAA or further inhibited with NOA and subsequently exposed to exogenous IAA (Stieger et al., 2002).

Unlike *abn* leaves treated with NPA, *abn* leaves without PIN1 show an enhanced *abn* phenotype. This apparent discrepancy is consistent with the reduced severity of the *pin1-1* leaf phenotype compared to NPA treated leaves, that has led to the suggestion that there is considerable redundancy in auxin efflux carriers in the leaves (Gälweiler et al., 1998; Mattsson et al., 1999). An explanation in accordance with the increased severity of the *abn* phenotype in the absence of PIN1 is that combined with the lack of carrier-

mediated auxin influx, decreased efflux causes auxin canalization to be at the control of random diffusion events. The redundancy in efflux carriers allows *abn pin1-1* leaves to retain some polar auxin transport and thus radially symmetrical leaves are not formed as seen with NPA treatment.

In the absence of active influx, cells accumulate auxin by diffusion

We propose that *abn* leaves are defective in active influx. However, auxin responses are evident in *abn* leaves; therefore, auxin enters cells independent of the influx carrier. IAA is able to enter cells both by diffusion and carrier-mediated uptake but cannot diffuse out of cells, thus carrier-mediated efflux is the sole mechanism for exporting auxin (Lomax et al, 1995; Goldsmith, 1997). NOA has been shown to be highly effective in inhibiting carrier-mediated auxin influx; however, NOA is not able to completely block polar auxin transport activity (Parry et al., 2001). This suggests that inhibiting carrier-mediated influx alone is not sufficient to stop auxin from entering cells. If diffusion, a slow and unregulated process, is the sole mechanism for auxin entry into cells in *abn* leaves, many cells will slowly accumulate auxin. In support of this idea, many *abn* leaves never establish a distal maximum, suggesting that diffusion alone is a less reliable process. When the establishment of a pronounced distal auxin response occurs in *abn* leaves, it occurs later than in wild type, further supporting the idea that auxin enters *abn* cells by diffusion.

Active auxin influx has been found necessary to establish an auxin gradient in developing leaves (Stieger et al., 2002). Based on our results, we hypothesize that active influx also regulates the direction of auxin canalization during midvein formation. If

influx is defective, polar auxin transport occurs solely by the action of efflux carriers. The *abn* phenotype is exacerbated when auxin efflux is decreased by introducing defective PIN1 into *abn* plants, suggesting that in *abn* leaves, polar auxin transport is being regulated by efflux carriers alone. Further support for this idea is our finding that NPA-treated *abn* leaves are similar to NPA-induced shoot apical pins treated with NOA and subsequently with IAA. This suggests that some auxin is able to diffuse into *abn* leaves, and allows leaf expansion to occur. However, radially symmetrical leaves form because the auxin gradient required for leaf patterning is not created. Moreover, both 2,4-D and 1-NAA treatment increase the number of primordia that do not expand or differentiate. This suggests that flooding the primordia with diffusible auxin disrupts the gradient required for leaf expansion and development. The effects seem to be more pronounced in *abn* leaves, presumably because of an already impaired auxin transport system.

Active auxin influx is required for higher order vein but not midvein formation

We are proposing that *abn* is defective in carrier-mediated auxin influx. The multiple midveins produced in *abn* leaves and in NOA treated wild type leaves indicate that the midvein differentiates independently of active auxin influx. Auxin efflux, on the other hand, is proposed to be required for midvein differentiation since NPA treated leaves form a ring of vascular tissue along the margin but do not develop a midvein (Mattsson et al., 1999; Sieburth, 1999). Consistent with this requirement, *abn* leaves, which only produce midveins, often cease leaf vascular differentiation and primordial expansion when treated with NPA. The fact that some *abn* leaves treated with NPA maintain midvein formation suggests that the requirement for efflux in midvein

development is not absolute. In the absence of controlled auxin transport, diffusion is sometimes sufficient for midvein formation suggesting that the position of the midvein within the leaf may be prepatterned .

The lack of differentiation of secondary and tertiary veins in *abn* leaves suggests that, in contrast to the midvein, higher order veins require active auxin influx. This further suggests that distinct developmental mechanisms control different levels of vein hierarchy: regulated midvein formation is normally dependent upon auxin efflux from external auxin sources, and higher order vein formation is dependent upon carrier-mediated auxin influx from internal auxin sources.

Active auxin influx is required for secondary, internal auxin responses

Our results suggest that the mechanisms by which auxin maxima are established in leaves are different at different times in development. PIN1is localized toward the distal tip (Benkova et al., 2003), which supports a requirement for auxin efflux in establishing the primary auxin response. Since *abn* has functional auxin efflux, it is not surprising that the primary auxin response in *abn* leaves at the distal tip often appears normal. However, both *abn* and NOA treated leaves often do not develop beyond primordia and do not establish a distal tip maxima suggesting that its establishment is somewhat compromised by the lack of active influx.

abn leaves do not show normal secondary auxin responses, but do show DR5:GUS expression at points proximal to the tip. The pattern of expression and its relationship to vein differentiation suggests that this later expression results from reiterations of the initial distal tip response. Late expression in *abn* leaves consists of a

ring of several individual areas of expression maxima that are similar to the expression observed at the distal tip and multiple midveins differentiate in directions toward the DR5:GUS expression maxima. As well, wild type leaves treated with NOA show reduced secondary DR5:GUS expression. The lack of active influx in *abn* and NOA treated wild type plants results in the reduction or abolishment of secondary auxin responses; thus, influx must be necessary to establish secondary auxin responses. Additionally, secondary auxin responses do not require efflux since wild type plants treated with NPA show secondary DR5:GUS expression. Therefore, we propose that efflux is required to establish the primary distal maximum and that carrier-mediated auxin influx is required to establish secondary auxin response.

The phenotype of *abn* leaves and wild type leaves treated with NOA suggests that carrier mediated influx is involved not only in switching on the secondary marginal auxin source, but also in turning off the primary auxin response. Without carrier-facilitated auxin influx, the secondary auxin source is not established and the primary auxin response continues causing a proliferation in midveins. Two models are consistent with these observations: 1) carrier-mediated influx is required to switch off the primary auxin response directly or 2) carrier-mediated influx is required to switch on the secondary auxin response directly, and the primary auxin response is switched off as an indirect consequence.

A surprising result is that *abn* leaves, defective in carrier-mediated influx, form midveins when treated with NPA whereas NPA treated wild type leaves form no midveins. One clear difference between NPA treated wild type and *abn* leaves is that wild type leaves show a strong secondary auxin response along the leaf margin whereas

abn leaves show no secondary response. One explanation for the formation of a midvein in NPA treated *abn* leaves is that because the secondary auxin response is never established, external auxin entering the primordia via diffusion is more able to direct formation of the midvein. This supports the model that carrier-mediated influx directly switches on the secondary auxin response, which indirectly switches off the primary auxin response.

References:

Aloni R (1995). The Induction of vascular tissues by auxin and cytokinin. In Plant Hormones: Physiology, biochemistry and molecular biology (Davies PJ ed), 531-546. Kluwer Academic Publishers, London.

Bartel B (1997). Auxin biosynthesis. *Annual Review of Plant Physiology and Plant Molecular Biology* **48,** 51–66.

Bell CJ and Ecker J (1994). Assignment of 30 microsatellite loci to the linkage map of *Arabidopsis*. *Genomics* **19**, 137-144.

Benkova E, Michniewicz M, Sauer M, Teichmann T, Seifertová D, Jürgens G and Friml J (2003). Local, efflux-dependent auxin gradients as a common module for plant organ formation. *Cell* **115**, 591-602.

Bennett MJ, Marchant A, May ST, and Swarup R (1998). Going the distance with auxin: Unraveling the molecular basis of auxin transport. *Philosophical Transactions of the Royal Society of London. B* **353**, 1511–1515.

Berleth T and Jurgens G (1993). The role of the *monopteros* gene in organising the basal body region of the *Arabidopsis* embryo. *Development* **118**, 575-87.

Berleth T and Sachs T (2001). Plant morphogenesis: long disntance coordination and local patterning. *Current opinion in Plant Biology* **4**, 57-62.

Blilou I, Xu J, Wildwater H, Willemsen V, Paponov I, Friml J, Heidstra R, Aida M, Palme K and Scheres B (2005). The PIN auxin efflux facilitator network controls growth and patterning in *Arabidopsis* roots. *Nature* **433**, 39-44.

Carland FM, Berg B, FitzGerald J, Jinamornphongs S, Nelson T and Keith B (1999). Genetic regulation of vascular tissue patterning in Arabidopsis. *The Plant Cell* **11**, 2123-2137.

Carland FM, Fujioka S, Takatsuto S, Yoshida S and Nelson T (2002).The identification of *CVP1* reveals a role for sterols in vascular patterning. *Plant Cell* **14,** 2045-2058.

Carland FM and Nelson T (2004). *COTYLEDON VASCULAR PATTERN2*-mediated inositol (1,4,5) triphosphate signal transduction is essential for closed venation patterns of Arabidopsis foliar organs. *The Plant Cell* **16**, 1263-1275.

Casimiro I, Marchant A, Bhalerao RP (2001). Auxin transport promotes Arabidopsis lateral root initiation. *The Plant Cell* **13**, 843-52.

Chen L, Ortiz-Lopez A, Jung A and Bush DR (2001). *ANT1*, an aromatic and neutral amino acid transporter in Arabidopsis. *Plant Physiology* **125**, 1813-1820.

Delbarre A, Muller P, Imhoff V, and Guern J (1996). Comparison of mechanisms controlling uptake and accumulation of 2,4-dichlorophenoxyacetic acid, naphthalene-1-acetic acid, and indole-3-acetic acid in suspension-cultured tobacco cells. *Planta* **198**, 532-541.

Dellaporta SL, Wood J, and Hicks JB (1983). A plant DNA minipreparation: version II. *Plant Molecular Biology Reports 1, 19.*

Dengler N and Kang J (2001). Vascular patterning and leaf shape. *Current opinion in Plant Biology* **4**, 50-56.

Deyholos M, Cordner G, Beebe D and Sieburth LE (2000). The *SCARFACE* gene is required for cotyledon and leaf vein patterning. *Development* **127**, 3205-3213.

Estelle M (1998). Polar auxin transport: new support for an old model. *The Plant Cell* **10**, 1775-78.

Estelle MA and Somerville C (1987). Auxin-resistant mutants of *Arabidopsis thaliana* with an altered morphology. *Molecular and General Genetics* **206,** 200-206.

Friml J (2003). Auxin transport - shaping the plant. *Current Opinions in Plant Biology* **6**, 7-12.

Friml J, Yang X, Michniewicz M, Weijers D, Quint A, Tietz O, Benjamins R, Ouwerkerk PBF, Ljung K, Sandberg G, Hooykaas PJJ, Palme K and Offringa R (2004). A PINOID-dependent switch in apical-basal PIN polar targeting directs auxin efflux. *Science* **306**, 862-865.

Friml J, Benkova E, Blilou I, Wisiewska J, Hamann T, Ljung K, Woody S, Sandberg G, Scheres B, Jurgens G, Palme K (2002). AtPIN4 mediates sink-driven auxin gradients and root patterning in *Arabidopsis*. *Cell*, **108**, 661-73.

Gälweiler L, Guan C, Müller A, Wisman E, Mendgen K, Yephremov A, Palme K (1998). Regulation of polar auxin transport at AtPIN1 in *Arabidopsis* vascular tissue. *Science*, **282**, 2226-2230.

Geldner N, Anders N, Wolters H, Keicher J, Kornberger W, Müller P, Delbarre A, Ueda T, Nakano A, Jürgens G (2003). The *Arabidopsis* GNOM ARF-GEF mediates endosomal recycling, auxin transport, and auxin-dependent plant growth. *Cell* **112**, 219-230.

Goldsmith MHM (1997). The polar transport of auxin. *Annual Review of Plant Physiology* **28**, 439-478.

Hamann T, Benkova E, Bäurle I, Kientz M, Jürgens G (2002). The *Arabidopsis BODENLOS* gene encodes an auxin response protein inhibiting *MONOPTEROS*-mediated embryo patterning. *Genes and Development*, **16**, 1610-1615.

Hamann T, Mayer U, Jürgens G (1999). The auxin-insensitive *bodenlos* affect primary root formation and apical-basal patterning in the *Arabidopsis* embryo. *Development*, **126**, 1387-1395.

Hardtke CS and Berleth T (1998). *Arabidopsis* gene *MONOPTEROS* encodes a transcription factor mediating embryo axis function and vascular development. *EMBO*, **17**, 1405-1411.

Hellmann H, Hobbie L, Chapman A, Dharmasiri S, Dharmasiri N, del Pozo C, Reinhardt D, Estelle M (2003). *Arabidopsis AXR6* encodes CUL1 implicating SCF E3 ligases in auxin regulation of embryogenesis. *EMBO*, **22**, 3314-3325.

Hobbie L, McGovern M, Hurwitz LR, Pierro A, Liu NY, Bandyopadhyay A, Estelle M (2000). The *axr6* mutants of *Arabidopsis thaliana* define a gene involved in auxin response and early development. *Development*, **127**, 23-32.

Hobbie, L and Estelle, M (1995) The axr4 auxin-resistant mutants of *Arabidopsis thalaiana* define a gene important for root gravitropism and lateral root initiation. *The Plant Journal,* **7,** 211-220.

Imhoff V, Muller P, Guern J, Delbarre A (2000) Inhibitors of the carrier-mediated influx of auxin in suspension-cultured tobacco cells. *Planta* **210,** 580-588

Jones AM, Kyung-Hoam I, Savka MA, Ming-Jing W, DeWitt NG, Shillito R and Binns AN (1998). Auxin-dependent cell expansion mediated by overexpressed auxin-binding protein 1. *Science* **282,** 1114-1117.

Jürgens G (2001). New EMBO member's review: apical-basal pattern formation in Arabidopsis embryogenesis. *EMBO* **20,** 3609-3616

Kang J and Dengler N (2002). Cell cycling frequency and expression of the homeobox gene *ATHB-8* during leaf vein development in *Arabidopsis*. *Planta* **216,** 212-219.

King JJ, Stimart D, Fisher R and Bleecker A (1995). A mutation altering auxin homeostasis and plant morphology in *Arabidopsis*. *Plant Cell* **7,** 2023-2037.

Koizumi K, Sugiyama M and Fukuda H (2000). A series of novel mutants of *Arabidopsis thaliana* that are defective in the formation of continuous vascular network:

calling the auxin signal flow canalization hypothesis into question. *Development* **127**, 3197-3204.

Leyser O (2002). Molecular genetics of auxin signaling. *Annual Review of Plant Biolog*, **53**, 377-398.

Leyser O (2001). Auxin signaling: the beginning, the middle and the end. *Current Opinion in Plant Biology* **4**, 382-386.

Lincoln D, Britton J and Estelle M (1990). Growth and development of the *axr1* mutants of *Arabidopsis*. *Plant Cell* **2**, 1071-1080.

Lomax TL, Muday GK and Rubery PH (1995). Auxin transport. In: Davies, PJ, ed. *Plant hormones: physiology, biochemistry and molecular biology.* Dordrecht, Netherlands: Kluwer Academic Publishers, 509-530.

Luschnig C (2002). Auxin transport: ABC proteins join the club. *Trends in Plant Science* **7, 8,** 329-332.

Marchant A, Bhalerao R, Casimiro I, Casero PJ and Bennett M (2002). AUX1 promotes lateral root formation by facilitating indole-3-acetic acid distribution between sink and source tissues in the Arabidopsis seedling. *The Plant Cell* **14**, 589-597.

Mattsson J, Ckurshumova W and Berleth T (2003). Auxin signaling in *Arabidopsis* leaf vascular development. *Plant Physiology* **131**, 1327-1339.

Mattsson J, Sung RZ and Berleth T (1999). Responses of plant vascular systems to auxin transport inhibition. *Development* **126**, 2979-2991.

McConnell JR, Emery J, Eshed Y, Bao N, Bowman J and Barton MK (2001). Role of *PHABULOSA* and *PHAVOLUTA* in determining radial patterning in shoots. *Nature* **411**, 709-713.

Muday GK, Peer WA and Murphy AS (2003). Vesicular cycling mechanisms that control auxin transport polarity. *Trends in Plant Science* **8**, 301-303.

Nagpal P, Walker LM, Young JC, Sonawala A, Timple C, Estelle M and Reed JW (2000). AXR2 encodes a member of the AUX/IAA protein family. *Plant Physiology* **123**, 563-573.

Napier RM (1995). Towards an understanding of ABP1. *Journal of Experimental Botany* **46**, 1787-95.

Napier RM, David KM and Perrot-Rechenmann C (2002). A short history of auxin-binding proteins. *Plant Molecular Biology* **49**, 339-348.

Nelson T (1998). Polarity, vascularization and auxin. *Trends in Plant Science* **3**, 245-246.

Nelson T and Dengler N (1997). Leaf vascular pattern formation. *The Plant Cell* **9**, 1121-1135.

Otsuga D, DeGuzman B, Prigge MJ, Drews GN and Clark SE (2001). *REVOLUTA* regulates meristem initiation at lateral positions. *The Plant Journal* **25**, 223-236.

Patton EE, Willems AR and Tyers M (1998). Combinatorial control in ubiquitin-dependent proteolysis: don't skip the F-box hypothesis. *Trends in Genetics* **14**, 236-243.

Parry G, Delbarre A, Marchant A, Swarup R, Perrot-Rechenmann C and Bennett MJ (2001). Novel auxin transport inhibitors phenocopy the auxin influx carrier mutation *aux1*. *The Plant Journal* **25**, 399-406.

Przemeck GKH, Mattsson J, Hardtke CS, Sung ZR and Berleth T (1996). Studies on the role of the *Arabidopsis* gene *MONOPTEROS* in vascular development and plant cell axialization. *Planta* **200**, 229-237.

Reinhardt D, Pesce E-R, Stieger P, Mandel T, Baltensperger K, Bennet M, Traas J, Friml J and Kuhlemeier C (2003). Regulation of phyllotaxis by polar auxin transport. *Nature* **426**, 255-260.

Rosen E, Chen R and Masson PH (1999). Root gravitropism: a complex response to a simple stimulus? *Trends in Plant Science* **4**, 407-412.

Ruegger M, Dewey E, Hobbie L, Brown D, Bernasconi P, Turner J, Muday G and Estelle M (1997). Reduced naphthylphthalamic acid binding in the *tir3* mutant of Arabidopsis is associated with a reduction in polar auxin transport and diverse morphological defects. *Plant Cell* **9**, 745-757.

Sachs T (1981). The control of patterned differentiation of vascular tissues. *Advances in Botanical Research* **9**, 151-262.

Sachs T (1989). The development if vascular networks during leaf development. *Current Topics in Plant Biochemistry and Physiology* **8**, 168-183.

Sachs T (1991). Cell polarity and tissue patterning in plants. *Development Supplement* **1**, 83-93.

Scarpella E, Francis P, and Berleth T (2004). Stage-specific markers define early steps of procambium development in *Arabidopsis* leaves and correlate termination of vein formation with mesophyll differentiation. *Development* **131**, 3445-3455

Sieburth LT (1999). Auxin is required for leaf vein pattern in Arabidopsis. *Plant Physiology* **121**, 1179-1190.

Skowyra D, Craig KL, Tyers M, Elledge SJ, and Harper JW (1997). F-box proteins are receptors that recruit phosphorylation substrates to the SCF ubiquitin-ligase complex. *Cell* **91**, 209-19.

Stieger P, Reinhardt D and Kuhlemeier C (2002). The auxin influx carrier is essential for correct leaf positioning. *The Plant Journal* **32**, 509-517.

Steynen Q and Schultz E (2003). The FORKED genes are essential for distal vein meeting in Arabidopsis. *Development* **130**, 4695-708.

Swarup R, Friml J and Marchant A (2001). Localization of the auxin permease AUX1 suggests two functionally distinct hormone transport pathways operate in the Arabidopsis root apex. *Genes and Development* **15**, 2648-2653.

Timpte C, Wilson A and Estelle M (1994). The *axr2-1* mutation in *Arabidopsis thaliana* is a gain-of-function mutation that disrupts an early step in auxin response. *Genetics* **138**, 1239-1249.

Ulmasov T, Murfett J, Hagen G and Guilfoyle TJ (1997). Aux/IAA proteins repress expression of reporter genes containing natural and highly active synthetic auxin response elements. *The Plant Cell* **9**, 1963-1971.

Warwicker, J (2001). Modelling of auxin-binding protein 1 suggests that its C-terminus and auxin could compete for a binding site that incorporates a metal ion and tryptophan residue 44. *Planta* **212,** 343-47.

Yamamoto M and Yamamoto K (1998). Differential effects of 1-naphathaleneacetic acid and 2,4-dichlorophenoxyacetic acid on the gravitropic response of roots in an auxin resistant mutant of *Arabidopsis*, *aux1*. *Plant Cell Physiology* **39**, 660.

Yang K-Y, Moon YH, Choi KH, Kim Y-H, Eun M-Y, Guh J-O, Kim K-C and Cho B-H (1997). Structure and expression of the *AWI31* gene specifically induced by wounding in *Arabidopsis thaliana*. *Molecular Cell* **7**, 131-135.

Zgurski J, Sharma R, Bolokoski DA and Schultz EA (2005). Asymmetric auxin response preceded asymmetric growth of *asymmetric leaf1* and *asymmetric leaf2* Arabidopsis leaves. *The Plant Cell* **17**, 77-91.

Table 1 – Genetic interactions between *abn* and other auxin mutants. *axr1-2* and *mp* recombination frequencies are consistent with the molecular map distance of *abn* to 24 cM on Chromosome 1.

Genotype (n)	Segregation	x^2 Value (d.f.)	Frequency of Double Mutants
abn fkd-1 (182)	Independent	2.3 (5)	0.0625
abn pin1-1 (259)	Independent	4.7 (5)	0.0625
abn aux1-7 (118)	Independent	7.1 (5)	0.0625
abn axr6-2 (306)	Independent	2.0 (5)	0.0625
abn axr4-2 (284)	*abn* epistatic	5.6 (4)	0
abn axr1-12 (357)	Linked	n/a	0.019
abn mp (473)	Linked	n/a	0.00211

Table 2 – Morphology of mature first leaves at 21 DAG (Significant difference from a = wild type, b = *abn*, c = single mutant, student's t-test, $p<0.05$). The double mutants were not tested to wild type.

Genotype (n)	Shape (L/W)	# FEVs	# Aeroles	# VI's	# BPs	Margin Size
wild type (23)	1.27	13.1	17.6	0.48	47.3	0.050
axr1-12 (18)	0.97^{a}	11.1	6.9^{a}	0.39	24.2^{a}	0.063
axr2 (3)	0.98^{a}	10.7	20.3	0.33	50.7	0.055
fkd-1 (32)	1.25	21.2^{a}	5.8^{a}	1.69^{a}	29.4^{a}	0.046
bdl (10)	0.99^{a}	14.1	22.7^{a}	0.00	59.5^{a}	0.050
pin1-1 (15)	1.05^{a}	11.3	15.2	0.53	40.6	0.080^{a}
axr4-2 (30)	1.23	15.2	20.0	0.40	54.5	0.054
aux1-7 (25)	1.21	21.0^{a}	25.0^{a}	0.20	70.6^{a}	0.049
abn het (54)	$1.42^{a,b}$	12.2^{b}	16.5	0.43	44.4^{b}	$0.073^{a,b}$
het::axr1-12 (21)	$1.19^{b,c}$	$8.0^{b,c}$	$11.3^{b,c}$	0	$30.7^{b,c}$	0.074
het::axr2 (4)	1.12^{b}	11.3	18.3	0.5	46.8	0.09
het::fkd-1 (40)	$1.32^{b,c}$	22.9b	$14.9^{b,c}$	0.65^{c}	$51.4^{b,c}$	0.066^{c}
het::bdl (44)	$1.19^{b,c}$	11.5	19.6^{b}	$0.14^{b,c}$	$50.4^{b,c}$	0.075^{c}
het::pin1-1 (19)	$1.32^{b,c}$	$19.4^{b,c}$	$26.4^{b,c}$	0.53	$71.1^{b,c}$	0.076
het::axr4-2 (18)	1.46^{c}	12.4	16.4	0.28	44.7^{c}	$0.094^{b,c}$
het::aux1-7 (47)	1.24^{b}	$18.0^{b,c}$	$28.0^{b,c}$	0.19	73.5^{b}	$0.062^{b,c}$
abn hom (23)	1.81^{a}	9.3^{a}	14.9	0.22	38.7^{a}	0.182^{a}
abn::axr1-12 (8)	1.45^{c}	10.3	13.4^{c}	0	37^{c}	0.168^{c}
abn::axr2 (5)	1.48^{c}	8	14^{c}	0	36^{c}	0.186^{c}
abn::fkd-1 (29)	1.97^{c}	22.3	14.8^{c}	0.62^{c}	50.8^{c}	0.148^{c}
abn::bdl (29)	1.33^{c}	7.6^{c}	16.2^{c}	0.03	39.9^{c}	0.139^{c}
abn::pin1-1 (10)	3.48^{c}	29.7^{c}	49.9^{c}	0.40	128.7^{c}	0.177^{c}
abn::axr4-2 (11)	1.99^{c}	13.8	13.5^{c}	0.00	40.9^{c}	0.236^{c}
abn::aux1-7 (35)	1.71^{c}	14.9^{c}	18.7^{c}	0.06	52.1^{c}	0.143^{c}

Table 3 – Morphology of mature cotyledons at 14 DAG (significant difference from a = wild type, b = *abn*, c = single mutant, student's t-test, $p<0.05$). The double mutants were not tested to wild type.

Genotype (n)	Shape (L/W)	# FEVs	# Aeroles	# BPs	Margin Size
wild type (23)	1.32	0.57	3.39	7.35	0.161
axr1-12 (11)	1.13[a]	1.91[a]	1.27[a]	4.45[a]	0.159
axr2 (4)	1.04[a]	1.50[a]	2.25[a]	6	0.179
fkd-1 (31)	1.20[a]	2.61[a]	1.19[a]	5.00[a]	0.174
bdl (11)	1.04[a]	0.36	3.64	7.64	0.134[a]
pin1-1 (14)	0.86[a]	1.57[a]	3.07	7.71	0.166
axr4-2 (31)	1.16[a]	0.45	3.26	6.97	0.152
aux1-7 (29)	1.14[a]	0.66	3.41	7.48	0.170
abn het (59)	1.33[b]	1.08[a,b]	4.12[a,b]	9.32[a,b]	0.155[b]
het::axr1-12 (10)	1.09[b]	2.70[b]	2.40[b,c]	7.50[b,c]	0.157
het::axr2 (8)	1.01[b]	1.875	2.88[b]	7.63[b]	0.232
het::fkd-1 (39)	1.25[b,c]	1.21[b,c]	2.26[b,c]	5.72[b,c]	0.189[b]
het::bdl (47)	1.07[b]	0.85[c]	3.74[b,c]	8.34[b,c]	0.151
het::pin1-1 (17)	1.09[b,c]	3.76[b,c]	6.71[b,c]	16.94[b,c]	0.174
het::axr4-2 (18)	1.21[b]	1.11[c]	3.33[b]	7.78[b,c]	0.164
het::aux1-7 (61)	1.06[b,c]	1.16[c]	3.46[b]	8.08[b,c]	0.167
abn hom (21)	1.59[a]	4.00[a]	8.57[a]	21.14[a]	0.256[a]
abn::axr1-12 (4)	1.29[c]	6.25[c]	0.50	7.25	0.328[c]
abn::axr2 (8)	1.22	3.63[c]	3.25	10.1[c]	0.297[c]
abn::fkd-1 (30)	1.37[c]	7.37[c]	1.57	10.5[c]	0.323[c]
abn::bdl (22)	1.21[c]	2.91[c]	5.00[c]	12.9[c]	0.274[c]
abn::pin1-1 (9)	1.13[c]	4.44[c]	11.44[c]	27.33[c]	0.207
abn::axr4-2 (16)	1.44[c]	3.81[c]	5.25[c]	14.3[c]	0.318[c]
abn::aux1-7 (35)	1.32[c]	3.69[c]	4.14[c]	11.97[c]	0.251[c]

DR5:GUS expression	AT			NOA			2,4D			NAA		
	wild type	*abn* het	*abn* hom	wild type	*abn* het	*abn* hom	wild type	*abn* het	*abn* hom	wild type	*abn* het	*abn* hom
Day 5 (wt); Day7 (NOA,2,4-D,NAA)	**(121)[d]**	**(86)**	**(30)**	**(108)**	**(84)**	**(30)**	**(107)**	**(86)**	**(24)**	**(55)**	**(91)**	**(36)**
Primordia (no DR5:GUS)	10.70%	16.30%	20%	20.40%	39.30%	60.00%	41.10%	62.80%	50%	21.80%	76.90%	83.30%
Distal tip[a] (dispersed in NOA/NPA)	39.30%	74.40%	0%	61.10%	15.50%	0%	35.50%	23.30%	0%	50.90%	19.80%	0%
Distal tip and Secondary loop	14.80%	0%	0%	3.70%	0%	0%	22.40%	0%	0%	20.00%	0%	0%
Secondary[b] loop alone	0%	0%	80%	0%	0%	13.30%	0%	0%	25%	0%	0%	16.70%
Tertiaries	14.00%	4.70%	0%	0%	0%	0%	0%	0%	0%	5.50%	1.10%	0%
Hydathodes (1)[c]	2.50%	4%	0%	0%	0%	0%	0%	0%	0%	1.80%	2.20%	0%
Hydathodes (2)[c]	23.10%	1%	0%	0%	0%	0%	0.90%	0%	0%	5.50%	0%	0%
Vascular lignification	25.20%	33.00%	30.40%	34.30%	82.10%	46.70%	1.90%	37.20%	16.60%		no data	
Day 6 (wt); Day10 (NOA,2,4-D); Day 9 (NAA)	**(43)**	**(82)**	**(36)**	**(124)**	**(76)**	**(32)**	**(161)**	**(82)**	**(26)**	**(61)**	**(103)**	**(50)**
Primordia (no DR5:GUS)	7.00%	20.70%	30.50%	29.80%	13.20%	6.30%	27.30%	41.50%	23.10%	4.90%	29.10%	72.20%
Distal tip* (dispersed in NOA/NPA)	41.90%	54.90%	30.50%	10.50%	0%	0%	20.50%	24.40%	0%	45.90%	67.00%	16.70%
Distal tip and Secondary loop	0%	0%	0%	0%	0%	0%	13.00%	0%	0%	3.30%	0%	0%
Secondary* loop alone	0%	0%	38.90%	0%	0%	0%	0%	0%	23.10%	0%	0%	5.60%
Tertiaries	39.50%	2%	0%	0%	0%	0%	1.20%	0%	0%	27.90%	0%	0%
Hydathodes (1)[c]	7%	9%	0%	0%	0%	0%	0%	0%	0%	20%	2%	0%
Hydathodes (2)[c]	30.20%	9%	0%	0%	0%	0%	1.90%	0%	0%	11.50%	0%	0%
Vascular lignification	38%	27.50%	15.00%	96.00%	94.30%	93.80%	57.80%	63.40%	65.40%		no data	
Day 10 (wt); Day14 (2,4-D,NAA)	**(60)**	**(93)**	**(20)**				**(86)**	**(27)**	**(4)**	**(74)**	**(72)**	**(41)**
Primordia (no DR5:GUS)	13.30%	28.00%	41.30%		no data		2.30%	7.40%	0%	23.00%	43.10%	70.70%
Distal tip* (dispersed in NOA/NPA)	5%	6.50%	2.20%				34.90%	29.60%	0%	36.50%	48.60%	12.20%
Distal tip and Secondary loop	1.70%	0%	0%				11.60%	0%	0%	0%	0%	0%
Secondary* loop alone	0%	0%	0%				0%	0%	0%	0%	0%	0%
Tertiaries	1.70%	0%	0%				4.70%	0%	0%	2.70%	0%	0%
Hydathodes (1)[c]	3%	25%	0%				9%	0%	0%	8%	1%	0%
Hydathodes (2)[c]	50%	27%	0%				2%	0%	0%	22%	1%	0%
Hydathodes (3)[c]	22%	1%	0%				0%	0%	0%	3%	0%	0%
Hydathodes (3)[c]	0%	1%	0%				0%	0%	0%	0%	0%	0%
Vascular lignification	77.80%	95.70%	72.60%				53.50%	77.80%	75%		no data	

Table 4 - Auxin response landmarks of vascular development in wild type, *abn* heterozygous and *abn* homozygous first leaves untreated (AT) or treated with 30 M NOA, 10-6 2,4-D or 40 M 1-NAA. Values represent the percentage of leaves showing DR5:GUS expression of each landmark. Parentheses indicate the total number of leaves scored for that character.

a - The distal tip expression occurs at a distinct maximum in AT and 1-NAA treated leaves, but is dispersed in NOA and 2,4-D treatments.

b - The secondary loop in *abn* homozygous leaves is not the same as the secondary loop in wild type and abn homozygous leaves.

c - The number of hydathodes showing DR5:expression are indicated in parentheses.

d - The total number of leaves scored.

Table 5 –Morphology of wild type, *abn* heterozygous and *abn* homozygous shoots. (Significant difference from a= wild type, b = *abn,* Student's t-test, $p<0.05$). * measured at 28 DAG.

Genotype (n)	2 cm bolt (Days)	Flowering (Days)	Maturation (Days)	# Rosette Leaves*	# Secondary Inflorescences*	Height* (mm)
Wild type (20)	26.1^{b}	26.9^{b}	28.4^{b}	7.6^{b}	3.8^{b}	71.7^{b}
abn het (58)	$23.5^{a,b}$	$24.2^{a,b}$	$25.1^{a,b}$	$5.4^{a,b}$	$2.5^{a,b}$	54.7^{a}
abn homo (21)	20.2^{a}	20.6^{a}	21.4^{a}	4.8^{a}	2.2^{a}	49.2^{a}

Table 6 – Morphology of roots. Primary root length was measured at 7 DAG while the number of lateral roots (LRs) and the distance from LRs to the root apical meristem (RAM) were measured at 14 DAG. No significant differences were determined (Student's t-test, $p<0.05$).

Genotype (n)	Primary Root Length (mm)	Number of LRs	Distance from LRs to RAM	LR Density (Length /LR)
Wild type (26)	24.9	5.3	17.9	5
abn het (73)	21	3.6	20.1	7.3
abn hom (23)	22.3	3.5	19.1	6.7

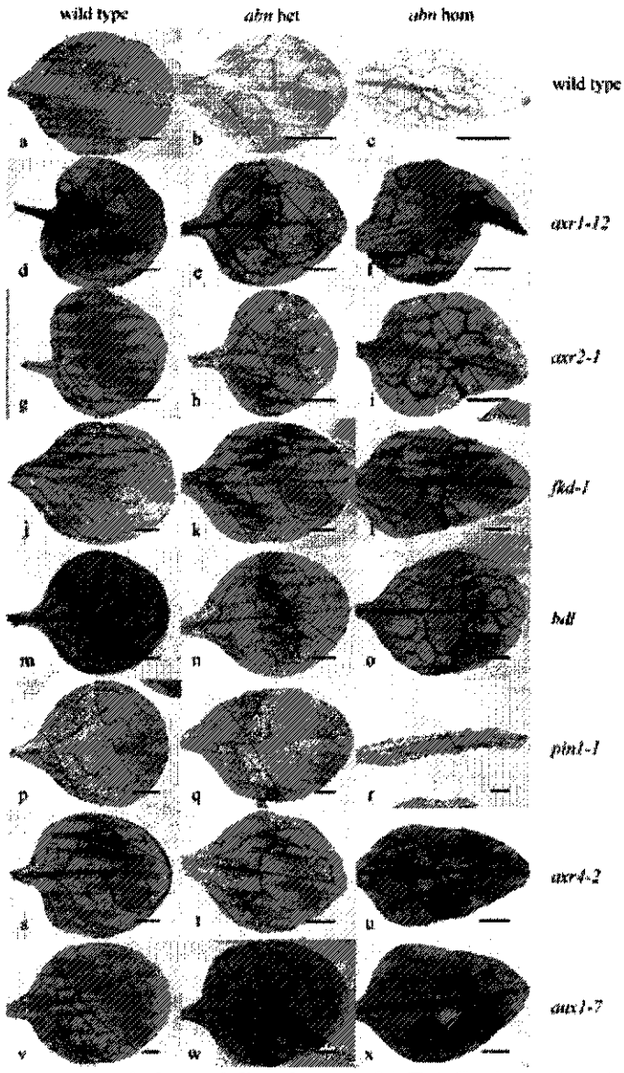

Figure 1 - Vascular pattern of cleared first leaves 21 DAG viewed under light microscopy (scale bar = 1 mm). The genotype of the *ABN* locus is shown along the top, while the genotype of a series of auxin related loci is shown along the right hand side.

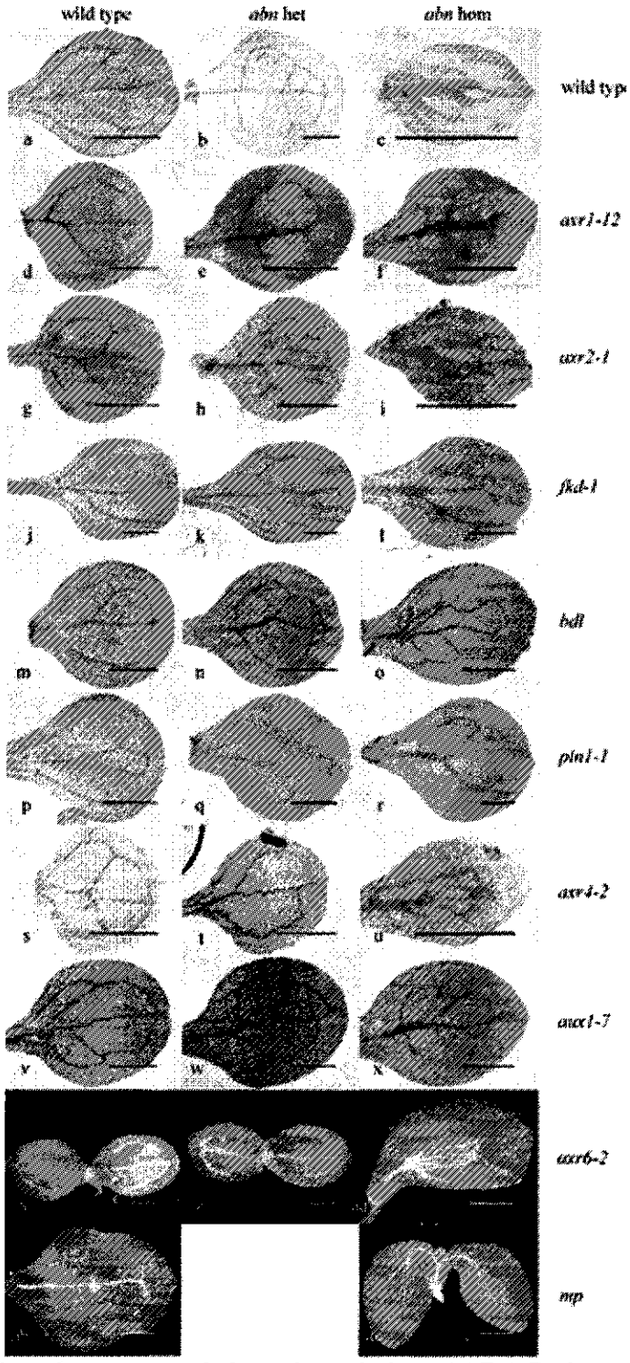

Figure 2 – Vascular pattern of cleared cotyledons 14 DAG viewed under light microscopy (a-x) or phase contrast optics (y-ac) (scale bar = 1 mm a-aa; 0.5mm y-ac). The genotype of the *ABN* locus is shown along the top, while the genotype of a series of auxin related loci is shown along the right hand side.

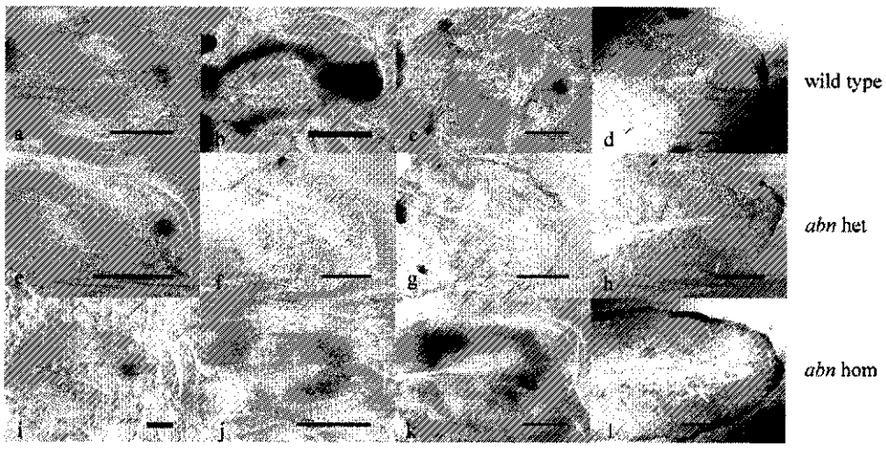

Figure 3 – DR5:GUS expression in developing leaves of wild type (a-d), *abn* heterozygous (e-h), and *abn* homozygous (i-l) seedlings. Viewed with differential interference contrast optics (scale bar = 0.05mm a,b,e,i-k; 0.1mm c,g; 0.2mm f; 0.5mm h; 1mm d,l).

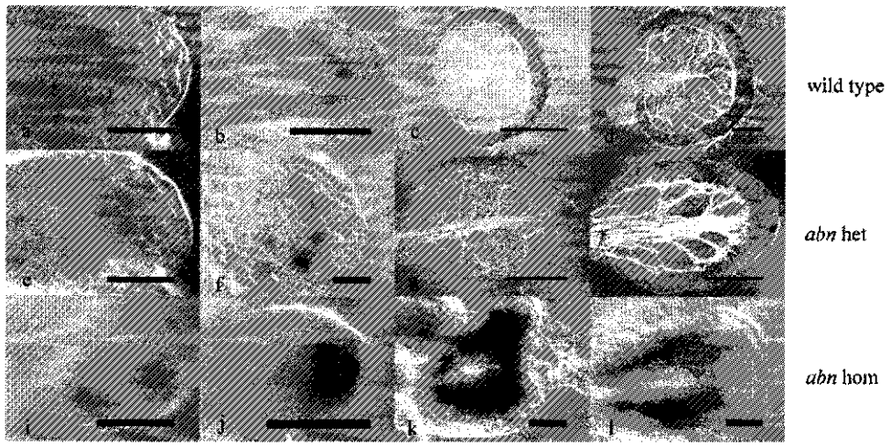

Figure 4 – DR5:GUS expression in developing leaves of wild type (a-d), *abn* heterozygous (e-h), and *abn* homozygous (i-l) seedlings treated with 30μM NPA. Viewed with differential interference contrast optics (scale bar = 0.01mm i; 0.05mm a,e,f,j-l; 0.1mm b, 0.5mm c,g; 0.2mm d; 0.5mm h).

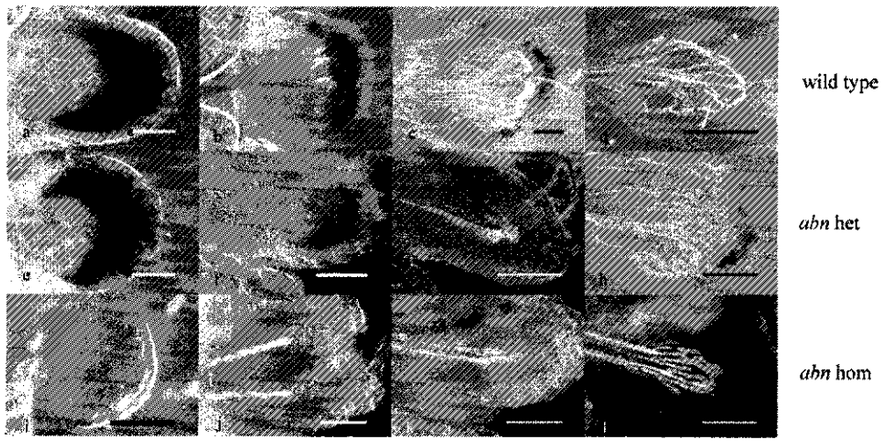

Figure 5 – DR5:GUS expression in developing leaves of wild type (a-d), *abn* heterozygous (e-h), and *abn* homozygous (i-l) seedlings treated with 30μM NOA. Viewed with differential interference contrast optics (scale bar = 0.05mm a,e,f,i-k; 0.1mm b,c,g,l; 0.2mm h; 0.5mm d).

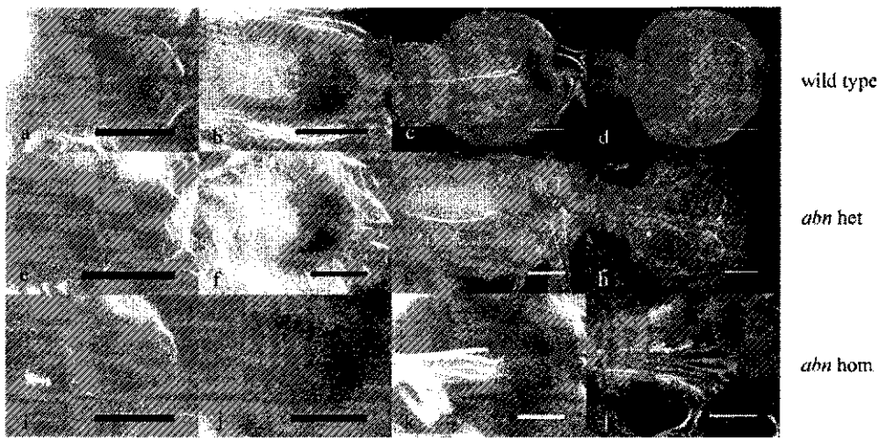

Figure 6 – DR5:GUS expression in developing leaves of wild type (a-d), *abn* heterozygous (e-h), and *abn* homozygous (i-l) seedlings treated with 1 μM *2*,4-D. Viewed with differential interference contrast optics (scale bar = 0.05mm a,b,e-g,i-k; 0.1mm c,l; 0.2mm d,h).

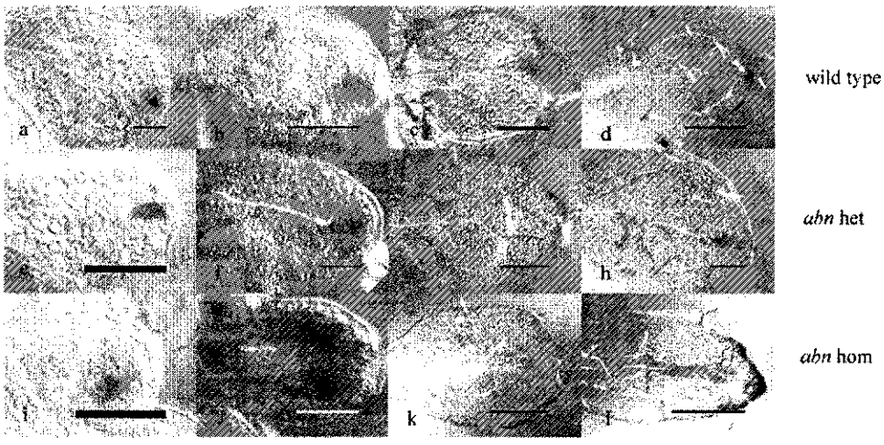

Figure 7 – DR5:GUS expression in developing leaves of wild type (a-d), *abn* heterozygous (e-h), and *abn* homozygous (i-l) seedlings treated with 0.40 μM 1-NAA. Viewed with differential interference contrast optics (scale bar = 0.05mm a,e,f,i,j; 0.1mm b,c; 0.2mm g,h; 0.5mm d,k,l).

AUTOBAHN: A GENE THAT HAS A ROLE IN AUXIN INFLUX IN *ARABIDOPSIS* LEAVES?

JASMINE JAY TAMARA GARRETT
B.Sc., University of Lethbridge, 2003

A Thesis
Submitted to the School of Graduate Studies
Of the University of Lethbridge
In Partial Fulfillment of the
Requirements for the Degree

MASTERS OF SCIENCE

Biological Sciences
University of Lethbridge
LETHBRIDGE, ALBERTA, CANADA

Your file Votre référence
ISBN: 978-0-494-17397-8
Our file Notre référence
ISBN: 978-0-494-17397-8

Abstract

The development of leaf vascular patterns is a highly regulated process. The plant hormone auxin is critical for vascular patterning: auxin canalization is proposed to cause files of cells to accumulate higher auxin levels and develop into veins. Thus, the response of cells to auxin and transport of auxin are critical to establish proper cell fate. We have characterized a mutation in the *Arabidopsis thaliana* gene named AUTOBAHN (ABN). *abn* leaves produce leaves that proliferate disorganized, overlapping veins parallel to the midvein with no differentiation of higher order veins. *abn* leaves show no normal aspects of the secondary auxin response though double mutant analysis suggest that ABN functions independently of previously characterized auxin response pathways. Wild type plants grown on an influx inhibitor phenocopy *abn* suggesting that *abn* is defective in carrier-mediated auxin influx.

Table of Contents

List of Tables

List of Figures

List of Abbreviations

Genes and Proteins

ABC	ATP-BINDING CASSETTE
ABN	AUTOBAHN
ABP	AUXIN BINDING PROTEIN
ARE	AUXINE-RESPONSE ELEMENT
ARF	AUXIN-RESPONSE FACTOR
ATHB8	ARABIDOPSIS THALIANA HOMEOBOX8
AUX	AUXIN
AXR1	AUXIN RESISTANT1
AXR2	AUXIN RESISTANT2
AXR4	AUXIN RESISTANT4
AXR6	AUXIN RESISTANT6
BDL	BODENLOS
CUL1	CULLIN1
CVP	COTYLEDON VASCULR PATTERN
FKD	FORKED
GEF	GTP EXCHANGE FACTOR
GL1-1	GLABROUS1-1
LAX	LIKE AUX1
MDR	MULTIPLE DRUG RESISTANCE
MRP	MULTIDRUG- RELATED PROTEIN

MP	MONOPTEROS
PID	PINOID
PIN1	PIN FORMED1
RTY	ROOTY
SCF	SKP1/CULLIN/F-BOX
SFC	SCARFACE
VAN	VASCULAR NETWORK
VEP1	VEIN PATTERNING1

Chemicals

2,4-D	2,4-dichlorophenoxyacetic acid
EMS	ethyl methane sulfonate
DMSO	dimethyl sulfoxide
IAA	indole-3-acetic acid
NAA	1-naphthaleneacetic acid
NOA	1-napthoxyacetic acid
NPA	naphthylphthalamic acid
X-gluc	5-bromo-4-chloro-3-indoyl glucuronide

Terms

AT	*Arabidopsis thaliana*
BP	branch point
Col	Columbia ecotype

CCD	charge-coupled device
DAG	days after germination
FEV	freely ending vein
Ler	Landsberg ecotype
PCR	polymerase chain reaction
RAM	root apical meristem
RF	recombination frequency
SAM	shoot apical meristem
SSLP	simple sequence length polymorphism
VI	vascular island

Introduction

Vascular systems are essential for the viability of plants and are comprised of two major types of conducting tissues: xylem and phloem. Xylem primarily transports water and dissolved minerals that are absorbed from the soil and phloem primarily transports photosynthates and hormones throughout the plant. Xylem and phloem are arranged into vascular bundles called veins. The spatial arrangement of leaf veins forms a multitude of patterns throughout different taxa in the plant kingdom. It is important to understand the development of venation patterns as they confer transport efficiency and mechanical stability to the entire plant.

In leaves of dicots, there are three major types of veins that contribute to the mature vascular pattern: 1) the midvein, which connects with the stem vascular system; 2) secondary veins, which branch from the midvein and develop into the lamina and; 3) tertiary and higher order veins, which branch from secondary veins or each other and do not meet with the midvein (Sieburth, 1999). Classical studies suggest that the midvein differentiates towards the leaf tip (acropetal differentiation) whereas secondary and higher order veins differentiate primarily towards the leaf base (basipetal differentiation) (Nelson and Dengler, 1997). However considerable debate over the direction of vein differentiation exists: recent analysis, based on proposed routes of auxin transport, suggests that the development of the midvein may be basipetal (Benkova et al., 2003) while ATHB8::GUS expression suggests that the development of secondary veins may be simultaneously acropetal and basipetal (Mattsson et al., 1999, Scarpella et al., 2004). The plant hormone auxin is known to be critical for plant vascular tissue formation and

patterning. Auxin has been shown to play a critical role in many aspects of plant growth and development (reviewed in Aloni, 1995) including tropisms (Rosen et al., 1999; Friml et al., 2002), patterning of early embryos (Jürgens, 2001; Friml 2003), root patterning and elongation (Blilou et al., 2005), lateral root initiation (Casimiro et al., 2001), the positioning and expansion of leaves and flowers (Berleth and Sachs, 2001; Benkova et al., 2003; Reindhardt et al, 2003), and vascular differentiation (Berleth et al, 2000; Aloni, 2003). Although the importance of auxin has been well established, we are only beginning to understand the molecular details of auxin signaling and transport.

Auxin is a unique signaling molecule as it is actively transported in a polar fashion from its source in young plant tissues and apical meristems to sites of action. Auxin transport in shoots is basipetal and is facilitated by the actions of specific influx and efflux carrier proteins located in the plasma membrane. The chemiosmotic hypothesis helps to explain polarized auxin transport. This model suggests that polar auxin flow is due to the asymmetrical distribution of influx and efflux carrier proteins (Estelle, 1998). The chemiosmotic model suggests that, in the shoot, influx carriers are located on the apical sides and that the efflux carriers are positioned to the basal sides of the cell; therefore, auxin can only be transported unidirectionally. In this model protonated IAA is cotransported into cells with a proton and loses its proton to become negatively charged. The anionic form of IAA can only be transported out of the cell through an efflux carrier. The *PIN1* gene encodes the transmembrane component of an auxin efflux carrier in shoot vascular tissue (Bennett et al., 1998; Galweiler et al., 1998, Blilou et al., 2005). Plants mutant for *PIN1* are defective in polar auxin transport resulting in a variety of defects including a lack of floral buds and an increase in marginal

venation in the leaves (Gälweiler et al., 1998, Mattsson et al., 1999). In shoots, PIN proteins are basally located in the cell corresponding with the direction of auxin flow (Friml, 2003), thus supporting the chemiosmotic hypothesis. To maintain their basal positioning, PIN proteins are proposed to continuously cycle between the plasma membrane and endosomes and may quickly respond to external cues (Geldner et al, 2003, Muday et al., 2003). Recycling of the PIN efflux carriers requires GNOM, an ADP ribosylation factor-GTP exchange factor (ARF-GEF) that regulates vesicle budding (Steinmann et al., 1999). Additionally PID, a protein kinase, is involved in ensuring the proper polarity of PIN (Friml et al., 2004). The exact involvement of PID is not known but it has been shown that high concentrations of PID lead to apical PIN localization and low levels of PID lead to basal localization of PIN (Friml et al., 2004).

Another class of proteins that are linked to auxin eflux belongs to the ATP-binding cassette (ABC) protein family (Luschnig, 2002). This large gene family is composed of several smaller clusters, of which cluster II are proposed to contain proteins that may be involved in auxin transport (Noh et al., 2001). Cluster II ABC proteins have several membrane-spanning domains and a cytosolic ATP-binding site. The multidrug resistance (MDR) and multidrug-related (MRPs) proteins belong to this group and have been shown to directly or indirectly remove substrates, such as organic anions, from the cytosol by hydrolyzing ATP (Noh et al., 2001). Plants mutant for AtMRP5 and AtMDR1 have defects similar to other auxin transport mutants such as decreased primary root elongation, early lateral root initiation and decreased apical dominance (Luschnig, 2002). It is suggested that these proteins may act independently or along with other transport proteins to transport auxin across the plasma membrane (Luschnig, 2002).

The importance of influx in polar transport has not been as well established as efflux but auxin influx carriers are proposed to catalyze the uptake of auxin from the extracellular space. The *AUX1* gene encodes a component of an influx carrier (Bennett at al., 1996, Marchant et al., 1998). *aux1* mutants have roots that are agravitropic, show decreased sensitivity to auxin and have defects in embryo patterning (Parry et al., 2001). Moreover, the agravitropic phenotype is rescued by exogenous application of 1-NAA, a highly permeable auxin that bypasses the influx carrier (Yamamoto and Yamamoto, 1998; Marchant et al., 1999). AUX1 is expressed in the shoot apical meristem; however, no shoot defects are apparent in *aux1* plants suggesting that different proteins may be involved in influx in the roots and shoots (Pickett et al., 1990; Marchant et al., 1999; Marchant et al., 2002). Influx is proposed to be important for directing the initial flux of auxin into leaf primordia as inhibiting influx with the chemical NOA, which sufficiently phenocopies *aux1* in roots, causes defects in the positioning of primordia but does not abolish organogenesis (Imhoff et al., 2000; Swarup et al., 2001). Plants mutant for AXR4, a proposed regulator of the influx carrier (Yamamoto and Yamamoto, 1999), are resistant to auxin, have agravitropic roots and the aerial portion of the plants is largely wild type (Hobbie and Estelle, 1995).

Other possible groups of genes controlling auxin influx in shoots are the LAX (Like AUX1) and ANT1 proteins. LAX proteins were identified based on their significant homology to AUX1 (Parry et al., 2001). ANT1 belongs to a small family of amino acid transporters that has been shown to transport IAA and 2,4-D (Chen et al., 2001). The role of these proteins in auxin influx has yet to be defined. More components

of auxin influx need to be identified to further characterize the role influx plays in developmental and regulatory processes.

Regulated auxin transport, both efflux and influx, is necessary to ensure that the proper cells receive auxin in order to respond and develop appropriately. Once inside the cell, auxin signals a cascade of events that eventually leads to the regulation of Aux/IAA gene expression. The signal cascade in response to auxin is proposed to initiate at the plasma membrane where IAA binds to ABP1 (auxin-binding protein 1), a specific receptor at the plasma membrane (Jones et al., 1998, reviewed in Napier, 1995). ABP1 primarily resides in the ER, but continuously cycles between the plasma membrane and the ER (Warwicker, 2001). It has been shown that binding of auxin to ABP1 can cause numerous changes at the cell membrane including modifications to ion channels or transporters (Napier et al., 2002).

Auxin is thought to modify the expression of auxin-inducible genes through a complex degradation pathway involving the SCF protein complex. SCF catalyzes the ubiquitination of specific proteins that targets them for degradation (Patton et al., 1998). The F-box subunit of SCF directly interacts with the targeted proteins allowing the Cullin and RBX1 subunits to catalyze the addition of ubiquitin, targeting the proteins for proteolysis by 26S proteosomes (Leyser, 2002). Support for the auxin-induced ubiquitination of target proteins is mounting as specific proteins involved in this system are identified (Leyser et al., 1993; Ruegger et al., 1998; del Prozo et al., 1998). Auxin's involvement in this pathway is not fully understood, though it is thought that auxin directly or indirectly increases the affinity of the F-box for the target proteins (Leyser,

2002). One model suggests that auxin initiates a phosphorylation cascade, the end product then mediating ubiquitination (Skowyra et al., 1997).

Aux/IAA proteins are some of the proteins targeted for degradation by SCF resulting in an endogenously short half-life (Leyser, 2002). Aux/IAA proteins also have a nuclear localization sequence allowing them to enter into the nucleus and modify gene expression by binding to auxin response factors (ARFs) (Leyser, 2002). In the absence of AUX/IAAs, ARF homodimers bind to auxin response elements (AREs) in auxin-regulated genes to up regulate gene expression (Ulmasov et al., 1997). A repeated sequence (TGTCTC-containing motif) has been shown to be sufficient to bind ARFs. An auxin-inducible reporter gene construct, DR5:GUS, was created by fusing tandem repeats of a modified ARE motif to the GUS reporter gene (Ulmasov et al., 1997). This construct enables the response to high levels of auxin to be easily assessed in plant tissues by providing the 5-bromo-4-chloro-3-indoyl glucuronide (x-gluc) substrate.

One well-characterized auxin response pathway in early embryonic development involves ARF5/MONOPTEROS (MP) (Hardtke and Berleth, 1998; Ulmasov et al, 1999), AUXIAA12/BODENLOS (BDL) (Hamann et al, 2002) and CUL1/AXR6 (Hellmann et al., 2003). *bdl*, *mp,* and *axr6* mutants are defective in apical-basal patterning in the embryo resulting in seedlings that lack basal structures (Berleth and Jurgens, 1993, Hardtke and Berleth, 1998; Hamman et al., 1999; Hobbie et al., 2000). Double mutant analyses have shown that all three are involved in the same pathway (Hellmann et al., 2003). The *mp* mutation is a loss of function allele consistent with the idea that MP cannot activate downstream genes in response to auxin. On the other hand, *bdl* is a gain of function mutation such that BDL, which normally binds to and represses ARFs, is not

degraded. Thus ARFs are continuously repressed causing the same negative effect on gene expression as the *mp* mutant (Hellmann et al., 2003). AXR6 is a component of the SCF complex and thus normally functions to degrade AUX/IAA proteins, such as BDL (Hellmann et al., 2003). *axr6* mutants are proposed to have an increased concentration of BDL causing the formation of BDL MP dimers and subsequent decreased gene expression in response to auxin (Hellmann et al., 2003). There are at least 24 AUX/IAA (Zrogg et al., 2001) and at least 10 ARF proteins (Ulmasov et al., 1999) that may interact in overlapping and distinct pathways to finely tune the cellular response to auxin.

The formation of files of vascular cells depends on both auxin transport and auxin response. The 'signal-flow canalization' hypothesis of auxin transport helps to explain vascular tissue development with respect to auxin transport and cellular response to auxin (Sachs, 1981, 1989, 1991). In this model, a small increase in the concentration of auxin in a cell ultimately causes more auxin to accumulate in that cell while draining neighboring cells of the hormone (Nelson and Dengler, 1997). The increased amount of auxin is proposed to cause the cell to become more efficient at transporting auxin as it elongates and situates auxin efflux carriers to the basal end of the cell. Furthermore, increased levels of auxin trigger the cells to differentiate into mature vascular tissue. Because of basipetal auxin transport, downstream cells accumulate auxin and the net effect is the formation of a canal of mature vascular tissue called a vein.

Mutants with defects in auxin transport or response may also have altered vasculature, consistent with the auxin canalization model. As well as being defective in polar auxin transport, *pin1* mutants have increased vasculature along the margin of leaves (Mattsson et al., 1999; Steinmann et al., 1999). *mp, bdl* and *axr6* are defective in auxin

response and show a reduction in cotyledon vasculature (Hardtke and Berleth, 1998; Hamman et al., 1999; Hobbie et al., 2000; Steynen and Schultz, 2003). AXR1 is involved in auxin response through an ubiquitin-degredation pathway (del Pozo and Estelle, 1999) and AXR2 is an auxin-inducible AUX/IAA protein (Nagpal et al., 2000). *axr1* and *axr2* mutants show a variety of auxin-related defects including a simplified vascular pattern (Steynen and Schultz, 2003). Furthermore, VASCULAR NETWORK (VAN) proteins are putative regulators of internal cell patterning and *van7* mutants, which are allelic to *gnom,* show disruptions in minor veins in leaves (Koizumi et al., 2000). *forked-1 (fkd-1)* mutants also show disrupted vascular patterning in leaves and the FKD-1 protein is proposed to respond to threshold levels of auxin required for distal vein meeting in leaves (Steynen and Schultz, 2003).

While the canalization model explains the differentiation of xylem and phloem from existing parenchyma cells it does not account for the existence of prepatterning of specific cells to become vasculature (Sachs 1990; Sachs 1991). Several vascular patterning mutants have been identified with unclear links to auxin canalization. The *cvp* (*cotyledon vascular pattern*) mutants show cotyledons with decreased vein meeting, however auxin synthesis, transport and perception appear normal (Carland et al, 1999). The altered venation pattern is due to a defect in the underlying prepatterning of cells to become vasculature that does not appear to depend on auxin canalization (Carland et al. 1999). CVP1 is a sterol methyltransferase and is important for signaling involved in cell differentiation and elongation along the cell axis (Carland et al., 2002). Sterol signaling has also been implicated for patterning processes beyond vasculature (Otsuga et al., 2001; McConnell et al., 2001). CVP2 is an inositol triphosphate signal that may regulate several

second messengers, including Ca^{2+}, important in a signal transduction pathway that leads to the specification of cells for a vascular cell fate (Carland and Nelson, 2004). The *scarface (scf)* mutant shows disrupted vascular patterning in leaves but shows normal differentiation resulting in a mutant phenotype that lacks vascular meeting (Deyholos et al., 2000). VEIN PATTERNING1 (VEP1) is a protein involved in apoptosis and *vep1* mutants show a reduction in vein meeting and a decrease in the total number of minor veins in leaves (Yang et al., 1997). The identification of such mutants suggests that the development of vascular patterns is a complex process involving several distinct and overlapping mechanisms in addition to auxin canalization.

A model is emerging to explain the role of auxin in the development of leaf venation patterns. Polar auxin transport creates sites of auxin maxima in the leaf where strong cellular auxin responses are evident (Aloni, 2003; Mattsson et al., 2003). Initially, an external source of auxin is transported into emerging leaf primordia from the stem vascular system toward the distal tip creating a strong distal auxin response that drives formation of the midvein (Aloni, 2003; Benkova et al., 2003; Reinhardt et al., 2003; Steynen and Schultz, 2003). Efflux carriers are localized and leaves with polar auxin transport inhibited by NPA or the *pin1* mutation show no distal auxin response or midvein differentiation (Mattsson et al., 1999; Sieburth, 1999). This result suggests that auxin efflux is required for midvein differentiation. Next, a secondary, internal source of auxin is positioned along the leaf margin, and internal transport accounts for the differentiation of secondary veins (Mattsson et al., 1999; Sieburth, 1999). In support of this idea, leaves treated with NPA show a ring of DR5::GUS expression along the leaf margin and differentiation of a thick band of vascular tissue follows (Mattsson et al.,

2003; Sieburth, 2003). Furthermore, there may be additional sources of auxin in the lamina of the leaf that have a role in the development of higher order veins (Aloni, 2003; Steynen and Schultz, 2003). Thus both polar auxin transport and auxin response are essential for vascular patterning formation in leaves.

To identify genes controlling the process of vascular development, mutants defective in vascular pattern formation have been isolated in the model plant, *Arabidopsis thaliana*. We have characterized a mutation in a gene named AUTOBAHN (ABN). The *abn* allele shows partial dominance with the heterozygotes showing an intermediate phenotype between that of wild type and *abn* homozygotes. *abn* plants produce leaves that proliferate disorganized, overlapping veins that are parallel to the midvein. Additionally the leaves show no differentiation of higher order veins. Our results suggest that *abn* is defective in carrier-mediated auxin uptake, a process required to establish the secondary source of auxin that allows for the differentiation of higher order veins.

Materials and Methods

Plant Materials

Glabrous (*gl1-1*) seed of Columbia ecotype (Col) used for EMS mutagenesis was obtained courtesy of George Haughn (Department of Botany, University of British Columbia, Vancouver, BC). *pin1-1*, mp^{G92}, mp^{BS1354} *and* mp^{G12} were generously provided by Thomas Berleth (University of Toronto, Toronto, ON) and *bdl* by Gerd Jurgens (University of Tubingen, Tubingen, Germany). DR5::GUS expressing seed was donated by Jane Murfett (University of Missouri, Columbia, MO). *fkd-1* was previously isolated from this laboratory (Steynen and Schultz, 2003). All other seed material was purchased from the Arabidopsis Biological Resource Center (Columbus, Ohio).

Chemicals

i) Hormones and Inhibitors

2,4-dichlorophenoxyacetic acid (2,4-D) and 1-naphthaleneacetic acid (NAA) were purchased from Sigma (St. Louis, MO); naphthylphthalamic acid (NPA) was purchased from Chem Service (West Chester, PA); 1-napthoxyacetic acid (NOA) was purchased from Lancaster Synthesis (Pelham, NH).

ii) AT medium (Estelle and Somerville, 1987)

$Ca(NO_3)_2$, $MgSO_4$, $MnCl_2$, NaCl and KNO_3 were obtained through BDH Inc. (Toronto, ON); KH_2PO_4, H_3BO_3, $CuSO_4$, $ZnSO_4$, Na_2MoO_4 and $CoCl_2$ were obtained from Sigma-Aldrich and FeEDTA was purchased from JT Baker (Phillipsburg, NJ). Agar was purchased from EM Science (Gibbstown, NJ).

iii) PCR and Gel Electrophoresis

KCl was from Fisher Scientific (Fair Lawn, NJ); ethidium bromide was purchased from Sigma; DNTP's and primers were synthesized by Invitrogen (Burlington, ON); Taq DNA Polymerase was purchased from Fischer Scientific (Ottawa, ON); agarose was purchased from EM Science; all other chemicals were purchased from BDH Inc..

iv) GUS Staining and Leaf Clearing (Kang and Dengler, 2002)

5-bromo-4-chloro-3-indoyl glucuronide (X-gluc) was purchased from Rose Scientific; $K_3Fe_3(CN)_6$ and dimethyl formamide were purchased from Sigma. $NaPO_4$ and EDTA were obtained from BDH Inc.; nonidet P40 was obtained from EM Science.

v) Solvents and Others

Dimethyl sulfoxide (DMSO) and ethyl methane sulfonate (EMS) were purchased from Sigma-Aldrich. Cytoseal was obtained though Stephen's Scientific (Kalamazoo, MI). All other chemicals and solvents were obtained from VWR.

Growth Conditions

Seed were either planted on Metromix 200 soil (W.R. Grace Co., Marysville, OK) in 100 cm^2 pots or on Petri plates containing Arabidopsis thaliana (AT) growth medium (Ruegger et. al., 1997). Pots were covered with plastic and both pots and plates were incubated at 4°C in the dark for 3 days, after which they were transferred to growth chambers (Percival Scientific, Perry, IA) with 24 hours of light at an intensity of 130 $\mu mol \bullet sec^{-1} \bullet m^{-2}$ from Sylvania Cool White, Grow Lux, and incandescent bulbs (Osram Sylvania Inc, Danvers, MA). Chambers were set at 20°C and 60% relative humidity. The

day of transfer to the growth chambers was considered to be the day of germination or 0 days after germination (DAG). Plastic wrap from the pots was removed 7 DAG.

Mutagenesis and Mutant Isolation

Approximately 2000 Columbia ecotype *gl1-1* seeds were treated with 0.25% v/v EMS for 16 hours then rinsed with distilled water and air dried on filter paper. The resultant M1 seeds were sown on soil at a density of 50 seeds per pot, grown to maturity and single plant M2 seeds were harvested for mutant screening. M2 seeds were sown on soil at a density of 25 seeds per pot. Cotyledons and first leaves were screened for aberrations in venation patterning at 14 DAG. Tissues were mounted in cytoseal, which provides partial clearing, and analyzed using a dissecting microscope. Putative vasculature mutants were grown to maturity and M3 seed was harvested and subsequently re-screened. The *abn* mutant was one of several identified from this initial screen. *abn* was back-crossed to Col three times before any analysis was performed.

Microscopy and Imaging

A Stemi 2000 dissecting light microscope was used for analysis of mature cotyledons, leaves and flowers (Carl Zeiss Inc., Thornwood, NY). Tissues were viewed using a CCD camera (RS-170, Cohu Inc., Electronics Division, San Diego, CA) that connected the microscope to a computer with NIH Image (http://rsb.info.nih.gov/nih-image/).

For cotyledon and leaf developmental analysis and the assessment of the effect of auxins and inhibitors on such development, an Eclipse E600 compound light microscope

was used (Nikon, Mississauga, ON). All photographs were taken with a Coolpix 990 digital camera (Nikon, Mississauga, ON) and images were adjusted using Adobe Photoshop 5.0 (Adobe Systems Inc., San Jose, CA).

Mapping

abn was crossed into the Landsberg (Ler) background and F2 seed was obtained for the mapping population. DNA was extracted from the leaves of plants showing the homozygous mutant phenotype according to Dellaporta et al. (1983). PCR-based mapping was performed using simple sequence length polymorphisms (SSLPs) between Col and Ler as described in Bell and Ecker (1994).

Phenotypic Analysis of Foliar Organs

To analyze and compare the cotyledons and leaves of all genotypes, seed were sown on soil at a density of 9 seed per pot. Cotyledons and first leaves were removed and mounted in cytoseal at 14 DAG and 21 DAG respectively. The shape and vascular pattern of tissues were scored using NIH Image. The shape was scored at the blade midpoint as a ratio of length to width. The vascular pattern was scored for the number of freely ending veins (FEV), branch points (BP), areoles, and vascular islands (VI). Additionally, the distance from the margin of the blade to the external-most vein was scored from both sides of the blade at the midpoint.

To assess floral morphology, whole flowers from *abn* homozygotes and Col flowers were removed and dissected when their petals had fully emerged. Dissections were performed under a dissecting light microscope and were scored for the number and

position of sepals, stigma, petals and stamens. In addition, the sepals and petals were cleared in 70% ethanol and the vascular pattern was scored using a compound light microscope.

Phenotypic Analysis of Whole Plant

To analyze whole plant morphology, F2 seed were sown on soil at a density of 9 seed per pot. Plants were scored for phyllotaxy, time of emergence of rosette leaves, time to flowering. Additionally the total number of rosette leaves, height of primary inflorescence, and number of main and secondary inflorescences were determined at 28 DAG. We also determined the rate of leaf intiation in wild type and an F2 population segregating for *abn*. The total number of rosette leaves was measured every 48 hours between 12 DAG and 21DAG and the rate was calculated as the number of leaves/day.

To assess root phenotype, *abn* F2, Col and *axr1-12* seed were planted on both AT plates and plates containing 1μM 2,4-D. Six seed were planted per plate and were grown vertically. Roots were scored for the length of the primary root at 7 DAG; the number of lateral roots (LRs), the distance from the root apical meristem (RAM) to the distal-most LR, and the length of the LRs were measured at 14 DAG. Additionally, root gravitropism was determined by rotating the plates 90° and measuring the ability to respond to gravity after 24 hours.

To assess stem vasculature, *abn* homozygote, heterozygote and Col wild type stems were sectioned by hand and stained with toluidine blue. Vascular pattern was viewed under a compound light microscope.

Generation of Double Mutants

Double mutants were generated between *abn* and the following mutants: *mp, axr6-2, bdl, pin1-1, axr2, axr1-12, axr4-2, fkd-1* and *aux1-7.* Double mutants were found in the F2 generations with the expected frequency (Table 1). Additionally, *mp* and *axr1-12* segregation data supports the molecular mapping of ABN to chromosome 1 (Table 1). For *bdl, axr2, axr1-12, axr4-2, fkd-1* and *aux1-7* double mutants, seed from the F2 plants that were heterozygous for *abn* but homozygous for the double mutant was harvested. Mature analysis on the cotyledons and leaves was done on the resultant F3 plants, with the exception of *axr1-12*and *axr2-1*, which were analyzed in an F2. For *mp, axr6* and *pin1-1*, the F2 seed was used for mature analysis as both mutants are infertile and a homozygous population was not obtainable.

Leaf Developmental Analysis on AT, NPA, NOA, 2,4-D and NAA

abn plants expressing the DR5:GUS fusion were created by crossing *abn* mutants with DR5:GUS plants (Ulmasov et al., 1997). F2 plants were screened for those showing root tip GUS expression and segregating for the *abn* mutation. These lines were pooled and used for all analysis. *abn* DR5:GUS and wild type DR5:GUS seeds were planted at a density of 50 seed per plate on unsuplemented AT plates and AT plates containing 30μM NPA, 30μM NOA, 1μM 2,4-D or 0.4 μM NAA. 100 *abn* DR5:GUS F2 seedlings and 25 DR5:GUS seedlings were GUS-stained and cleared as described by Steynen and Schultz (2003) for each day of analysis. Seedlings were dissected by hand under a dissecting microscope and were mounted on slides with 50% glycerol. Analysis was done using a compound light microscope.

Results

Mutant Isolation and Mapping

A population of Columbia ecotype (Col-0) Arabidopsis seed was mutagenized with EMS and the resultant M1 generation was single plant harvested. M2 families were screened for putative leaf vascular patterning mutants. We identified from this initial screen a mutant that proliferates disorganized, overlapping veins that develop parallel to the midvein in both the cotyledons and leaves. The resulting vascular pattern looks like a multi-lane highway of veins, therefore, we named the mutant *autobahn (abn). abn* plants produce narrow, irregularly shaped leaves and are male sterile. The remaining plant morphology appears normal.

After back-crossing *abn* to wild-type, the F1 has a vascular pattern phenotype intermediate between the *abn* homozygote and wild type in both the cotyledons and leaves. The F2 population segregates in accordance with Mendelian ratios for a single, nuclear, semi-dominant mutation (1:2:1, $x^2 = 0.613$, df = 2, n=1043).

In order to map the ABN gene, *abn* was crossed to Landsberg erecta (Ler) and the segregating F2 population was used for molecular mapping (Bell and Ecker, 1994). The ABN gene mapped to Chromosome I to a position of 24 cM using the simple sequence length polymorphism markers nga248 (1-40) (R.F.=15.8%, n=48 chromosomes) and nga63 (1-11) (R.F.=13.6%, n=82 chromosomes).

First Leaf Phenotype and Vascular Development

In order to characterize the *abn* leaf phenotype, the mature vascular pattern of *abn* homozygotes, *abn* heterozygotes and wild type leaves was quantified and compared (Table 2). We scored the complexity and openness of the vascular pattern by determining the number of freely ending veins (FEV), branch points (BP), areoles (an area completely enclosed by veins) and vascular islands (VIs) (Table 2). The placement of the vascular pattern was assessed by determining the margin size, providing a measure of whether the veins are centralized or expand towards to the margin. The margin size was scored by measuring, at the midpoint of the blade, the distance from the margin to the outer-most vein on each half of the leaf and then averaging the distances and dividing by the total leaf width. Thus, a larger margin represents a more centralized venation pattern. Finally, the shape of the leaves was determined as the ratio of the length to the width at the blade midpoint.

Wild type leaves have a single midvein, several secondary loops that most often meet proximally, and higher order veins that either end freely in the leaf lamina or connect with veins other than the midvein to form small, closed areoles (Figure 1a). The *abn* heterozygous venation pattern is similar to wild type in that it consists of a single midvein, several secondary branches that form areoles, and higher order veins that branch into the lamina. A distinction from wild type is seen at the distal tip of the midvein, where the initial secondary veins often branch slightly proximal to the distal tip of the midvein and several small veins form at this site (Figure 1b). Whereas in wild type the distal junction between the first secondaries is relatively smooth, the additional veins in *abn* heterozygote leaves results in a much more complex, disorganized junction.

Additionally, the secondary branches are not as regularly spaced as in wild type and the vasculature is significantly more centralized than in wild type (Table 2). Furthermore the leaf shape of *abn* heterozygotes is more elongate than wild type (Table 2). The venation pattern of *abn* homozygotes (Figure 1c) is much more centralized and has reduced complexity compared to both wild type and *abn* heterozygotes (Table 2). Branches from the midvein are more randomly spaced and develop at irregular angles compared to wild type (Figure 1c). Furthermore, the size and shape of aeroles are irregular in *abn* homozygotes and *abn* leaf shape is significantly more elongate compared to wild type and heterozygous leaves (Figure 1c, Table 2).

To study the development of the vascular pattern, we assessed developing first leaves for the appearance of xylem cell wall thickening, which we considered equivalent to the differentiation of veins. In wild type, the differentiation of the midvein, which connects to the stem vasculature and extends to the distal tip of the leaf, is complete at 6 DAG. Two distal secondary veins branch from the distal tip of the midvein and differentiate in opposite directions along the margin. They loop back into the lamina in a basipetal direction and reconnect to the midvein at a more proximal location by 7 DAG. Additional secondary veins branch from existing secondaries and are regularly spaced. They develop in the same direction as previous secondaries and connect to the midvein proximally. Tertiary veins branch from the secondaries and quaternary branch from tertiaries. The later secondary veins develop simultaneously with higher order veins to create the mature reticulate vascular pattern. The development of the *abn* heterozygous leaf vascular pattern is a very similar to wild type with the midvein differentiating at 6 DAG and secondary branches extending from it and differentiating basipetally. The

midvein of *abn* homozygous leaves also differentiates first and is complete at 6 DAG, although it terminates farther from the distal tip than in wild type. There are no clear secondary branches that form at the distal tip of the midvein; rather, subsequent veins initiate at proximal points along the midvein and differentiate apically. These veins have a similar appearance and form very close to the midvein producing a mature phenotype that appears to be the result of a proliferation of midveins without the development of regularly patterned secondary veins.

Characteristics of the *abn* first leaf vein and midrib thickness support our hypothesis that *abn* leaves proliferate midveins at the expense of higher order veins. The midvein is the thickest vein in leaves with higher order vein thickness decreasing hierarchically (Nelson and Dengler, 1997; Dengler and Kang, 2001). The mid rib develops along with the midvein: leaves with midveins occupying more cells develop mid ribs that are correspondingly more pronounced (Nelson and Dengler, 1997). In *abn* leaves, all veins are of similar thickness to the wild type midvein. As well, the mid rib in *abn* leaves is more pronounced than in wild type.

Cotyledon Phenotype

Cotyledons have a much simpler venation pattern than leaves and thus cotyledons are useful for assessing basic patterning defects. We quantified the mature venation pattern of *abn* homozygotes, *abn* heterozygotes and wild type cotyledons by the same criteria as leaves (Table 3). Wild type cotyledons have a single midvein and most often 4 secondary veins that loop to form 4 areoles (Figure 2a). However there are occasionally

fewer areoles (average = 3.4) due to a smaller number of secondary veins or secondary veins that do not meet the midvein proximally.

Like wild type, *abn* heterozygote cotyledons always have a single midvein and most often four secondary veins that form closed areoles (Figure 2b). In contrast to wild type cotyledons, but like *abn* heterozygous leaves, the heterozygous cotyledons have additional veins that often extend from the distal tip of the midvein and either end freely or close to form small areoles. Thus *abn* heterozygotes have a more complex vascular pattern than wild type (Table 3). The placement of veins and the cotyledon shape are not significantly different to wild type (Table 3).

Like *abn* homozygous leaves, *abn* homozygote cotyledons have a disorganized vein pattern that consists of a midvein from which additional veins extend distally from the midvein at irregular positions (Figure 2c). The venation of *abn* homozygotes is significantly more complex and is more centralized than either heterozygote and wild type cotyledons (Table 3). Additionally, *abn* homozygote cotyledons are significantly more elongate than either wild type or heterozygote cotyledons (Table 3). Like the leaf phenotype, we believe the mature cotyledon phenotype is the result of midvein proliferation; however, we were unable to assess the development of the venation pattern in *abn* cotyledons; the sterility of *abn* homozygotes requires that a segregating population be used for all analyses. Within this population, the genotype of individual plants is certain only after the mature vascular pattern has been established in the cotyledons.

Auxin Response in *abn* Leaves

DR5:GUS Expression Pattern

Auxin plays a critical role in the development of leaf vascular patterns. Current models suggest that there are predominantly two distinct sources of auxin involved in leaf vascular development. The external, primary auxin source is transported into the leaf and is required for midvein development (Benkova et al., 2003; Reinhardt et al., 2003). The internal, secondary auxin source along the margin is transported into the interior of the leaf and may account for the development of secondary veins (Mattsson et al., 1999; Sieburth, 1999). The mature vascular pattern of *abn* leaves appears to result from a proliferation of midveins with no higher order vein differentiation, which may result from a defective secondary auxin source. Two models are consistent with such a defect: 1) *abn* leaves have aberrant cellular responses to auxin required for higher order vein differentiation or 2) *abn* leaves are defective in auxin transport required for higher order veins.

To test if *abn* leaves show altered auxin response, *abn* was introduced into the DR5:GUS background to assess auxin response in the leaves. This line, segregating for *abn* and homozygous for the DR5:GUS construct, was grown on AT plates and seedlings were scored at 24-hour intervals. We compared the intensity and pattern of DR5:GUS expression in *abn* leaves to that in wild type (Table 4). We found no change in the intensity of DR5:GUS expression in *abn* but the pattern of expression was altered.

In wild type first leaves, DR5:GUS expression is first evident in a single cell at the distal tip at 4 DAG before any vascular lignification has occurred (90.2%, n=122,

Table 4) (Figure 3a). At 5 DAG, expression remains at the distal tip but is also evident along the marginal zone predicting the position of secondary veins (14.8%, n=121) (Table 4, Figure 3b). As well, DR5:GUS expression is first observed in the lamina at 5 DAG in areas that seem to predict higher order vein formation (14%, n=121, Table 4). This lamina expression is most strongly observed at 6 DAG (39.5%, n=43) (Table 4, Figure 3c). Hydathode DR5:GUS expression is also first observed at 5 DAG, most often in 2 hydathodes (90.3%, n=31, Table 4). Hydathode expression continues through remaining leaf development (Figure 3c,d, Table 4).

Like wild type, *abn* heterozygous first leaves initially express DR5:GUS at the distal tip at 4 DAG (43.6%, n=110, Table 4), but expression is most prominent at 5 DAG (74.4%, n = 86) (Table 4, Figure 3e). The secondary marginal expression is never observed and tertiary expression is much less common than in wild type at 6 DAG (2.4%, n=82) (Table 4, Figure 3f). Furthermore, as in wild type expression in the hydathodes is evident at 5 DAG but is most often seen in only one hydathode (75%, n=4) (Table 4, Figure 3f,g).

Many *abn* homozygous leaf primordia did not expand or show any DR5:GUS expression at 10 DAG (44.3%, n=20, Table 4), which is significantly more than seen in *abn* heterozygotes (28%, n=93, Table 4) or wild type (13.3%, n=60, Table 4). A smaller proportion of *abn* homozygous first leaves express DR5:GUS in the distal tip compared to wild type (22.2%, n=27 at 4 DAG and 30.5% at 6 DAG) (Table 4, Figure 3i). *abn* homozygotes, like heterozygotes, do not express DR5:GUS along the secondary margin; however a thick band of cells just internal to the margin shows expression at 5 DAG (80%, n=30) (Table 4, Figure 3j,k). While this pattern is similar in timing and superficial

appearance to the secondary marginal expression in wild type leaves, we feel it is distinct since the expression is more central and the number of expressing cells staining is increased. As well, expression in this thick band never occurs simultaneously with expression at the distal tip (Table 4). Finally, *abn* homozygous leaves completely lack tertiary and hydathode staining (Table 4, Figure 3l).

In *abn* leaves, the initial auxin response at the distal tip occurs in fewer leaves, but when it does occur, expression is as in wild type. In contrast, subsequent auxin response in *abn* is altered. This suggests that the initial, distal auxin maximum required for the midvein development can form normally, but the internal, marginal auxin is altered. The altered response to the internal, marginal auxin may be due to a change in the source of auxin itself, altered auxin transport from that source, or a change in the cellular response to auxin.

Sepal and Petal Venation Pattern

All floral organs are thought to be derived from leaves. Therefore, we predicted that the venation pattern of other foliar organs in *abn* plants may show defects similar to those observed in leaves. The venation pattern of the sepals and petals in *abn* homozygous and wild type plants was examined and compared. The pattern of wild type sepals usually consists of 3 main veins (avg=3.4, n=43) that most often interconnect to form two closed loops (avg=2.05, n=43). While *abn* sepals have more major veins (avg=8.7, n=99) than wild type, they nevertheless form fewer closed loops (avg=1.72, n=99). The venation pattern of wild type petals always consist of a single main vein with several secondary branches (avg=4.3, n=40). *abn* petals have many more veins than wild

type petals (avg=7.4, n = 31). Thus, like *abn* leaves and cotyledons, *abn* perianth organs seem to proliferate major veins.

Plant Morphology

If an altered auxin response pattern exists in other parts of *abn* plants, we may see phenotypic changes. Additionally, vascular systems have a critical role for ensuring nutrients and water are appropriately transported throughout the plant; thus, the altered venation pattern in *abn* plants may have pleiotropic effects elsewhere in the plant. To assess if the *abn* mutation affects other areas of the plant, we examined *abn* flower, shoot, stem and root morphologies and compared them to wild type.

In addition to the vascular pattern of floral organs, we compared the structure of *abn* and wild type flowers to assess if *abn* shows aberrations in the positioning or number of pistils, stamen, sepals or petals. Wild type flowers consist of 4 concentric organ whorls in which organs are symmetrically arranged around a central pistil. We always observed 6 stamen, 4 petals and 4 sepals in wild type flowers (n=10). In contrast, *abn* homozygous flowers lack symmetrical organ arrangement and show altered numbers of organs as well as organ fusion. *abn* flowers (n=30) consist of a pistil surrounded by fewer stamen (avg=4.6) and petals (avg=2.2) but the same average number of sepals (avg=4.0) as observed in wild type. The morphology of *abn* floral organs is often aberrant; stamens may fuse in pairs (10%) or triplets (6.7%); petals are sometimes tubular (15.6%), folded at their distal tip (26.6%) or fused in pairs (1.6%); sepals also fuse in pairs (20%).

The aerial morphology of *abn* homozygote, *abn* heterozygote and wild type plants was compared by scoring the number of rosette leaves, number of secondary

inflorescences and the height of the plants at 28 DAG (Table 5). Additionally the time of bolting (2 cm inflorescence), flowering, and maturity (1 cm internode between first silique-bearing nodes) was compared between the genotypes (Table 5). Phylotaxy was also measured and no observable difference was discernable between the genotypes.

abn heterozygous plants bolt, produce flowers and mature several days earlier than wild type plants (Table 5). Additionally, *abn* heterozygotes produce fewer rosette leaves, secondary inflorescences and are significantly shorter than wild type plants at maturity (Table 5). Correspondingly, *abn* homozygotes produce bolts, flowers and reach maturation significantly earlier than both *abn* heterozygote and wild type plants (Table 5). Furthermore, *abn* homozygote plants produce significantly fewer rosette leaves, secondary inflorescences and are shorter than both heterozygous and wild type plants at maturity (Table 5). The rate of leaf initiation was determined in an F2 population segregating for *abn*. Within the entire population, the rate of initiation was significantly slower compared to a wild type population (data not shown), suggesting that the *abn* plants have a slower rate of leaf initiation than wild type.

abn homozygous, heterozygous and wild type stems were cross- sectioned and the vascular patterns were compared. There were no visible differences among the genotypes.

Auxin has well quantified effects on roots including response to gravity stimulus, lateral root initiation and elongation of the primary root. To assess auxin-related defects in root phenotype, *abn* homozygote, *abn* heterozygote, wild type and *axr1-12* plants were grown vertically on both unsuplemented AT plates and AT plates containing 1 μM 2,4-D. *axr1-12* plants served as a control group for the effects of 2,4-D.

Roots were scored for the number of lateral roots (LRs), the distance from the root apical meristem (RAM) to the distal-most LR, the length of the LRs, and the density of LRs (length of primary root / number of LRs) (Table 6). Additionally, gravitropism was assessed. For all properties scored, there was no significant difference between *abn* homozygote, heterozygote and wild type roots (Student's t-test, Table 6), while *axr1-12* roots were significantly different from all other genotypes (Student's t-test, data not shown).

Effects of Auxin Response Mutants on the *abn* Phenotype

axr1-12, axr2-1, fkd-1

Plants mutant for *AXR1* and *AXR2* have a decreased sensitivity to auxin (Lincoln et al., 1990; Timpte et al., 1994) and share similar phenotypes including decreased gravitropism, slowed growth of inflorescences, curled rosette leaves due to aberrant marginal leaf cell expansion, and simplified vascular patterns (Hobbie and Estelle, 1995; Steynen and Schultz, 2003). Plants mutant for *FKD1* show leaf specific defects including decreased distal vein meeting and *fkd-1* leaves show a more open vein pattern (Steynen and Schultz, 2003). We assessed *axr1-12, axr2-1* and *fkd-1* in combination with *abn* to provide some insight into the auxin defects in *abn* plants. If *abn* is defective in auxin response, we predict genetic intereactions to occur in the double mutants.

Both *axr1-12* and *axr2-1* have a more open venation pattern (Steynen and Schultz, 2003) and *axr1-12* leaf pattern is also simpler (Tables 2 and 3) (Figures 1d,g and 2d,g). *fkd1* cotyledons (Figure 2j) and leaves (Figure 2d) have significantly more FEV

and consequentially a reduction in the number of areoles and branch points (BPs) (Tables 2 and 3). *fkd1* leaves additionally show a marked increase in the number of vascular islands (VIs) (Table 2). As well, *axr1-12* and *axr2-1* cotyledons and leaves are rounder than wild type (Tables 2 and 3).

axr1-12, *axr2-1* and *fkd-1* in combination with both heterozygous and homozygous *abn* show essentially additive phenotypes. The *axr* double mutant cotyledons (Figure 2e,f,h,i) and leaves (Figure 1e,f,h,i) show a shape intermediate between the single mutants and centralized veins like *abn* single mutants (Tables 2 and 3). Like the *axr* single mutants, the double mutant cotyledons have a more open pattern (Table 3). The *fkd-1* double mutant cotyledons (Figure 2k,l) have an intermediate phenotype with a significant reduction in the number of areoles compared to *abn* single mutants (Table 3). The double mutant leaves (Figure 1k,l) show an intermediate venation pattern with an increase in FEVs like *fkd-1* and a similar number of areoles compared to *abn* (Table 2). The veins of the cotyledons are centralized like *abn* single mutants but are positioned intermediately in the leaves (Tables 2 and 3). These additive phenotypes suggest that ABN functions independently of these genes

mp, bdl and *axr6* Double Mutants

One explanation for the altered auxin response pattern observed in *abn* leaves is that *abn* is defective in a molecular auxin response pathway. MP, AXR6 and BDL act in auxin-response pathways and double mutants between *mp, axr6-2*and *bdl* with *abn* were generated to determine if ABN functions in the same pathway. *mp* and *axr6* mutants lack hypocotyls and roots, have incomplete vasculature in the cotyledons and produce few

leaves (Berleth and Jurgens, 1993; Przemeck et al., 1996; Hobbie et al., 2000), whereas *bdl* mutants have a weaker phenotype with normal shoots with fertile flowers (Hamman et al., 1999).

We observed that *mp* and *axr6-2* seedlings most often produce two cotyledons (70.2%, n=121; 80%, n=45) with severely reduced vasculature (Figure 2ab,y). Most *mp* cotyledons only developed a midvein (43.7%, n=206) and less frequently a midvein and one (25.2%, n=206) or two (14.1%, n=206) incomplete secondary veins that do not reconnect to the midvein to produce closed loops. Occasionally a small loop of vasculature was formed above the distal tip of the midvein (17.0%, n=206) that often had multiple small secondaries extending from it (10.2%, n=206). Most *axr6-2* cotyledons have a midvein and one (15.1%, n=53) or two secondaries (83%, n=53) that do not meet with the midvein proximally. Often there were vascular islands along the region where the secondary loops would usually form (45.3%, n=53) and very rarely the pattern consisted of only a midvein (1.9%, n=53). *bdl* seedlings produce normal shoots with fully developed cotyledons (Figure 2m) and leaves (Figure 1m). In our analysis, *bdl* cotyledons were more round than wild type with otherwise normal vascular pattern (Table 3) and leaves were more round and show a more complex vascular pattern than wild type (Table 2).

mp abn , *axr6-2 abn*, and *bdl abn* double mutants show additive phenotypes suggesting that ABN functions independently from this auxin response pathway. *axr6-2 abn* double mutants (Figure 2aa) make up 21.3 % of the population that is homozygous for *axr6-2* (n=94); like *axr6-2* single mutants they lack roots and a hypocotyl but the cotyledon venation pattern is like *abn* single mutants. While we expect half of the

remaining *axr6-2* seedlings to be heterozygous for *abn* (based on a 1:2:1 *abn* ratio), only 28.4% (n=74) have cotyledons with characteristics similar to *abn* heterozygotes (Figure 2z) indicating that a single copy of the mutant *ABN* gene is often not distinguishable in an *axr6* background. In the *axr6-2 abn* heterozygous cotyledons that had a visible phenotype, the venation pattern consists of a midvein with many small vascular strands at the distal tip and a reduction in the remaining vasculature. There is most often only one (14.3%) or two (33.3%) secondary veins formed that are freely ending proximally and vascular islands are infrequently observed (4.8%). Occasionally the secondary veins do meet distally to the midvein to form a closed loop (33.3%), which is never observed in *axr6* single mutant cotyledons.

The *mp abn* double mutant phenotype appears to be additive as it has characteristics of both single mutants (Figure 2ac): like *mp* single mutants, the seedling lacked a hypocotyl and roots and the venation pattern was like *abn* single mutants. Due to the small number of *mp abn* double mutants, no statistical analysis of the phenotype was possible. As in *axr6-2* seedlings, within the *mp* homozygous seedlings, plants with a single copy of the *abn* mutation were not distinguishable.

The *bdl abn* double mutant phenotype appears to be additive. The cotyledons (Figure 2n,o) have an intermediate venation pattern complexity that is centralized like *abn* single mutants (Table 3), and the leaves, on the other hand, show a venation pattern like *abn* single mutant that is intermediately centralized (Table 2). The cotyledons and leaves have an intermediate shape between the single mutants (Tables 2 and 3).

The additive phenotypes of these double mutants indicate that the aberrant auxin response pattern in *abn* leaves is not due to a defect in the molecular response to auxin.

Another explanation for the altered auxin response pattern in *abn* leaves is that auxin transport is altered. To examine auxin transport, we grew *abn* plants on different sources of exogenous auxin, transport inhibitors and generated double mutants with mutants defective in different aspects of auxin transport.

Effects of Polar Auxin Transport on *abn* Leaf Vascular Patterning

Efflux: NPA and *pin1-1*

pin1-1 mutants are defective in polar auxin transport and sometimes produce leaves with increased marginal venation (Galweiler et al., 1998; Mattson et al., 1999). *pin1-1* cotyledons (Figure 2p) and leaves (Figure 1p) are wider than wild type though the vein pattern does not differ greatly from wild type (Tables 2 and 3). The phenotype of *abn* leaves seems to be enhanced in the *pin1-1* background (Table 2). The *pin1-1 abn* double mutant cotyledons (Figure 2q,r) show an intermediate shape and the venation pattern does not differ significantly from *abn* single mutants (Table 3). The leaves of the double mutants, however, are highly elongated (Figure 1q,r) and the venation pattern is significantly more complex than either single mutant (Table 2). One explanation for the enhancement of the *abn* phenotype in the presence of the *pin1-1* mutation is that some aspect of transport is defective in *abn* and decreasing auxin efflux exacerbates the defect.

The effects of the *pin1-1* mutant can be phenocopied by growing seedlings on the auxin efflux inhibitor NPA which binds to and disrupts the ability of PIN1 to export auxin from cells (Lomax et al., 1995). High concentrations of NPA results in a proliferation of vascular tissue along the leaf margin without the development of a

midvein. Afterward, vascular strands emerge from the marginal zone and develop basipetally to create parallel veins that exit the leaf at the petiole. This observation has led to the hypothesis that the leaf margin is a source of auxin and for normal vascular differentiation in discrete cell files requires auxin efflux to transport auxin away from this source (Mattsson et al., 1999; Sieburth, 1999).

Wild type and *abn* plants expressing DR5:GUS were grown on 30μM NPA to assess the molecular auxin response and vascular development in leaves under the inhibitory effects of NPA. Like untreated leaves, NPA treated wild type leaves initially show an auxin response at the distal tip; however, it is not confined to a single cell but rather is diffuse across several cells (Figure 4a). This response spreads along the margin (Figure 4b). No acropetal midvein differentiation occurs. Later DR5:GUS expression is observed along two loops, one at the margin and one slightly interior to the margin (Figure 4c). Vascular tissue later differentiates basipetally from the interior loop toward the center of the leaf and parallel veins exit the leaf at the petiole. Late DR5:GUS expression is evident throughout the interior of the leaf blade concurrently with the marginal loops (Figure 4d). Unlike untreated wild type leaves, this internal expression pattern in NPA treated leaves does not appear to predict future vascular differentiation. Furthermore, no hydathode expression is evident.

abn heterozygotes show an initial response at the distal tip like wild type leaves (Figure 4e). The auxin response spreads along the margin but is discontinuous (Figure 4f). Like wild type, *abn* heterozygotes show a double loop of expression and vascular tissue forms along the interior loop but the loops are less uniform (Figure 4g). In contrast to wild type, a midvein differentiates acropetally along with the development of veins

from the marginal ring of vasculature. There is very little expression of DR5:GUS evident in the interior of the leaf and none in the hydathodes (Figure 4h).

abn homozygotes treated with NPA most often produce a large number of small leaf primordia (88.2% n =68, Table 4) that never develop into distinct leaves. In contrast, only 58.2% (n=153) of *abn* heterozygotes and a very small number of wild type seedlings (7.7% n=117) proliferate leaf primordia with no subsequent leaf development when treated with NPA (Table 4). Interestingly, this response is reminiscent of the effects of treating NPA induced pins with NOA, an influx inhibitor (Stieger et al., 2002). Later in development some of these primordia develop into leaves that are often tubular with an initial auxin response at the distal tip that is restricted to the distal-most ring of tissue (Figure 4j,k). This expression, in contrast to wild type and *abn* heterozygotes, does not predict vascular development. *abn* homozygote leaves maintain a similar, though more extreme, vascular pattern as untreated seedlings and show a proliferation of midveins. There is never any late DR5:GUS expression predicting higher order veins observed in the interior of the leaf nor in the hydathodes (Table 4, Figure 4l).

Influx: NOA, *aux1-7* and *axr4*

The increased severity of the *abn* phenotype in the presence of NPA or *pin1* suggests that *abn* may be defective in polar auxin transport. Moreover, like NPA-induced pins treated with NOA, *abn* seedlings treated with NPA proliferate undeveloped primordia. This suggests that like NOA, *abn* may inhibit active auxin influx. To test this, we treated *abn* homozygotes, *abn* heterozygotes and wild type seedlings with NOA and additionally generated double mutants of *abn* with *aux1-7* and *axr4-2*.

The molecular function of AXR4 is still unknown though it is proposed to be involved in the regulation of auxin influx (Hobbie and Estelle, 1995). *axr4* plants show global auxin-related defects including a decreased sensitivity to auxin and defects in root gravitropism. They have curled rosette leaves but do not show a vascular pattern defect in the cotyledons and leaves (Hobbie and Estelle, 1995). We found that *axr4-2* cotyledons (Figure 2s) are rounder than wild type though the vascular pattern is indistinguishable (Table 3). *axr4-2* mutants do not show any leaf abnormalities (Figure 1s) (Table 2). *abn* was observed to be epistatic to *axr4-2:* leaves that show the *abn* vascular phenotype do not curl downward like *axr4-2* mutant and are thus indistinguishable from the *abn* single mutants (Figures 1t,u and 2t,u). This suggests that the gene product of *ABN* acts upstream of AXR4 and may be involved with auxin influx in leaves.

To further examine the role of influx in *abn* plants, we generated double mutants with *aux1-7*. AUX1 encodes a protein that facilitates auxin uptake into cells (Marchant et al., 2002). AUX1 regulates the transport of auxin from its source in young leaf primordia toward its sink in root tissues (Marchant et al., 2002). *aux1-7* mutants are defective in AUX1-mediated auxin influx and show defects specific to roots including a reduced number of lateral roots and altered gravitropism (Parry et al., 2001). We found that *aux1* cotyledons (Figure 2v) do not differ significantly from wild type except that they are rounder (Table 3), while the leaves (Figure 1v) are the same shape but have a vascular pattern that is slightly more complex than wild type (Table 2). ABN and AUX1 appear to be functionally independent as the phenotype of the double mutants appears to be additive. The double mutant cotyledons (Figure 2w,x) have an intermediate shape and venation pattern complexity (Table 3). The double mutant leaves (Figure 1w,x) have the

same shape as *abn* single mutants with a venation pattern that shows an intermediate complexity between the two single mutants (Table 3). If ABN is involved directly with auxin influx, these results suggest that there may be a different mechanism for influx in the roots and shoots with AUX1 functioning in the roots and perhaps ABN in the shoots.

NOA, an auxin influx inhibitor, has been shown to phenocopy *aux1* mutants (Parry et al., 2001) and to affect leaf primordial initiation (Stieger et al., 2002). If *abn* is defective in auxin influx, treating wild type with NOA may phenocopy the *abn* leaf phenotype. *abn* and wild type plants expressing DR5:GUS were grown on 30 μM NOA to assess both the molecular auxin response and vascular development in leaves under the inhibitory effects of NOA. Like many *abn* homozygous leaves, NOA treated wild type leaves initially do not show a discrete auxin response at the distal tip but rather show a strong response in a crescent shape along a sizeable region of the distal tip and margin (Table 4, Figure 5a). Later expression is more confined to a lateral region along the distal margin (Figure 5b) with vascular differentiation initiating at the zone of expression and extending proximally (Figure 5b,c). Veins develop parallel to one another and meet distally though no distinct midvein is evident. The final vascular pattern appears similar to untreated *abn* heterozygotes (Figure 5d).

NOA treated *abn* heterozygotes have a similar initial auxin response as NOA treated wild type leaves (Table 4, Figure 5e). Also like wild type, later expression in *abn* heterozygotes is confined to the distal marginal zone and vascular differentiation initiates at the sites of DR5:GUS expression (Figure 5f-h). Unlike wild type leaves, *abn* heterozygous leaves acropetally develop a distinctive midvein (Figure 5g). The final

vascular pattern consists of an abundance of parallel veins with little distal meeting and closely resembles the vascular pattern of untreated *abn* homozygotes (Figure 5h).

abn homozygotes grown on NOA do not show a strong initial auxin response (Table 4, Figure 5i). Later DR5:GUS expression occurs along the periphery of the midvein, interior to the margin (Figure 5j,k). Vascular differentiation in *abn* does not appear to be affected by NOA treatment (Figure 5i-l). NOA treatment appears to phenocopy the *abn* mutation supporting the hypothesis that ABN is involved in auxin influx.

The effects of exogenous auxins on the *abn* phenotype: 2,4 D and NAA

The result that NOA partially phenocopies *abn* in wild type leaves but does not affect the *abn* homozygous phenotype supports the idea that *abn* is defective in auxin influx. If this is true, one would expect a synthetic auxin, such as 2,4-D, that relies on auxin influx to enter cells, to have no effect on the *abn* phenotype.

Wild type leaves treated with 1 μM 2,4-D often do not express DR5:GUS at the distal tip (Table 4). When they do, expression is evident in several cells simultaneously (Table 4, Figure 6a). Strong expression occurs next in a crescent shape that may cover more than half of the developing leaf primordium (Figure 6b). Late expression is constrained to the marginal tip as in untreated leaves (figure 6c,d). Tertiary and hydathode DR5:GUS expression are absent. Vascular differentiation is relatively unchanged however the distal vasculature recedes slightly from the distal tip causing a flattened apical ridge of vasculature (Figure 6d).

abn heterozygotes grown on 2,4-D show similar DR5:GUS expression as wild type at all stages though the strength of the auxin response is somewhat reduced (Table 4, Figure 6e-h). Like wild type leaves treated with 2,4-D, the vasculature in *abn* heterozygote leaves treated with 2,4-D appears unchanged except for a reduction in a prominent distal tip of vasculature to a more flattened apical ridge (Figure 6h). *abn* homozygotes grown on 2,4-D do not appear to have an altered auxin response compared to untreated *abn* leaves and the vascular development also appears unchanged (Figure 6i-l). That 2,4-D does not affect the *abn* phenotype supports the notion that the auxin response changes in *abn* leaves are due to defective carrier-mediated auxin influx.

To further assess if *abn* is defective in carrier-mediated influx or auxin uptake in general, we can expose *abn* plants to 1-NAA. This auxin is able to easily enter cells by diffusion, thus bypassing the influx carrier (Delbarre et al., 1996). If the *abn* defects are the result of a lack of auxin entering the cell, NAA should rescue the *abn* phenotype; however, if the *abn* defects are due to processes that require active auxin influx, NAA should not rescue the phenotype. 1-NAA has been shown to rescue the agravitropic roots of *aux1* plants (Yamamoto and Yamamoto, 1998; Marchant et al., 1999); however, 1-NAA is not able to rescue influx related defects in the shoot as primordial placement defects in plants inhibited with NOA were not rescued with NAA treatment (Stieger et al., 2002).

To assess if auxin response and vascular differentiation in the leaves is affected by 1-NAA, wild type and *abn* plants expressing DR5:GUS were grown on AT plates supplemented with 0.4 μM 1-NAA. For all genotypes, treatment with 1-NAA caused an increase in the number of seedlings whose primordia did not expand or express

DR5:GUS (Table 4). For those primordia that did expand, no change in auxin response or vascular development was noted for any genotype (Figure 7). The lack of phenotypic change in developing primordial supports that *abn* is defective in carrier-mediated auxin influx. Auxin enters *abn* leaves by diffusion thus the availability of a diffusible auxin, 1-NAA, does not change the phenotype. The increase in undeveloped primordia may be the result of increasing the amount of auxin entering the leaf via unregulated diffusion.

Discussion

We have identified a new vascular pattern mutant in *Arabidopsis thaliana* named *autobahn (abn)*. *abn* produces elongated leaves that proliferate disorganized, overlapping veins parallel to the midvein without higher order vein differentiation. *abn* flowers are male sterile and perianth organs have similar vein patterning defects as the leaves. Stems do not show vascular defects and roots have normal auxin responses, thus ABN seems to be specific to foliar organs. All aspects of the *abn* heterozygous phenotype are intermediate between wild type and *abn* homozygous phenotypes indicating that the phenotype is dosage dependent.

We have observed that *abn* leaves have an altered pattern of auxin response from analysis of an *abn* line that contains the DR5:GUS construct. In wild type leaves, three distinct classes of auxin response are evident: 1) primary, at the distal tip, 2) secondary, along the margin and, 3) higher order, in hydathodes as well as areas within the lamina that predict the differentiation of higher order veins (Aloni, 2003). The primary auxin response pattern is proposed to result from auxin entering leaves from the stem and forming a sink at the distal tip (Aloni, 2003; Benkova et al., 2003; Steynen and Schultz, 2003). Auxin from a secondary, internal source exists along the leaf margin and is proposed to be canalized into the leaf interior (Sieburth, 1999; Mattsson et al, 1999). Some *abn* leaves never establish the distal maxima and do not expand or form veins, while others show normal primary DR5:GUS expression and develop midveins. In contrast, the secondary and tertiary auxin responses never occur normally and no higher

order veins form. Thus, the primary transport of auxin into the *abn* leaves can be established normally while the secondary response cannot.

The aberrant secondary auxin response in *abn* may be explained by two different mechanisms: 1) *abn* is defective in the secondary molecular response to auxin or 2) *abn* is defective in auxin transport required for secondary auxin responses. Our results suggest that the altered auxin response pattern observed in *abn* leaves is due to a defect in carrier-mediated auxin influx. *abn* leaves are often not defective in establishing the distal tip maximum required for midvein formation but the defect in auxin influx causes multiple, rather than singular, midveins to differentiate at the expense of higher order veins. Additionally, the secondary source of auxin that is proposed to exist along the margin fails to be established in *abn* leaves and thus no higher order auxin response is observed and subsequent vasculature does not develop. Therefore, we suggest that auxin influx is important for regulated auxin transport into the leaf, activation of the marginal source of auxin and inhibition of the primary auxin source. ABN is a critical component for each of these processes.

abn is defective in carrier-mediated auxin influx

Wild type plants grown on NOA are agravitropic and insensitive to exogenously supplied auxin, thus phenocopying the *aux1* mutant, which is defective in auxin uptake in roots (Imhoff et al., 2000). Previous studies have not examined the effects of NOA on the venation pattern of leaves. When treated with NOA, wild type leaves show an auxin response pattern similar to *abn* followed by a proliferation of midveins that meet distally, closely resembling untreated *abn* heterozygotes. Furthermore, when grown on NOA, *abn*

heterozygote leaves show an altered auxin response pattern and a more extreme venation phenotype that closely resembles untreated *abn* homozygotes. The venation pattern phenotype and auxin response of *abn* homozygotes does not appear to be affected by NOA treatment. The result that NOA phenocopies the *abn* phenotype in wild type and *abn* heterozygous leaves but does not change *abn* homozygous phenotype suggests that *abn* is defective in carrier-mediated influx with a dosage effect seen in the heterozygote.

Double mutants constructed with mutants defective in auxin efflux, auxin response and auxin influx support this idea. Double mutant combinations with *abn* and several well-characterized auxin efflux and response mutants show additive phenotypes indicating that ABN is not involved in these pathways. *aux1-7* is defective in carrier-mediated influx; however, mutant plants show root-specific defects. Since *abn* shows shoot specific defects it is not surprising that *aux1-7 abn* double mutants show an additive phenotype. In contrast, *axr4-2* mutants show both root and shoot defects. The AXR4 protein is proposed to be a regulator of carrier-mediated influx (Hobbie and Estelle, 1995). *aux1-7* is epistatic to *axr4-2* with respect to the root phenotype (Hobbie and Estelle, 1995), and we have found that *abn* is epistatic to *axr4-2* with respect to the shoot phenotype.

Further support for our hypothesis comes from the lack of response of the *abn* phenotype to either 2,4-D or 1-NAA. 2,4-D enters cells via the influx carrier but exits independently of the efflux carrier (Delbarre et al., 1996). If *abn* is defective in carrier-mediated influx, *abn* seedlings should be resistant to 2,4-D. In support of our idea, *abn* seedlings grown on 2,4-D show no detectible change in auxin response or vascular development in the developing leaves whereas, 2,4-D treated wild type leaves show a

slight increase in auxin response at the distal tip and a widening of the vasculature. 1-NAA has been shown to diffuse readily into cells (Yamamoto and Yamamoto, 1998; Marchant et al., 1999) but cannot rescue leaf primordial positioning defects in NOA influx-inhibited plants (Stieger et al., 2002). This suggests that some aspects of leaf formation require auxin to enter via a carrier protein and that entry by diffusion cannot substitute. Developing *abn* leaves grown on 1-NAA show no detectible changes in auxin response or vascular differentiation compared to untreated leaves, supporting our proposal that *abn* is specifically defective in carrier-mediated auxin influx.

Shoots that have both influx and efflux inhibited by NOA and NPA respectively, are unable to undergo leaf organogenesis (Stieger et al., 2002). Consistent with the notion that *abn* is defective in carrier-mediated influx, *abn* plants treated with NPA show a similar phenotype to NOA treated plants exposed to NPA: they often do not form leaves and instead produce a large number of primordia from the SAM. Moreover, in the exceptional case of primordial expansion, leaves are often ring-shaped, similar to the leaves that form when NPA-induced shoot apical pins are exogenously exposed to 1-NAA or further inhibited with NOA and subsequently exposed to exogenous IAA (Stieger et al., 2002).

Unlike *abn* leaves treated with NPA, *abn* leaves without PIN1 show an enhanced *abn* phenotype. This apparent discrepancy is consistent with the reduced severity of the *pin1-1* leaf phenotype compared to NPA treated leaves, that has led to the suggestion that there is considerable redundancy in auxin efflux carriers in the leaves (Gälweiler et al., 1998; Mattsson et al., 1999). An explanation in accordance with the increased severity of the *abn* phenotype in the absence of PIN1 is that combined with the lack of carrier-

mediated auxin influx, decreased efflux causes auxin canalization to be at the control of random diffusion events. The redundancy in efflux carriers allows *abn pin1-1* leaves to retain some polar auxin transport and thus radially symmetrical leaves are not formed as seen with NPA treatment.

In the absence of active influx, cells accumulate auxin by diffusion

We propose that *abn* leaves are defective in active influx. However, auxin responses are evident in *abn* leaves; therefore, auxin enters cells independent of the influx carrier. IAA is able to enter cells both by diffusion and carrier-mediated uptake but cannot diffuse out of cells, thus carrier-mediated efflux is the sole mechanism for exporting auxin (Lomax et al, 1995; Goldsmith, 1997). NOA has been shown to be highly effective in inhibiting carrier-mediated auxin influx; however, NOA is not able to completely block polar auxin transport activity (Parry et al., 2001). This suggests that inhibiting carrier-mediated influx alone is not sufficient to stop auxin from entering cells. If diffusion, a slow and unregulated process, is the sole mechanism for auxin entry into cells in *abn* leaves, many cells will slowly accumulate auxin. In support of this idea, many *abn* leaves never establish a distal maximum, suggesting that diffusion alone is a less reliable process. When the establishment of a pronounced distal auxin response occurs in *abn* leaves, it occurs later than in wild type, further supporting the idea that auxin enters *abn* cells by diffusion.

Active auxin influx has been found necessary to establish an auxin gradient in developing leaves (Stieger et al., 2002). Based on our results, we hypothesize that active influx also regulates the direction of auxin canalization during midvein formation. If

influx is defective, polar auxin transport occurs solely by the action of efflux carriers. The *abn* phenotype is exacerbated when auxin efflux is decreased by introducing defective PIN1 into *abn* plants, suggesting that in *abn* leaves, polar auxin transport is being regulated by efflux carriers alone. Further support for this idea is our finding that NPA-treated *abn* leaves are similar to NPA-induced shoot apical pins treated with NOA and subsequently with IAA. This suggests that some auxin is able to diffuse into *abn* leaves, and allows leaf expansion to occur. However, radially symmetrical leaves form because the auxin gradient required for leaf patterning is not created. Moreover, both 2,4-D and 1-NAA treatment increase the number of primordia that do not expand or differentiate. This suggests that flooding the primordia with diffusible auxin disrupts the gradient required for leaf expansion and development. The effects seem to be more pronounced in *abn* leaves, presumably because of an already impaired auxin transport system.

Active auxin influx is required for higher order vein but not midvein formation

We are proposing that *abn* is defective in carrier-mediated auxin influx. The multiple midveins produced in *abn* leaves and in NOA treated wild type leaves indicate that the midvein differentiates independently of active auxin influx. Auxin efflux, on the other hand, is proposed to be required for midvein differentiation since NPA treated leaves form a ring of vascular tissue along the margin but do not develop a midvein (Mattsson et al., 1999; Sieburth, 1999). Consistent with this requirement, *abn* leaves, which only produce midveins, often cease leaf vascular differentiation and primordial expansion when treated with NPA. The fact that some *abn* leaves treated with NPA maintain midvein formation suggests that the requirement for efflux in midvein

development is not absolute. In the absence of controlled auxin transport, diffusion is sometimes sufficient for midvein formation suggesting that the position of the midvein within the leaf may be prepatterned .

The lack of differentiation of secondary and tertiary veins in *abn* leaves suggests that, in contrast to the midvein, higher order veins require active auxin influx. This further suggests that distinct developmental mechanisms control different levels of vein hierarchy: regulated midvein formation is normally dependent upon auxin efflux from external auxin sources, and higher order vein formation is dependent upon carrier-mediated auxin influx from internal auxin sources.

Active auxin influx is required for secondary, internal auxin responses

Our results suggest that the mechanisms by which auxin maxima are established in leaves are different at different times in development. PIN1is localized toward the distal tip (Benkova et al., 2003), which supports a requirement for auxin efflux in establishing the primary auxin response. Since *abn* has functional auxin efflux, it is not surprising that the primary auxin response in *abn* leaves at the distal tip often appears normal. However, both *abn* and NOA treated leaves often do not develop beyond primordia and do not establish a distal tip maxima suggesting that its establishment is somewhat compromised by the lack of active influx.

abn leaves do not show normal secondary auxin responses, but do show DR5:GUS expression at points proximal to the tip. The pattern of expression and its relationship to vein differentiation suggests that this later expression results from reiterations of the initial distal tip response. Late expression in *abn* leaves consists of a

ring of several individual areas of expression maxima that are similar to the expression observed at the distal tip and multiple midveins differentiate in directions toward the DR5:GUS expression maxima. As well, wild type leaves treated with NOA show reduced secondary DR5:GUS expression. The lack of active influx in *abn* and NOA treated wild type plants results in the reduction or abolishment of secondary auxin responses; thus, influx must be necessary to establish secondary auxin responses. Additionally, secondary auxin responses do not require efflux since wild type plants treated with NPA show secondary DR5:GUS expression. Therefore, we propose that efflux is required to establish the primary distal maximum and that carrier-mediated auxin influx is required to establish secondary auxin response.

The phenotype of *abn* leaves and wild type leaves treated with NOA suggests that carrier mediated influx is involved not only in switching on the secondary marginal auxin source, but also in turning off the primary auxin response. Without carrier-facilitated auxin influx, the secondary auxin source is not established and the primary auxin response continues causing a proliferation in midveins. Two models are consistent with these observations: 1) carrier-mediated influx is required to switch off the primary auxin response directly or 2) carrier-mediated influx is required to switch on the secondary auxin response directly, and the primary auxin response is switched off as an indirect consequence.

A surprising result is that *abn* leaves, defective in carrier-mediated influx, form midveins when treated with NPA whereas NPA treated wild type leaves form no midveins. One clear difference between NPA treated wild type and *abn* leaves is that wild type leaves show a strong secondary auxin response along the leaf margin whereas

abn leaves show no secondary response. One explanation for the formation of a midvein in NPA treated *abn* leaves is that because the secondary auxin response is never established, external auxin entering the primordia via diffusion is more able to direct formation of the midvein. This supports the model that carrier-mediated influx directly switches on the secondary auxin response, which indirectly switches off the primary auxin response.

References:

Aloni R (1995). The Induction of vascular tissues by auxin and cytokinin. In Plant Hormones: Physiology, biochemistry and molecular biology (Davies PJ ed), 531-546. Kluwer Academic Publishers, London.

Bartel B (1997). Auxin biosynthesis. *Annual Review of Plant Physiology and Plant Molecular Biology* **48,** 51–66.

Bell CJ and Ecker J (1994). Assignment of 30 microsatellite loci to the linkage map of *Arabidopsis*. *Genomics* **19**, 137-144.

Benkova E, Michniewicz M, Sauer M, Teichmann T, Seifertová D, Jürgens G and Friml J (2003). Local, efflux-dependent auxin gradients as a common module for plant organ formation. *Cell* **115**, 591-602.

Bennett MJ, Marchant A, May ST, and Swarup R (1998). Going the distance with auxin: Unraveling the molecular basis of auxin transport. *Philosophical Transactions of the Royal Society of London. B* **353**, 1511–1515.

Berleth T and Jurgens G (1993). The role of the *monopteros* gene in organising the basal body region of the *Arabidopsis* embryo. *Development* **118**, 575-87.

Berleth T and Sachs T (2001). Plant morphogenesis: long disntance coordination and local patterning. *Current opinion in Plant Biology* **4**, 57-62.

Blilou I, Xu J, Wildwater H, Willemsen V, Paponov I, Friml J, Heidstra R, Aida M, Palme K and Scheres B (2005). The PIN auxin efflux facilitator network controls growth and patterning in *Arabidopsis* roots. *Nature* **433**, 39-44.

Carland FM, Berg B, FitzGerald J, Jinamornphongs S, Nelson T and Keith B (1999). Genetic regulation of vascular tissue patterning in Arabidopsis. *The Plant Cell* **11**, 2123-2137.

Carland FM, Fujioka S, Takatsuto S, Yoshida S and Nelson T (2002).The identification of *CVP1* reveals a role for sterols in vascular patterning. *Plant Cell* **14,** 2045-2058.

Carland FM and Nelson T (2004). *COTYLEDON VASCULAR PATTERN2*-mediated inositol (1,4,5) triphosphate signal transduction is essential for closed venation patterns of Arabidopsis foliar organs. *The Plant Cell* **16**, 1263-1275.

Casimiro I, Marchant A, Bhalerao RP (2001). Auxin transport promotes Arabidopsis lateral root initiation. *The Plant Cell* **13**, 843-52.

Chen L, Ortiz-Lopez A, Jung A and Bush DR (2001). *ANT1*, an aromatic and neutral amino acid transporter in Arabidopsis. *Plant Physiology* **125**, 1813-1820.

Delbarre A, Muller P, Imhoff V, and Guern J (1996). Comparison of mechanisms controlling uptake and accumulation of 2,4-dichlorophenoxyacetic acid, naphthalene-1-acetic acid, and indole-3-acetic acid in suspension-cultured tobacco cells. *Planta* **198**, 532-541.

Dellaporta SL, Wood J, and Hicks JB (1983). A plant DNA minipreparation: version II. *Plant Molecular Biology Reports 1, 19.*

Dengler N and Kang J (2001). Vascular patterning and leaf shape. *Current opinion in Plant Biology* **4**, 50-56.

Deyholos M, Cordner G, Beebe D and Sieburth LE (2000). The *SCARFACE* gene is required for cotyledon and leaf vein patterning. *Development* **127**, 3205-3213.

Estelle M (1998). Polar auxin transport: new support for an old model. *The Plant Cell* **10**, 1775-78.

Estelle MA and Somerville C (1987). Auxin-resistant mutants of *Arabidopsis thaliana* with an altered morphology. *Molecular and General Genetics* **206,** 200-206.

Friml J (2003). Auxin transport - shaping the plant. *Current Opinions in Plant Biology* **6**, 7-12.

Friml J, Yang X, Michniewicz M, Weijers D, Quint A, Tietz O, Benjamins R, Ouwerkerk PBF, Ljung K, Sandberg G, Hooykaas PJJ, Palme K and Offringa R (2004). A PINOID-dependent switch in apical-basal PIN polar targeting directs auxin efflux. *Science* **306**, 862-865.

Friml J, Benkova E, Blilou I, Wisiewska J, Hamann T, Ljung K, Woody S, Sandberg G, Scheres B, Jurgens G, Palme K (2002). AtPIN4 mediates sink-driven auxin gradients and root patterning in *Arabidopsis*. *Cell*, **108**, 661-73.

Gälweiler L, Guan C, Müller A, Wisman E, Mendgen K, Yephremov A, Palme K (1998). Regulation of polar auxin transport at AtPIN1 in *Arabidopsis* vascular tissue. *Science*, **282**, 2226-2230.

Geldner N, Anders N, Wolters H, Keicher J, Kornberger W, Müller P, Delbarre A, Ueda T, Nakano A, Jürgens G (2003). The *Arabidopsis* GNOM ARF-GEF mediates endosomal recycling, auxin transport, and auxin-dependent plant growth. *Cell* **112**, 219-230.

Goldsmith MHM (1997). The polar transport of auxin. *Annual Review of Plant Physiology* **28**, 439-478.

Hamann T, Benkova E, Bäurle I, Kientz M, Jürgens G (2002). The *Arabidopsis BODENLOS* gene encodes an auxin response protein inhibiting *MONOPTEROS*-mediated embryo patterning. *Genes and Development*, **16**, 1610-1615.

Hamann T, Mayer U, Jürgens G (1999). The auxin-insensitive *bodenlos* affect primary root formation and apical-basal patterning in the *Arabidopsis* embryo. *Development*, **126**, 1387-1395.

Hardtke CS and Berleth T (1998). *Arabidopsis* gene *MONOPTEROS* encodes a transcription factor mediating embryo axis function and vascular development. *EMBO*, **17**, 1405-1411.

Hellmann H, Hobbie L, Chapman A, Dharmasiri S, Dharmasiri N, del Pozo C, Reinhardt D, Estelle M (2003). *Arabidopsis AXR6* encodes CUL1 implicating SCF E3 ligases in auxin regulation of embryogenesis. *EMBO*, **22**, 3314-3325.

Hobbie L, McGovern M, Hurwitz LR, Pierro A, Liu NY, Bandyopadhyay A, Estelle M (2000). The *axr6* mutants of *Arabidopsis thaliana* define a gene involved in auxin response and early development. *Development*, **127**, 23-32.

Hobbie, L and Estelle, M (1995) The axr4 auxin-resistant mutants of *Arabidopsis thalaiana* define a gene important for root gravitropism and lateral root initiation. *The Plant Journal,* **7,** 211-220.

Imhoff V, Muller P, Guern J, Delbarre A (2000) Inhibitors of the carrier-mediated influx of auxin in suspension-cultured tobacco cells. *Planta* **210,** 580-588

Jones AM, Kyung-Hoam I, Savka MA, Ming-Jing W, DeWitt NG, Shillito R and Binns AN (1998). Auxin-dependent cell expansion mediated by overexpressed auxin-binding protein 1. *Science* **282,** 1114-1117.

Jürgens G (2001). New EMBO member's review: apical-basal pattern formation in Arabidopsis embryogenesis. *EMBO* **20,** 3609-3616

Kang J and Dengler N (2002). Cell cycling frequency and expression of the homeobox gene *ATHB-8* during leaf vein development in *Arabidopsis*. *Planta* **216,** 212-219.

King JJ, Stimart D, Fisher R and Bleecker A (1995). A mutation altering auxin homeostasis and plant morphology in *Arabidopsis*. *Plant Cell* **7,** 2023-2037.

Koizumi K, Sugiyama M and Fukuda H (2000). A series of novel mutants of *Arabidopsis thaliana* that are defective in the formation of continuous vascular network:

calling the auxin signal flow canalization hypothesis into question. *Development* **127**, 3197-3204.

Leyser O (2002). Molecular genetics of auxin signaling. *Annual Review of Plant Biolog*, **53**, 377-398.

Leyser O (2001). Auxin signaling: the beginning, the middle and the end. *Current Opinion in Plant Biology* **4**, 382-386.

Lincoln D, Britton J and Estelle M (1990). Growth and development of the *axr1* mutants of *Arabidopsis*. *Plant Cell* **2**, 1071-1080.

Lomax TL, Muday GK and Rubery PH (1995). Auxin transport. In: Davies, PJ, ed. *Plant hormones: physiology, biochemistry and molecular biology.* Dordrecht, Netherlands: Kluwer Academic Publishers, 509-530.

Luschnig C (2002). Auxin transport: ABC proteins join the club. *Trends in Plant Science* **7, 8,** 329-332.

Marchant A, Bhalerao R, Casimiro I, Casero PJ and Bennett M (2002). AUX1 promotes lateral root formation by facilitating indole-3-acetic acid distribution between sink and source tissues in the Arabidopsis seedling. *The Plant Cell* **14**, 589-597.

Mattsson J, Ckurshumova W and Berleth T (2003). Auxin signaling in *Arabidopsis* leaf vascular development. *Plant Physiology* **131**, 1327-1339.

Mattsson J, Sung RZ and Berleth T (1999). Responses of plant vascular systems to auxin transport inhibition. *Development* **126**, 2979-2991.

McConnell JR, Emery J, Eshed Y, Bao N, Bowman J and Barton MK (2001). Role of *PHABULOSA* and *PHAVOLUTA* in determining radial patterning in shoots. *Nature* **411**, 709-713.

Muday GK, Peer WA and Murphy AS (2003). Vesicular cycling mechanisms that control auxin transport polarity. *Trends in Plant Science* **8**, 301-303.

Nagpal P, Walker LM, Young JC, Sonawala A, Timple C, Estelle M and Reed JW (2000). AXR2 encodes a member of the AUX/IAA protein family. *Plant Physiology* **123**, 563-573.

Napier RM (1995). Towards an understanding of ABP1. *Journal of Experimental Botany* **46**, 1787-95.

Napier RM, David KM and Perrot-Rechenmann C (2002). A short history of auxin-binding proteins. *Plant Molecular Biology* **49**, 339-348.

Nelson T (1998). Polarity, vascularization and auxin. *Trends in Plant Science* **3**, 245-246.

Nelson T and Dengler N (1997). Leaf vascular pattern formation. *The Plant Cell* **9**, 1121-1135.

Otsuga D, DeGuzman B, Prigge MJ, Drews GN and Clark SE (2001). *REVOLUTA* regulates meristem initiation at lateral positions. *The Plant Journal* **25**, 223-236.

Patton EE, Willems AR and Tyers M (1998). Combinatorial control in ubiquitin-dependent proteolysis: don't skip the F-box hypothesis. *Trends in Genetics* **14**, 236-243.

Parry G, Delbarre A, Marchant A, Swarup R, Perrot-Rechenmann C and Bennett MJ (2001). Novel auxin transport inhibitors phenocopy the auxin influx carrier mutation *aux1*. *The Plant Journal* **25**, 399-406.

Przemeck GKH, Mattsson J, Hardtke CS, Sung ZR and Berleth T (1996). Studies on the role of the *Arabidopsis* gene *MONOPTEROS* in vascular development and plant cell axialization. *Planta* **200**, 229-237.

Reinhardt D, Pesce E-R, Stieger P, Mandel T, Baltensperger K, Bennet M, Traas J, Friml J and Kuhlemeier C (2003). Regulation of phyllotaxis by polar auxin transport. *Nature* **426**, 255-260.

Rosen E, Chen R and Masson PH (1999). Root gravitropism: a complex response to a simple stimulus? *Trends in Plant Science* **4**, 407-412.

Ruegger M, Dewey E, Hobbie L, Brown D, Bernasconi P, Turner J, Muday G and Estelle M (1997). Reduced naphthylphthalamic acid binding in the *tir3* mutant of Arabidopsis is associated with a reduction in polar auxin transport and diverse morphological defects. *Plant Cell* **9**, 745-757.

Sachs T (1981). The control of patterned differentiation of vascular tissues. *Advances in Botanical Research* **9**, 151-262.

Sachs T (1989). The development if vascular networks during leaf development. *Current Topics in Plant Biochemistry and Physiology* **8**, 168-183.

Sachs T (1991). Cell polarity and tissue patterning in plants. *Development Supplement* **1**, 83-93.

Scarpella E, Francis P, and Berleth T (2004). Stage-specific markers define early steps of procambium development in *Arabidopsis* leaves and correlate termination of vein formation with mesophyll differentiation. *Development* **131**, 3445-3455

Sieburth LT (1999). Auxin is required for leaf vein pattern in Arabidopsis. *Plant Physiology* **121**, 1179-1190.

Skowyra D, Craig KL, Tyers M, Elledge SJ, and Harper JW (1997). F-box proteins are receptors that recruit phosphorylation substrates to the SCF ubiquitin-ligase complex. *Cell* **91**, 209-19.

Stieger P, Reinhardt D and Kuhlemeier C (2002). The auxin influx carrier is essential for correct leaf positioning. *The Plant Journal* **32**, 509-517.

Steynen Q and Schultz E (2003). The FORKED genes are essential for distal vein meeting in Arabidopsis. *Development* **130**, 4695-708.

Swarup R, Friml J and Marchant A (2001). Localization of the auxin permease AUX1 suggests two functionally distinct hormone transport pathways operate in the Arabidopsis root apex. *Genes and Development* **15**, 2648-2653.

Timpte C, Wilson A and Estelle M (1994). The *axr2-1* mutation in *Arabidopsis thaliana* is a gain-of-function mutation that disrupts an early step in auxin response. *Genetics* **138**, 1239-1249.

Ulmasov T, Murfett J, Hagen G and Guilfoyle TJ (1997). Aux/IAA proteins repress expression of reporter genes containing natural and highly active synthetic auxin response elements. *The Plant Cell* **9**, 1963-1971.

Warwicker, J (2001). Modelling of auxin-binding protein 1 suggests that its C-terminus and auxin could compete for a binding site that incorporates a metal ion and tryptophan residue 44. *Planta* **212,** 343-47.

Yamamoto M and Yamamoto K (1998). Differential effects of 1-naphathaleneacetic acid and 2,4-dichlorophenoxyacetic acid on the gravitropic response of roots in an auxin resistant mutant of *Arabidopsis*, *aux1*. *Plant Cell Physiology* **39**, 660.

Yang K-Y, Moon YH, Choi KH, Kim Y-H, Eun M-Y, Guh J-O, Kim K-C and Cho B-H (1997). Structure and expression of the *AWI31* gene specifically induced by wounding in *Arabidopsis thaliana*. *Molecular Cell* **7**, 131-135.

Zgurski J, Sharma R, Bolokoski DA and Schultz EA (2005). Asymmetric auxin response preceded asymmetric growth of *asymmetric leaf1* and *asymmetric leaf2* Arabidopsis leaves. *The Plant Cell* **17**, 77-91.

Table 1 – Genetic interactions between *abn* and other auxin mutants. *axr1-2* and *mp* recombination frequencies are consistent with the molecular map distance of *abn* to 24 cM on Chromosome 1.

Genotype (n)	Segregation	x^2 Value (d.f.)	Frequency of Double Mutants
abn fkd-1 (182)	Independent	2.3 (5)	0.0625
abn pin1-1 (259)	Independent	4.7 (5)	0.0625
abn aux1-7 (118)	Independent	7.1 (5)	0.0625
abn axr6-2 (306)	Independent	2.0 (5)	0.0625
abn axr4-2 (284)	*abn* epistatic	5.6 (4)	0
abn axr1-12 (357)	Linked	n/a	0.019
abn mp (473)	Linked	n/a	0.00211

Table 2 – Morphology of mature first leaves at 21 DAG (Significant difference from a = wild type, b = *abn*, c = single mutant, student's t-test, $p<0.05$). The double mutants were not tested to wild type.

Genotype (n)	Shape (L/W)	# FEVs	# Aeroles	# VI's	# BPs	Margin Size
wild type (23)	1.27	13.1	17.6	0.48	47.3	0.050
axr1-12 (18)	0.97^{a}	11.1	6.9^{a}	0.39	24.2^{a}	0.063
axr2 (3)	0.98^{a}	10.7	20.3	0.33	50.7	0.055
fkd-1 (32)	1.25	21.2^{a}	5.8^{a}	1.69^{a}	29.4^{a}	0.046
bdl (10)	0.99^{a}	14.1	22.7^{a}	0.00	59.5^{a}	0.050
pin1-1 (15)	1.05^{a}	11.3	15.2	0.53	40.6	0.080^{a}
axr4-2 (30)	1.23	15.2	20.0	0.40	54.5	0.054
aux1-7 (25)	1.21	21.0^{a}	25.0^{a}	0.20	70.6^{a}	0.049
abn het (54)	$1.42^{a,b}$	12.2^{b}	16.5	0.43	44.4^{b}	$0.073^{a,b}$
het::axr1-12 (21)	$1.19^{b,c}$	$8.0^{b,c}$	$11.3^{b,c}$	0	$30.7^{b,c}$	0.074
het::axr2 (4)	1.12^{b}	11.3	18.3	0.5	46.8	0.09
het::fkd-1 (40)	$1.32^{b,c}$	22.9b	$14.9^{b,c}$	0.65^{c}	$51.4^{b,c}$	0.066^{c}
het::bdl (44)	$1.19^{b,c}$	11.5	19.6^{b}	$0.14^{b,c}$	$50.4^{b,c}$	0.075^{c}
het::pin1-1 (19)	$1.32^{b,c}$	$19.4^{b,c}$	$26.4^{b,c}$	0.53	$71.1^{b,c}$	0.076
het::axr4-2 (18)	1.46^{c}	12.4	16.4	0.28	44.7^{c}	$0.094^{b,c}$
het::aux1-7 (47)	1.24^{b}	$18.0^{b,c}$	$28.0^{b,c}$	0.19	73.5^{b}	$0.062^{b,c}$
abn hom (23)	1.81^{a}	9.3^{a}	14.9	0.22	38.7^{a}	0.182^{a}
abn::axr1-12 (8)	1.45^{c}	10.3	13.4^{c}	0	37^{c}	0.168^{c}
abn::axr2 (5)	1.48^{c}	8	14^{c}	0	36^{c}	0.186^{c}
abn::fkd-1 (29)	1.97^{c}	22.3	14.8^{c}	0.62^{c}	50.8^{c}	0.148^{c}
abn::bdl (29)	1.33^{c}	7.6^{c}	16.2^{c}	0.03	39.9^{c}	0.139^{c}
abn::pin1-1 (10)	3.48^{c}	29.7^{c}	49.9^{c}	0.40	128.7^{c}	0.177^{c}
abn::axr4-2 (11)	1.99^{c}	13.8	13.5^{c}	0.00	40.9^{c}	0.236^{c}
abn::aux1-7 (35)	1.71^{c}	14.9^{c}	18.7^{c}	0.06	52.1^{c}	0.143^{c}

Table 3 – Morphology of mature cotyledons at 14 DAG (significant difference from a = wild type, b = *abn*, c = single mutant, student's t-test, $p<0.05$). The double mutants were not tested to wild type.

Genotype (n)	Shape (L/W)	# FEVs	# Aeroles	# BPs	Margin Size
wild type (23)	1.32	0.57	3.39	7.35	0.161
axr1-12 (11)	1.13[a]	1.91[a]	1.27[a]	4.45[a]	0.159
axr2 (4)	1.04[a]	1.50[a]	2.25[a]	6	0.179
fkd-1 (31)	1.20[a]	2.61[a]	1.19[a]	5.00[a]	0.174
bdl (11)	1.04[a]	0.36	3.64	7.64	0.134[a]
pin1-1 (14)	0.86[a]	1.57[a]	3.07	7.71	0.166
axr4-2 (31)	1.16[a]	0.45	3.26	6.97	0.152
aux1-7 (29)	1.14[a]	0.66	3.41	7.48	0.170
abn het (59)	1.33[b]	1.08[a,b]	4.12[a,b]	9.32[a,b]	0.155[b]
het::axr1-12 (10)	1.09[b]	2.70[b]	2.40[b,c]	7.50[b,c]	0.157
het::axr2 (8)	1.01[b]	1.875	2.88[b]	7.63[b]	0.232
het::fkd-1 (39)	1.25[b,c]	1.21[b,c]	2.26[b,c]	5.72[b,c]	0.189[b]
het::bdl (47)	1.07[b]	0.85[c]	3.74[b,c]	8.34[b,c]	0.151
het::pin1-1 (17)	1.09[b,c]	3.76[b,c]	6.71[b,c]	16.94[b,c]	0.174
het::axr4-2 (18)	1.21[b]	1.11[c]	3.33[b]	7.78[b,c]	0.164
het::aux1-7 (61)	1.06[b,c]	1.16[c]	3.46[b]	8.08[b,c]	0.167
abn hom (21)	1.59[a]	4.00[a]	8.57[a]	21.14[a]	0.256[a]
abn::axr1-12 (4)	1.29[c]	6.25[c]	0.50	7.25	0.328[c]
abn::axr2 (8)	1.22	3.63[c]	3.25	10.1[c]	0.297[c]
abn::fkd-1 (30)	1.37[c]	7.37[c]	1.57	10.5[c]	0.323[c]
abn::bdl (22)	1.21[c]	2.91[c]	5.00[c]	12.9[c]	0.274[c]
abn::pin1-1 (9)	1.13[c]	4.44[c]	11.44[c]	27.33[c]	0.207
abn::axr4-2 (16)	1.44[c]	3.81[c]	5.25[c]	14.3[c]	0.318[c]
abn::aux1-7 (35)	1.32[c]	3.69[c]	4.14[c]	11.97[c]	0.251[c]

DR5:GUS expression	AT			NOA			2,4D			NAA		
	wild type	*abn* het	*abn* hom	wild type	*abn* het	*abn* hom	wild type	*abn* het	*abn* hom	wild type	*abn* het	*abn* hom
Day 5 (wt); Day7 (NOA,2,4-D,NAA)	**(121)[d]**	**(86)**	**(30)**	**(108)**	**(84)**	**(30)**	**(107)**	**(86)**	**(24)**	**(55)**	**(91)**	**(36)**
Primordia (no DR5:GUS)	10.70%	16.30%	20%	20.40%	39.30%	60.00%	41.10%	62.80%	50%	21.80%	76.90%	83.30%
Distal tip[a] (dispersed in NOA/NPA)	39.30%	74.40%	0%	61.10%	15.50%	0%	35.50%	23.30%	0%	50.90%	19.80%	0%
Distal tip and Secondary loop	14.80%	0%	0%	3.70%	0%	0%	22.40%	0%	0%	20.00%	0%	0%
Secondary[b] loop alone	0%	0%	80%	0%	0%	13.30%	0%	0%	25%	0%	0%	16.70%
Tertiaries	14.00%	4.70%	0%	0%	0%	0%	0%	0%	0%	5.50%	1.10%	0%
Hydathodes (1)[c]	2.50%	4%	0%	0%	0%	0%	0%	0%	0%	1.80%	2.20%	0%
Hydathodes (2)[c]	23.10%	1%	0%	0%	0%	0%	0.90%	0%	0%	5.50%	0%	0%
Vascular lignification	25.20%	33.00%	30.40%	34.30%	82.10%	46.70%	1.90%	37.20%	16.60%		no data	
Day 6 (wt); Day10 (NOA,2,4-D); Day 9 (NAA)	**(43)**	**(82)**	**(36)**	**(124)**	**(76)**	**(32)**	**(161)**	**(82)**	**(26)**	**(61)**	**(103)**	**(50)**
Primordia (no DR5:GUS)	7.00%	20.70%	30.50%	29.80%	13.20%	6.30%	27.30%	41.50%	23.10%	4.90%	29.10%	72.20%
Distal tip* (dispersed in NOA/NPA)	41.90%	54.90%	30.50%	10.50%	0%	0%	20.50%	24.40%	0%	45.90%	67.00%	16.70%
Distal tip and Secondary loop	0%	0%	0%	0%	0%	0%	13.00%	0%	0%	3.30%	0%	0%
Secondary* loop alone	0%	0%	38.90%	0%	0%	0%	0%	0%	23.10%	0%	0%	5.60%
Tertiaries	39.50%	2%	0%	0%	0%	0%	1.20%	0%	0%	27.90%	0%	0%
Hydathodes (1)[c]	7%	9%	0%	0%	0%	0%	0%	0%	0%	20%	2%	0%
Hydathodes (2)[c]	30.20%	9%	0%	0%	0%	0%	1.90%	0%	0%	11.50%	0%	0%
Vascular lignification	38%	27.50%	15.00%	96.00%	94.30%	93.80%	57.80%	63.40%	65.40%		no data	
Day 10 (wt); Day14 (2,4-D,NAA)	**(60)**	**(93)**	**(20)**				**(86)**	**(27)**	**(4)**	**(74)**	**(72)**	**(41)**
Primordia (no DR5:GUS)	13.30%	28.00%	41.30%		no data		2.30%	7.40%	0%	23.00%	43.10%	70.70%
Distal tip* (dispersed in NOA/NPA)	5%	6.50%	2.20%				34.90%	29.60%	0%	36.50%	48.60%	12.20%
Distal tip and Secondary loop	1.70%	0%	0%				11.60%	0%	0%	0%	0%	0%
Secondary* loop alone	0%	0%	0%				0%	0%	0%	0%	0%	0%
Tertiaries	1.70%	0%	0%				4.70%	0%	0%	2.70%	0%	0%
Hydathodes (1)[c]	3%	25%	0%				9%	0%	0%	8%	1%	0%
Hydathodes (2)[c]	50%	27%	0%				2%	0%	0%	22%	1%	0%
Hydathodes (3)[c]	22%	1%	0%				0%	0%	0%	3%	0%	0%
Hydathodes (3)[c]	0%	1%	0%				0%	0%	0%	0%	0%	0%
Vascular lignification	77.80%	95.70%	72.60%				53.50%	77.80%	75%		no data	

Table 4 - Auxin response landmarks of vascular development in wild type, *abn* heterozygous and *abn* homozygous first leaves untreated (AT) or treated with 30 M NOA, 10-6 2,4-D or 40 M 1-NAA. Values represent the percentage of leaves showing DR5:GUS expression of each landmark. Parentheses indicate the total number of leaves scored for that character.

a - The distal tip expression occurs at a distinct maximum in AT and 1-NAA treated leaves, but is dispersed in NOA and 2,4-D treatments.

b - The secondary loop in *abn* homozygous leaves is not the same as the secondary loop in wild type and abn homozygous leaves.

c - The number of hydathodes showing DR5:expression are indicated in parentheses.

d - The total number of leaves scored.

Table 5 –Morphology of wild type, *abn* heterozygous and *abn* homozygous shoots. (Significant difference from a= wild type, b = *abn,* Student's t-test, $p<0.05$). * measured at 28 DAG.

Genotype (n)	2 cm bolt (Days)	Flowering (Days)	Maturation (Days)	# Rosette Leaves*	# Secondary Inflorescences*	Height* (mm)
Wild type (20)	26.1^{b}	26.9^{b}	28.4^{b}	7.6^{b}	3.8^{b}	71.7^{b}
abn het (58)	$23.5^{a,b}$	$24.2^{a,b}$	$25.1^{a,b}$	$5.4^{a,b}$	$2.5^{a,b}$	54.7^{a}
abn homo (21)	20.2^{a}	20.6^{a}	21.4^{a}	4.8^{a}	2.2^{a}	49.2^{a}

Table 6 – Morphology of roots. Primary root length was measured at 7 DAG while the number of lateral roots (LRs) and the distance from LRs to the root apical meristem (RAM) were measured at 14 DAG. No significant differences were determined (Student's t-test, $p<0.05$).

Genotype (n)	Primary Root Length (mm)	Number of LRs	Distance from LRs to RAM	LR Density (Length /LR)
Wild type (26)	24.9	5.3	17.9	5
abn het (73)	21	3.6	20.1	7.3
abn hom (23)	22.3	3.5	19.1	6.7

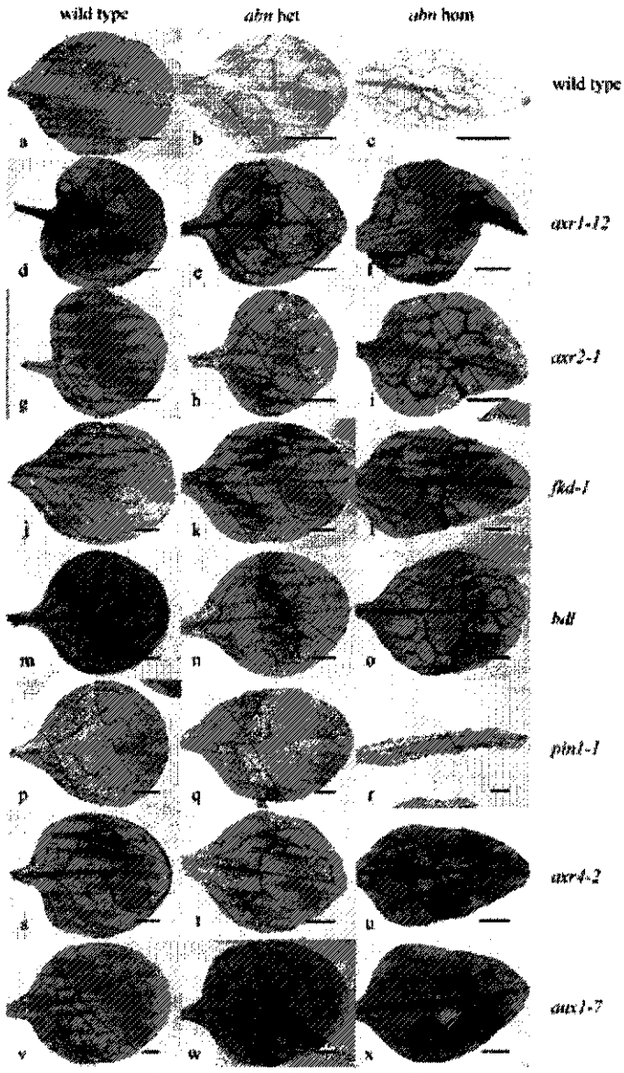

Figure 1 - Vascular pattern of cleared first leaves 21 DAG viewed under light microscopy (scale bar = 1 mm). The genotype of the *ABN* locus is shown along the top, while the genotype of a series of auxin related loci is shown along the right hand side.

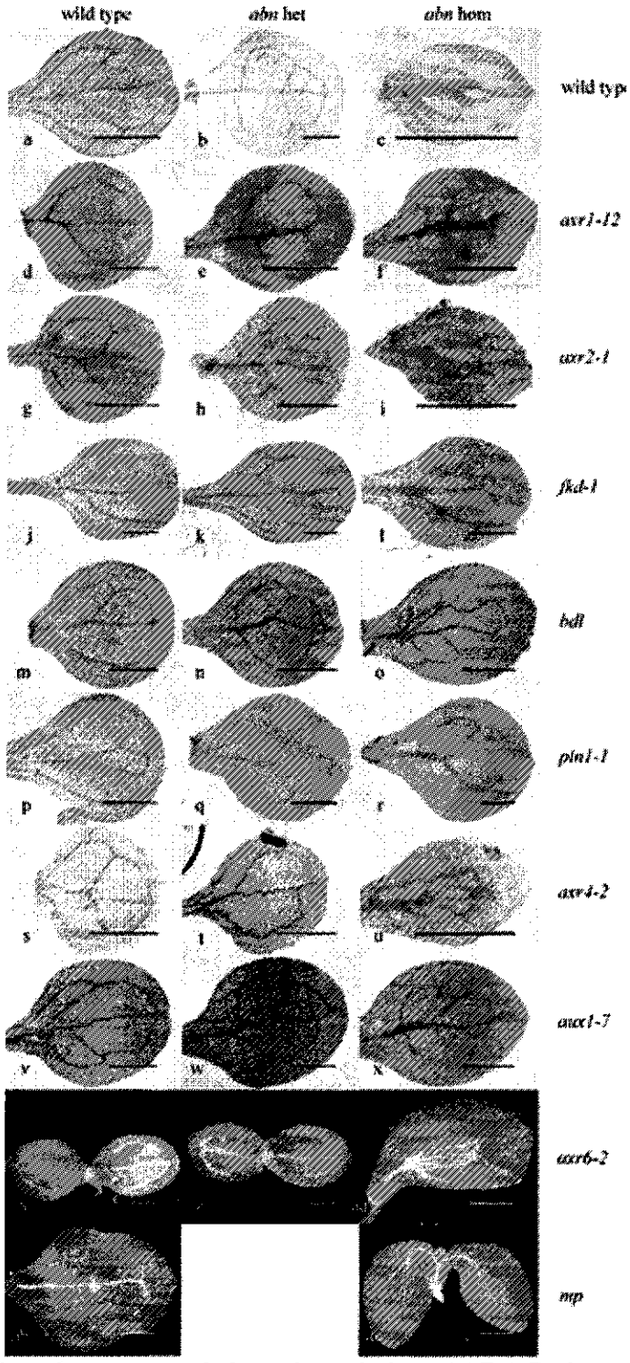

Figure 2 – Vascular pattern of cleared cotyledons 14 DAG viewed under light microscopy (a-x) or phase contrast optics (y-ac) (scale bar = 1 mm a-aa; 0.5mm y-ac). The genotype of the *ABN* locus is shown along the top, while the genotype of a series of auxin related loci is shown along the right hand side.

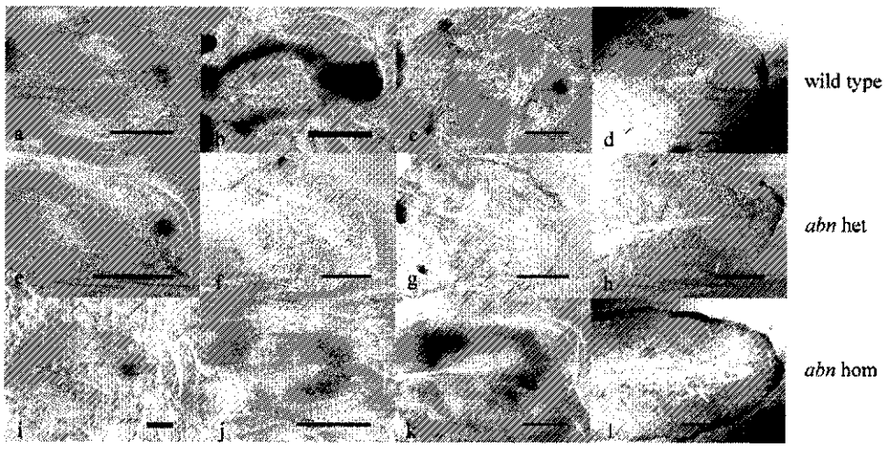

Figure 3 – DR5:GUS expression in developing leaves of wild type (a-d), *abn* heterozygous (e-h), and *abn* homozygous (i-l) seedlings. Viewed with differential interference contrast optics (scale bar = 0.05mm a,b,e,i-k; 0.1mm c,g; 0.2mm f; 0.5mm h; 1mm d,l).

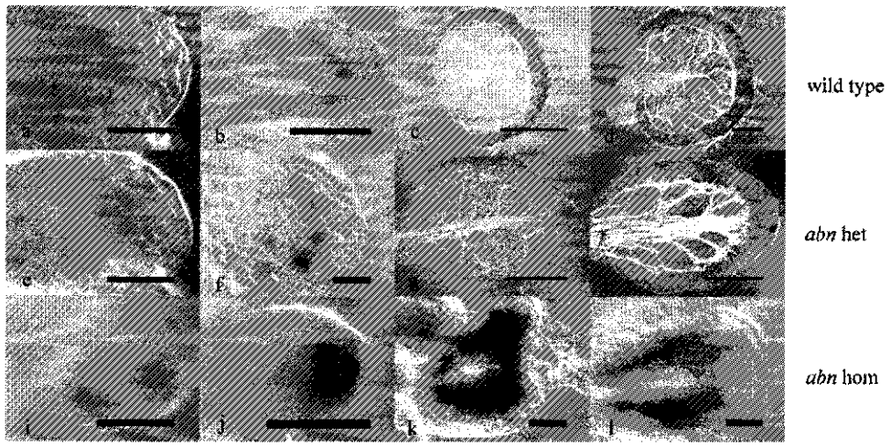

Figure 4 – DR5:GUS expression in developing leaves of wild type (a-d), *abn* heterozygous (e-h), and *abn* homozygous (i-l) seedlings treated with 30μM NPA. Viewed with differential interference contrast optics (scale bar = 0.01mm i; 0.05mm a,e,f,j-l; 0.1mm b, 0.5mm c,g; 0.2mm d; 0.5mm h).

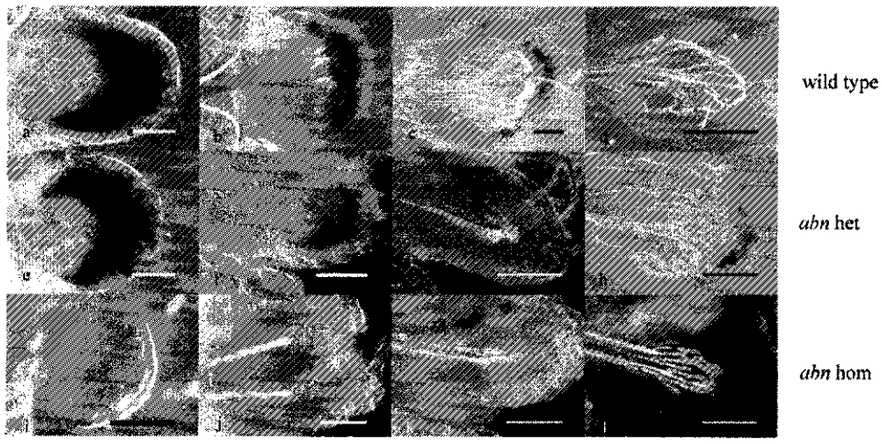

Figure 5 – DR5:GUS expression in developing leaves of wild type (a-d), *abn* heterozygous (e-h), and *abn* homozygous (i-l) seedlings treated with 30μM NOA. Viewed with differential interference contrast optics (scale bar = 0.05mm a,e,f,i-k; 0.1mm b,c,g,l; 0.2mm h; 0.5mm d).

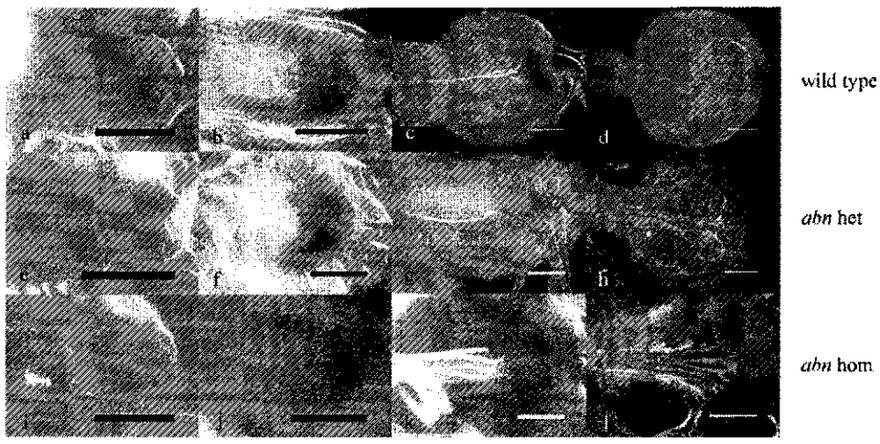

Figure 6 – DR5:GUS expression in developing leaves of wild type (a-d), *abn* heterozygous (e-h), and *abn* homozygous (i-l) seedlings treated with 1 μM *2*,4-D. Viewed with differential interference contrast optics (scale bar = 0.05mm a,b,e-g,i-k; 0.1mm c,l; 0.2mm d,h).

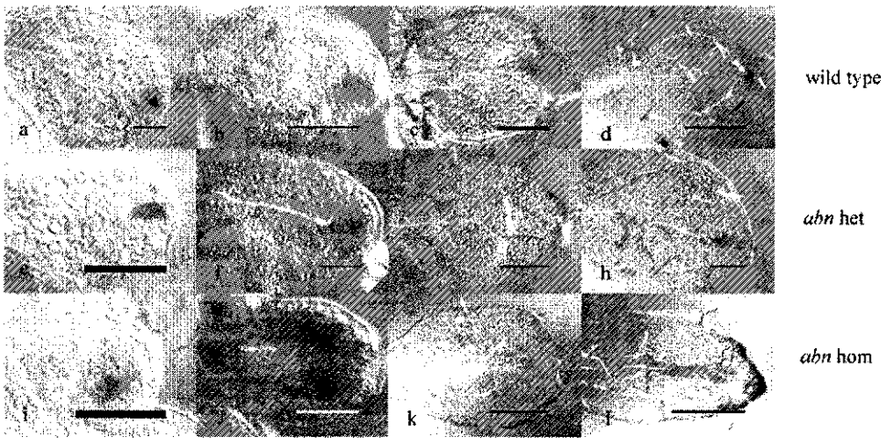

Figure 7 – DR5:GUS expression in developing leaves of wild type (a-d), *abn* heterozygous (e-h), and *abn* homozygous (i-l) seedlings treated with 0.40 μM 1-NAA. Viewed with differential interference contrast optics (scale bar = 0.05mm a,e,f,i,j; 0.1mm b,c; 0.2mm g,h; 0.5mm d,k,l).